POLITECNICO
MILANO 1863

SCUOLA DI INGEGNERIA INDUSTRIALE
E DELL'INFORMAZIONE

Enhancing Sustainability for Wide and High Additive Manufacturing through Material Recycling and Zero-Defects Production

TESI DI LAUREA MAGISTRALE IN
MANAGEMENT ENGINEERING

Author: **Andrea Bellia**

Student ID:	953319
Advisor:	Bianca Maria Colosimo
Co-advisor:	Fabio Caltanissetta
Academic Year:	2020-21

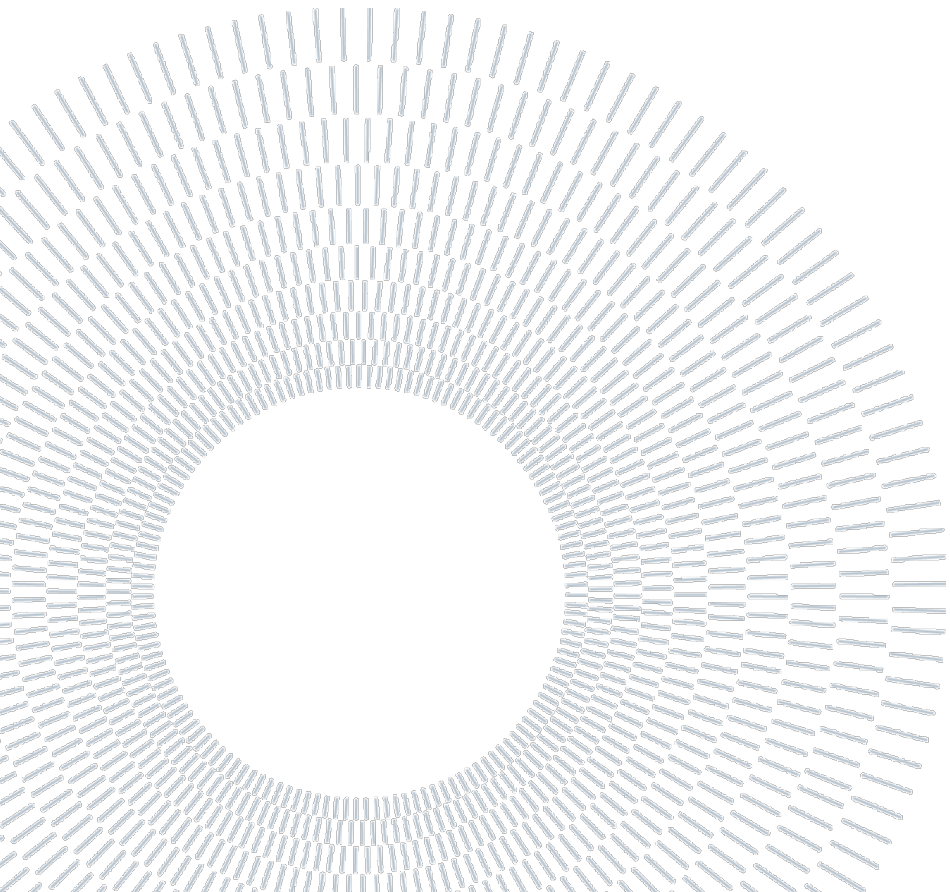

Abstract

Among the current industrial proceedings, Additive Manufacturing (AM) has been recognized as one of the most disruptive technologies in changing the paradigm of the current manufacturing industry. In particular, Wide and High Additive Manufacturing (WHAM) is emerging for the 3D printing of functional large-scale objects. Recent studies have demonstrated that the nature of these processes enables the reduction of scraps and material use with respect to the traditional manufacturing processes, paving the way towards a more sustainable production of large-volume products of thermoplastic or composites parts. However, few study still investigate the environmental impact of WHAM process and the different ways of reducing CO_2 emissions. This study will deepen the sustainability in WHAM, with the main purpose of reducing the CO_2 emissions related to thermoplastic material production. More in details, two paths have been followed. In the first part, material recycling was investigated. ABS filled with 20% of chopped carbon fibers was recycled and reused for a new part's production. Here, the CO_2 emissions related to material recycling and virgin material production have been calculated, as well as the associated costs with the production of the virgin material compared to its mechanical recycling process, highlighting the advantages of the reuse of the material. Moreover, a study regarding the mechanical properties of the recyclates has been conducted, underlining a decrease when adding recycled material to the mix. The second considered way to reduce material wastes consisted in reducing production scraps thanks to the prompt detection of part defect. For this purpose, in-situ thermal monitoring of the process was applied to limit the occurrence of defects. During the first experimental campaign, different cooling behaviors have been noted for the different parts of the structures, highlighting a faster cooling rate for the surface in contact with the floor. Moreover, other peculiarities of the process have been underlined, focusing the attention on the re-heating effect of the extruder for a multi-bead structure.

Key-words: Sustainability, WHAM, Recycling, Monitoring.

Abstract in lingua italiana

Tra le attuali tecnologie industriali, l'Additive Manufacturing, o Stampa 3D, si è affermata come una delle tecniche più rivoluzionarie del settore, andando a sconvolgere i paradigmi nel campo dell'industria manifatturiera. In particolare, la Wide and High Additive Manufacturing (WHAM), o stampa 3D di grande dimensione, sta guadagnando quote di mercato per la produzione di oggetti funzionali con volumi superiori al m^3. Studi recenti hanno dimostrato che la natura di questi processi favorisce l'utilizzo di meno materiale e riduce gli scarti rispetto alle tecniche di manifattura tradizionale, aprendo la strada verso una produzione sostenibile di oggetti di grande dimensione in materiale termoplastico o composito. Parallelamente, sono pochi gli studi dedicati all'analisi dell'impatto ambientale per i processi WHAM con l'obiettivo di andare a ridurre le emissioni di CO_2. Questo studio approfondisce il tema della sostenibilità in ambito WHAM, con l'obiettivo principale di andare a ridurre le emissioni di CO_2 legate alla produzione di oggetti in materiale termoplastico. Sono stati seguiti due percorsi col fine di raggiungere questo obiettivo. Nella prima parte si è approfondito il riciclo del materiale. In particolare, si è riciclato e riutilizzato ABS caricato al 20% con fibre di carbonio corte per la produzione di nuovi oggetti. Per questo scenario, sono state calcolate le emissioni di CO_2 collegate al riciclo del materiale e alla sua produzione, andando a calcolare e paragonare i relativi costi, evidenziando un vantaggio nel riutilizzo del materiale. A conclusione di questa parte, si è condotto uno studio sulle proprietà meccaniche del materiale riciclato, riscontrando una diminuzione delle proprietà alla presenza di materiale riutilizzato. Nella seconda parte si è approfondita la riduzione degli scarti di produzione grazie alla rilevazione dei difetti di stampa. A questo scopo, il monitoraggio termico in-situ è stato applicato col fine di limitare l'emergere di difetti. Durante la prima campagna sperimentale si sono evidenziati diversi comportamenti in relazione al punto considerato, osservando un raffreddamento più veloce per le regioni a contatto con il suolo. Inoltre, per strutture multi-bead, si è evidenziato un effetto di re-heating delle zone adiacenti al passaggio dell'estrusore.

Parole chiave: Sostenibilità, WHAM, Riciclo, Monitoraggio.

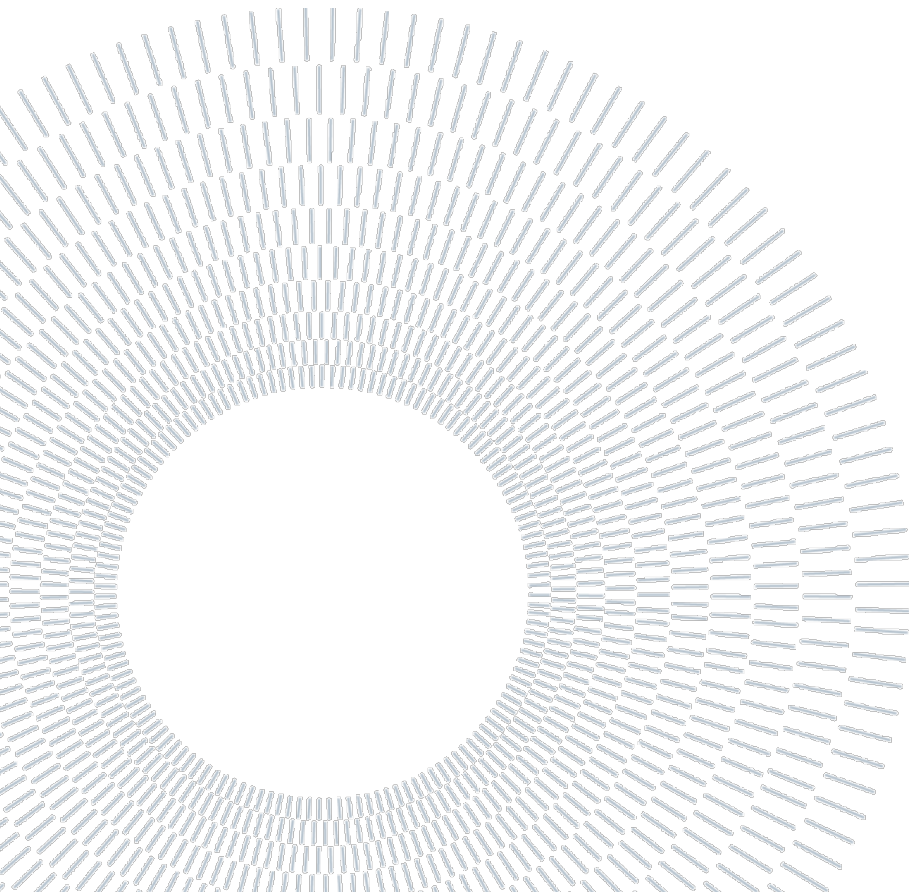

Contents

Introduction

In today's world, the environmental issue is increasingly worrying governments around the world, pushing an ecological transition towards a circular economy and a more sustainable consumption of resources in all areas. The attention of governments to the problem is also demonstrated by numerous deals, like the “Paris Agreement”, in which states around the world are committed to contain carbon emissions, in particular for the world of manufacturing.

Among the manufacturing technologies, Additive Manufacturing plays a central role in the ongoing industrial revolution and has an enormous potential in limiting pollution, saving materials and reconfiguring the value chains. Thanks to the characteristics of this technology, functional parts are produced by adding material where needed, decreasing its use and reducing wastes. At the same time, the logistics and the supply chains are simplified due to the reduction or elimination of intermediaries. Moreover, physical inventories are not needed since the products can be manufactured using a “make-to-order” policy, staring from digital CAD files.

Among the AM technologies, one of the most promising for the production of large functional parts is Wide and High Additive Manufacturing (WHAM). Within this category are included those systems capable of building objects whose volume is bigger than 1 m^3. The most utilized materials are composites and techno-polymers, used to produce ready-to-use tools like molds or prototypes. WHAM’s horizon is expanding, and as build volumes increase, so does the demand for the related products, resulting in a generation of new markets. On the other hand, the most used materials for Wide and High Additive Manufacturing are plastics and composite materials with glass and carbon fibers.

This thesis was born from the collaboration between Camozzi Group and Politecnico of Milano. It aims at the limitation of CO_2 emissions for Wide and High Additive Manufacturing through the reduction of the use of virgin material for industrial production.

Considering the related CO_2 emissions, the reduction in the use of plastic or composites is a central theme throughout the world and in particular in the European Union, where there is a tendency to prefer recycling over the production of new plastic. In addition, when we consider the fillers in the materials used for

WHAM, glass and carbon fibers require an incredible amount of energy to be produced, increasing energy requirements and, consequently, the associated CO_2 emissions. Moreover, recent studies (Witten et al., 2018) have shown a trend of increasing demand for these composite materials, making it necessary to take a different approach to the problem than just producing new material.
Among the existing possibilities for CO_2 emissions reduction, two main options have been considered for the reduction of CO_2 emissions in WHAM. They concern the mechanical recycling of the material and the thermal monitoring of 3D printing. The objective of material recycling consists in reusing production waste or end-of-life (EOL) products to introduce circularity in the use of raw materials, emitting less CO_2 and reducing production costs. As regards "zero-defects" production, it consists in limiting as much as possible the production of waste during the printing process. The entire work has been performed on the Ingersoll MasterPrint, the Large-scale Additive Manufacturing system owned by Innse Berardi.
This work, therefore, will be articulated by exploring the two paths mentioned above. The thesis will be structured as follow:

- The first chapter is dedicated to the review of the state of the art. It describes the characteristics of 3D printing and WHAM, and it analyzes the main methods of recycling and the main types of defects that may arise during the printing process, devoting brief attention to the technologies developed for in-situ monitoring.
- The second chapter is focused on the practical aspects concerning the recycling of the material taken as a benchmark for the process, the ABS filled with 20% carbon fibers. It presents the effect of recycling in CO_2 reduction and costs savings. Moreover, the results of the mechanical tests performed on the raw and recycled materials are presented to assess the possibility of the reuse for functional application.
- The third chapter is focused on a preliminary evaluation of the thermal monitoring of the process. In this section, a data acquisition campaign will be discussed, and qualitative evaluations regarding the cooling process of the part, printed with ABS filled with 20% glass fiber, will be made.
- The fourth and last chapter will deal with the conclusions of the work, summarizing the results of the thesis and the future perspectives.

1. State of the Art

Additive Manufacturing (AM) is a specific 3D printing technique that consists in building parts layer by layer by depositing material according to precise digital 3D design data. The word 3D Printing (or 3DP) is increasingly used as a synonym for Additive Manufacturing. However, the latter better reflects the manufacturing process that significantly differs from the traditional, subtractive manufacturing methods (EOS, 2021). Nowadays, with the new paradigm of "Industry 4.0" based on the integration of the physical and digital world, AM has acquired great importance due to its characteristics of flexibility and design freedom, and it's now considered an essential constituent of this industrial revolution (Ugur et al., 2017). In order to better understand the peculiarities of this technology, firstly some words need to be spent to clarify how AM works and how the designed parts are produced. The following framework is intended to explain the typical steps involved in the manufacturing of a 3D-printed part. All AM products must be developed starting from a software model that fully represents the part: usually, Computer Aided Design (CAD) softwares are used for this purpose, but also 3D scanners can be utilized (Gibson et al., 2015). Once the piece has been successfully designed, the file must be converted in the .STL file format, widely accepted as a standard for almost every machine, that is responsible for the "slicing" of the piece: this is the formal division in layers that once deposited will form the physical object. Subsequently, this type of file needs to be transferred to the AM machine where some minor changes concerning the scaling of the object and the orientation inside the building chamber are applied. Before budling the object, the machine needs to be set up properly according to the material used and other parameters, such as the temperature inside the hollow, need to be established. Then, the part can be automatically built by the AM machine, without the direct supervision of the operators. Once the product is printed and removed from the machine, post-processes may be required to finish the manufactured item

before its final application. Once finished, the object can be successfully used for what it has been designed for (Gibson et al., 2015).
The picture below (Fig. 1) summarizes the above-mentioned steps to produce a part using additive manufacturing.

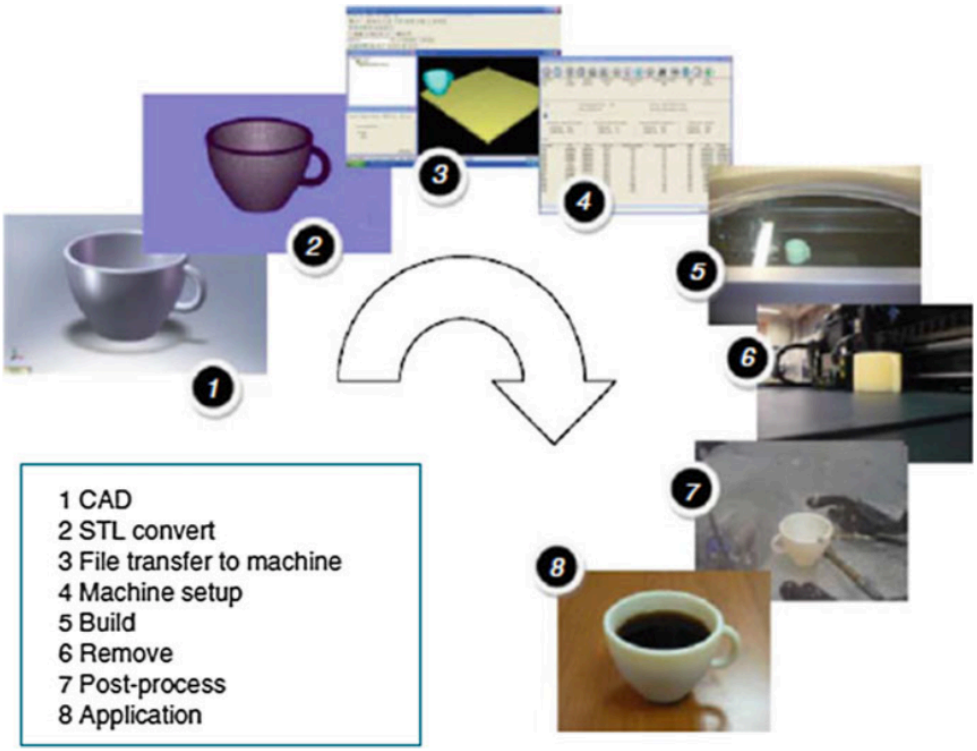

Figure 1 - Generic process used to manufacture a product using AM (Source: Gibson et al., 2015)

As it is noticeable, this process deeply differs from the traditional way of producing objects. Indeed, using AM, the material is deposited only where needed, following precise instructions established by the .STL file. This characteristic allows the development of complex patterns and geometries resulting useful for reducing wastes of material during the production process and for saving weights (Gibson et al., 2015).

The history of additive manufacturing began in 1983 when the engineer Charles Hull firstly manufactured an object using the technique of stereolithography (SLA). Once he had registered the patent for this technology in 1986, Hull founded his company

specialized in 3D printing, the 3D Systems, still today one of the most important companies in the sector. At the same time, the founder developed the file format ".STL" (stereolithography interface format), meant to be the main standard used today. In 1986 researchers Carl Deckard and Joe Beaman, starting from Hull's concepts, developed another technology capable to produce parts using AM, the so-called selective laser sintering (SLS). The development of new technologies for AM didn't stop there, in fact, in 1989 Scott Crump patented a new technique: the fused deposition modeling (FDM) starting the Stratasys, the main competitor of the 3D Systems. After a period of stagnation regarding the development of new AM technologies, in 1993 the Massachusetts Institute of Technology patented its personal technology, called "Three-Dimensional Printing". Subsequently, in 1995 the Fraunhofer Institute in Germany invented another manufacturing process based on AM, the selective laser melting (SLM), a process similar to the SLS but different in its main fundamentals (Wholers Associates, 2014). From 1995 other technologies have been patented, it is the case of Material Jetting (MJ), Binder Jetting (BJ), Sheet Lamination processes (SL), and Direct Energy Deposition processes (DED). Even nowadays the innovation in this field has never stopped: always more and more firms are approaching this world and their collaboration with universities has allowed a rapid growth in the development of know-how concerning these technologies.

To be more precise, since 2010, AM processes have been classified according to a set of standards developed by ASTM (American Society for Testing and Material) F42, in which the different technologies developed so far have been grouped. These seven processes are:

- Vat Photopolymerization processes,
- Powder Bed Fusion processes,
- Extrusion-Based systems,
- Material Jetting,
- Binder Jetting,
- Sheet Lamination processes,
- Direct Energy Deposition processes.

Since the topic of this work concerns Wide and High Additive Manufacturing (WHAM) systems, which are extrusion-based, it has been decided to provide a general overview of the above-mentioned technology describing its main

characteristics, the machine types, the material processed, and the sector of applications.
The core of this work is related to enhancing sustainability by limiting the material usage, in particular composites and plastics. Due to the peculiarity of the technology, the pieces that can be produced by these systems can weigh, on average, 500 kilograms, requiring a stunning material quantity. The idea from which this work has been developed has been born from the previous statement: in fact, achieving a way to reduce the material usage can lead to big savings in terms of costs and enhance the attention on the environmental problem. To be more precise, two paths will be defined along this thesis: the possibility of recycling scraps and end-of-life products to achieve a sustainable production reusing the material already printed, and the monitoring of the printing from a thermal point of view, preventing the rising of defects and limiting the material waste from the beginning.

1.1 AM Technology – Extrusion Based Systems

Extrusion-based technologies are currently the most widespread in the business of 3D printing (Gibson et al., 2015; Brian et al., 2014). In these types of processes, a material contained in a reservoir is melted and extruded through a nozzle by applying pressure. Once a layer is completed, the machine moves upward of a layer thickness and continues with the process. There are some key characteristics that are peculiar of these technologies (Brian et al., 2014):

- Loading of material: the material used to print the object is stored in a reservoir in a solid-state form.
- Melting of the material: to be successfully extruded and selectively deposited the solid material need to be melted to form the desired geometries.
- Pressure application to force the material through the nozzle and extrusion: to successfully deposit and extrude the material through the nozzle, pressure must be applied, the more the pressure is maintained constant the more regular is the filament extruded.
- Deposition of the material through a predetermined path: when starting the printing of the object the path of the extruder needs to be already determined in order to optimize the deposition of the material (i.e. to avoid over-

deposition of the material, pressure needs to be adjusted to vary the flow rate when the nozzle change the printing direction).

- Support generation to enable complex geometrical features: to assist the production of complex geometries since the material is not self-supporting when melted, supports need to be printed and then removed at the end of the printing.

Hereafter (Fig. 2) is represented a typical extrusion-based machine to give a visual representation of the apparatus.

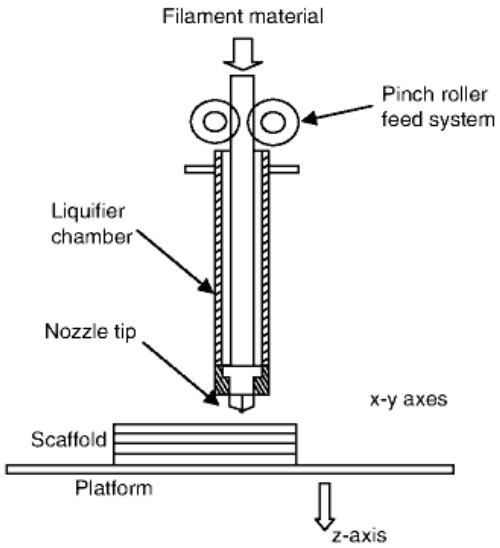

Figure 2 - Representation of an extrusion-based machine (Source: Colosimo et al., 2020)

As previously anticipated, these processes are usually characterized by the presence of post-processes to remove printed supports and to improve the surface's quality of the final product.

Among the different Extrusion-Based Systems, the most common are Fused Deposition Modeling (FDM), Fused Filament Fabrication (FFF) and Melt Extrusion Manufacturing (MEM) or Hot Melt Extrusion (HME) (Brian et al., 2014).

As far as FDM is concerned, to produce a piece, the raw material is fed into a temperature-controlled extrusion nozzle continuously, and liquified to facilitate its extrusion. The printing head extrudes and deposits the material along the printing platform, thanks to a control system.

When a layer is complete, the machine moves up or the platform lowers down in the z-axis and starts the printing of the following one (Singh et al., 2016). Ideally, when the material is extruded, it should remain unchanged in shape and size. On the other hand, since the material has been brought to a semi-liquid state, while cooling some shrinkage phenomena could happen. To control the shrinkage and to limit residual stress, FDM machines come with a heated chamber developed to mitigate the arise of problems (Gibson et al., 2015). The chamber maintains constant the environmental temperature and the temperature of the material, increasing the bonding between the layers and avoiding layer separation (delamination). With this extrusion technology, some features may result impossible to be printed from scratch. To overcome these problems and print, for example, a piece with an inclination lower than 45° with respect to the building plate, supports are needed (Roschli et al., 2018). Supports are extra components, aside from the material needed for the piece, printed to support the building of the most complex geometries.

Concerning Fused Filament Fabrication (FFF), the definition of the technology is a bit controversial: often these two names are wrongly used interchangeably but refer to two different apparatus. Since FDM is a proprietary technology patented by Stratasys in 1989, the world of 3D printing needed to develop a similar technique for printing parts. FFF, like FDM, uses a filament extruded by a heated nozzle to produce parts but, in this case, there is not a heated chamber to facilitate the control during the printing phase (3D Shop, 2021). According to literature, this is the main difference between the two processes, with the fact that FDM is thought for industrial application, while FFF is more open access also for a mass market, due to its peculiarity of affordability in terms of costs. As far as MEM processes are concerned, these technologies differ significantly from the ones previously described. The main differences of melt extrusion manufacturing concern the material feedstock and the extrusion technique of the material. In this case, granulates from injection molding are used, not filament coming from a coil (Verlag, 2018). If in FDM and FFF a filament is extruded by two rollers, in HME a screw is responsible for the melting of the pellets. Indeed, the granules, after some pre-processes, are fed into a hopper and transported to the nozzle by a three-section screw. Heat is applied to melt the material which is then deposited on the building plate (Valkenaers et al.,2013).

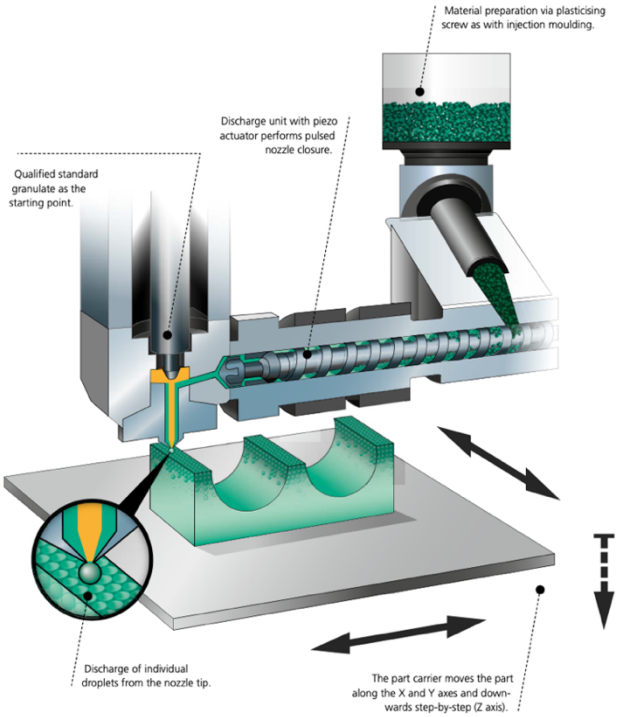

Figure 3 - Representation of HME machine with screw extruder (Source: Arburg plastic freeformer pamphlet)

As we can see from the figure above (Fig. 3), the material is contained in a granulate form inside the reservoir, where it is usually dried from moisture. Then, the pellets are processed by the screw that heats them through the presence of resistances positioned along the structure. Usually, three heat zones are identified with increasing temperature to gradually melt the material. When fully melted, the substance is extruded by the nozzle to be deposited over the building platform. When a layer is finished, the nozzle goes up of a sheet's thickness and starts printing the subsequent blanket. The process is repeated till the object is complete (Valkenaers et al.,2013).

The most important factors to be considered when dealing with material-extrusion processes are the process parameters. Indeed, these need to be optimized to achieve the correct accuracy and mechanical properties useful for the final application of the part. Among them, according to Gibson (Gibson et al., 2015), the most important are:

- Input pressure: which is one of the factors responsible for the flow rate of the material through the nozzle.
- Temperature: maintaining constant the inversion for the melted material would be ideal because temperature affects the flow of the material.
- Nozzle diameter: usually it is constant and define the quantity of the material that can be deposited.
- Material characteristics: such as viscosity, glass and melting temperatures, and mechanical properties. These are factors that could influence the parameters of the machine, the printability and the application of the material.
- Gravity and other factors: if no pressure is applied, it is still possible that the material will flow autonomously through the nozzle causing dimensional problems for the final part.
- Temperature build-up between the parts: as soon as the material is being extruded, it starts to cool down. This represents a problem for layer adhesion since, to achieve the best bonding between the sheets, the material needs to be within a certain range of temperature to avoid delamination (no bonding between layers) and the collapsing of the part (if the lower layer is not capable of sustaining the weight of the following one).

Due to the high variability of uses and the necessity to cope with different needs, firstly concerning the dimensions, a wide range of 3D printers machine using extrusion technology has been developed. In particular, the two main companies that are guiding the commercial sector, Stratasys and 3D Systems, released a lot of models serving different needs. Also, other companies have entered the market in recent years, primarily addressing the different opportunities rising in multiple sectors. According to previous research (Bertoli, 2020), a possible classification of the FDM machines concerns the different ways in which the paradigm of deposition is declined. In particular, four categories can be identified (3D Natives, 2021):

- Cartesian FDM 3D printers: this is the most diffused and utilized system for FDM. It is based on the Cartesian coordinate system and it uses three axes, X, Y, and Z to elaborate the correct position and path of the printing head. With this technology the platform moves on the Z axis while the head is moving on X and Y. On the other hand, especially with printers with bigger dimensions, it is the nozzle that is moving on all the axis, leaving the plate stable.

- Delta FDM printers: as for cartesian printers, Delta printers use a system of cartesian coordinates. This technology requires a plate combined with an extruder secured at three points. Each of these points moves up and down determining the position of the head. The system does not differ widely from the ones previously described, the main dissimilarity consists in the axis in which the print head can move, three instead of two of the Cartesian printers.
- Polar 3D FDM printers: in this technology the coordinates are determined by a polar system, involving angles and lengths. A circular plate rotates while the printing head is moving up and down.
- FDM 3D Printing with robotic arms: usually this process is used for assembling components inside the factories, but due to the high flexibility of the technology it is now implemented on lots of FDM systems. Mainly, this is due to the fact that the absence of a plate gives more printing freedom, allowing the development of more complex geometries.

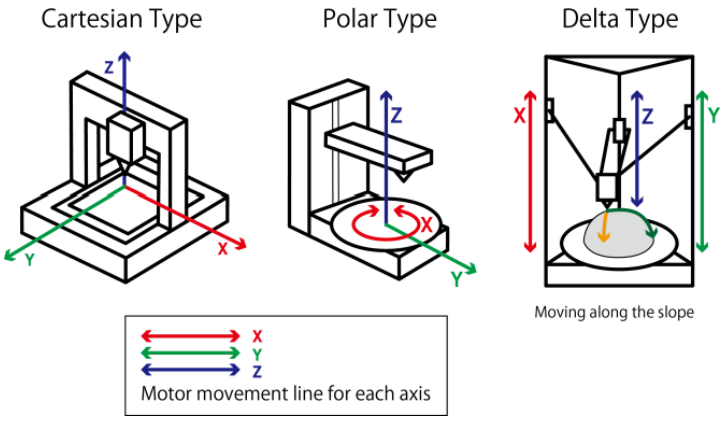

Figure 4 - A schematic representation of three different FDM 3D printing (Source: Wakimoto, 2018)

In Fig. 4-5 the above-mentioned systems are illustrated to provide clear examples. Each system come with its own pros and cons and the most widespread deposition technology, also created and adapted for apparatus of bigger dimensions, is the Cartesian Type.

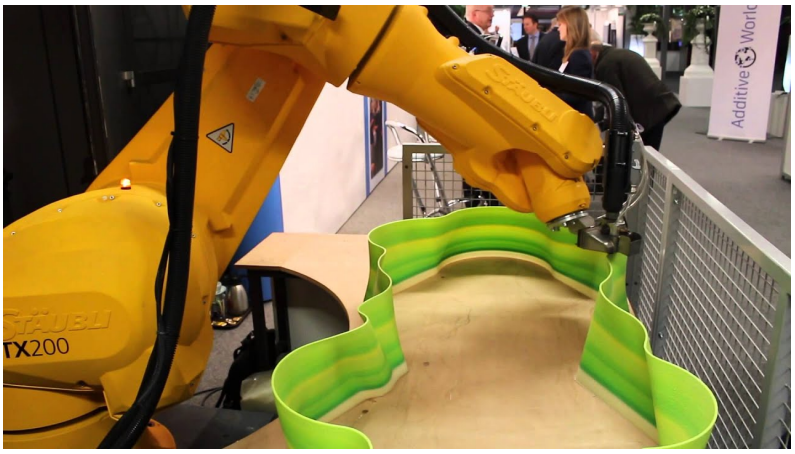

Figure 5 – FDM 3D printing with robotic arm (Source: www.all3dp.com)

After an introduction concerning the main characteristics of FDM and the typologies of machines developed to exploit this technology, a close examination on the materials used needs to be done.

The typical material managed by these technologies are thermoplastic polymers and composites like polycarbonate (PC), acrylonitrile butadiene styrene (ABS), and polylactic acid (PLA), also with insert of carbon fiber (CF) and glass fiber (GF) to enhance their mechanical and thermal properties (Andrzejewski et al., 2020; Billah et al., 2020).

As mentioned before, these materials could only be found in a filament form specific to the 3D printing process, resulting in high costs for the feedstock (up to $200/kg). Thanks to the introduction of the screw technology, materials available for the injection molding became available for 3D printing, resulting in a significant decrease in costs for raw material ($10/kg) and expansion in terms of possible fabrics to be used (Chad et al., 2017). At the same time, the expansion of 3D printing is highly related to the material and their processability: indeed, the future rate of adhesion concerning additive manufacturing is expected to grow in order to reach a global market of 28 B$ by 2023, but only if the research on technologies and feedstocks will proceed (EY, 2019) ensuring a higher range of applications and quality of printed parts.

Regarding the current applications of FDM technology, it is worthy to mention the ones concerning rapid prototyping and ready-to-use parts (Deepak et al., 2019). As mentioned before, the typical material processed by FDM are thermoset and thermoplastic polymers, sometimes reinforced with fillers to enhance their

properties. Due to the characteristics of these materials, the sectors of application vary, from the automotive and naval industries to aerospace, energy, and medical businesses (Gibson et al., 2015). Usually, FDM can be used in the following areas (Chartier et al., 2013; Post et al., 2017):

- Concept visualization, it can help visualizing concept models in the early stages of product development to shorten the time to market.
- Functional prototyping, it creates functional prototypes for testing purposes. In particular, these objects allow to test the product in real-world environment and take fundamental decisions to develop the product.
- Fabrication of end-use part, leveraging on the short time needed to fabricate one piece, FDM can be exploited to produce complex and customized objects without following the typical path of subtractive manufacturing, also avoiding assembly and intermediate processing.
- Fabrication of manufacturing tools, molds and tools for traditional manufacturing are expensive to be produced with conventional techniques. With the use of FDM and Wide & High Additive Manufacturing big tools can be realized more economically and using less time.

1.1.1 Wide and High Additive Manufacturing

One of the main problems regarding additive manufacturing is the printing time. As objects grow in dimensions, more and more time to print a part is necessary, impacting also on the economical point of view (Post et al., 2016). Indeed, it has been calculated (Colosimo et al., 2020) that the machine costs, which also include the amortization of the machine, are responsible for the 63% of the costs to produce a part. It is a direct consequence that if printing time increases there will be fewer pieces on which dividing the fixed cost of the machine, resulting in an increase of the price for the final product. To produce a part in an appropriate time to exploit the potential of additive manufacturing and to solve problems linked to the growth in dimensions of the pieces required, new systems have been developed. As build volumes increase, so does the demand for these products, resulting in a generation of new markets (Nieto et al., 2019) that wants to take the advantages of 3D printing: high customization degrees, relatively low processing time, the possibility of realization of complex geometries impossible with traditional systems, rapid prototyping (Nieto et al., 2019; Post et al., 2016; Brian et al., 2017). To face this

increasing demand for big products, the so-called Large-Format Additive Manufacturing (LFAM) systems have been developed. To be clear, a system is included in the category of LFAM if capable of printing objects with a volume higher than 1 m^3 (Nieto et al., 2019). The first machines of this kind started to be developed in 2014. The first company to develop its 3D printing satisfying this requisite has been the Cincinnati Incorporated (CI) that, thanks to an agreement with Oak Ridge National Laboratories (ORNL), launched its systems patented as Big Area Additive Manufacturing (BAAM) at the end of 2014. Consequently, the first papers concerning this argument have been published. In 2015 the first pieces obtained with this technology have been presented: indeed, ORNL presented a 3D printed Shelby Cobra at Detroit Auto Show, printed at full scale using carbon fiber enhanced polymers (Fig. 6) (Department of energy, 2019).

Figure 6 – 3D printed Shelby Cobra (Source: Department of energy, 2019)

Subsequently, in September 2016, Ingersoll Machine Tools and ORNL partnered together to develop a Wide and High Additive Manufacturing systems (WHAM) that culminated in the following years with the launch of the Ingersoll MasterPrint. Finally, in 2020, thanks to a collaboration of Ingersoll Machine Tools and Innse Berardi, both companies belonging to Camozzi Group S.p.A., the MasterPrint developed by Ingersoll has been installed in Milan, becoming the largest 3D printing machine in Europe. At the same time, other LFAM systems have been developed in

parallel all over the world. In particular, these companies have to be mentioned: BLB Industries, in Sweden, for the development of the Magnum Printer, CEAD, from The Netherlands, for the development of BEAD Printer, and Colido, in China, that have developed the Colido Mega Printer. In the picture below a map with the location of all the systems above-mentioned is presented, to give an idea of their geographical distribution (Fig. 7).

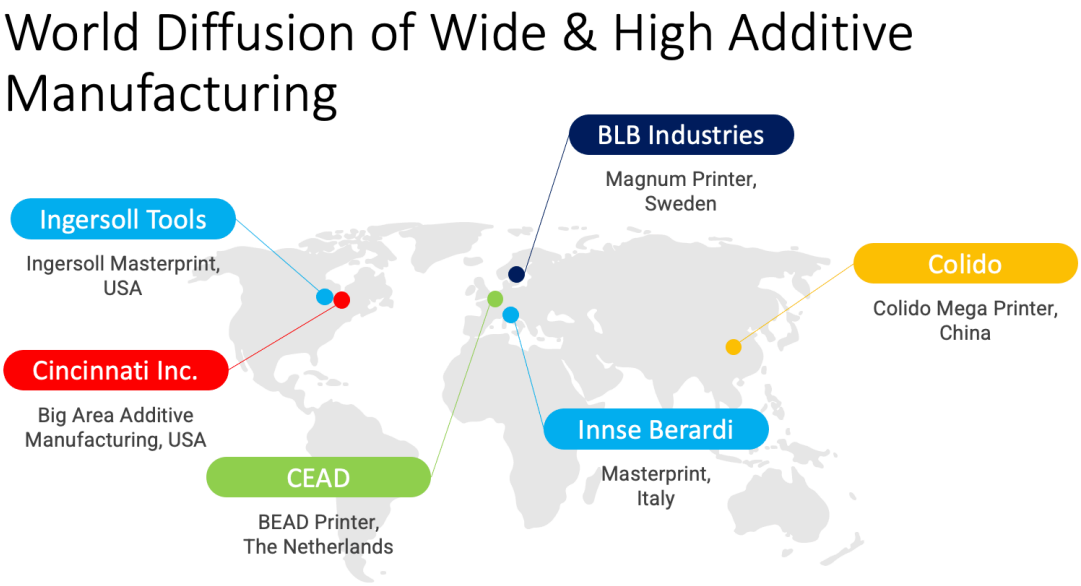

Figure 7 - World Diffusion of the main Wide and High Additive Manufacturing systems

The WHAM systems belong to the category of Fused Deposition Modelling, as the material is extruded through a nozzle and selectively deposited to create the part (Post et al., 2017; Nieto et al., 2019). These kinds of systems work similarly to their precursors of smaller dimensions, but with some significant differences. First of all, the operating dimensions. Indeed, these printers are capable of producing objects in a working environment whose volume exceeds 1 m^3 (Nieto et al., 2019) overcoming the limits of the previous technology. The scale of the printers and the capability to print big objects introduce the problem of printing velocity, which must be high enough to guarantee the realization of a piece in a reasonable time. To solve this issue, engineers and designers have decided to adopt the technology of injection molding (IM) and adapt it to be used in an Additive Manufacturing system (Holshouser et al.,

2013; Post et al., 2016). To guarantee printing velocity, accuracy, and a good flow through the nozzle, it has been decided to abandon the filament as feedstock material and to concentrate on plastic pellets, typical of IM technologies and capable to guarantee quicker production times (Nieto et al., 2019). To process these pellets optimally, a screw system has been adopted. To be more precise, the raw material is stocked in unit loads in a pellet form, away from sunlight, at room temperature, and as far away as possible from moisture. Then, before being processed by the machine, the pellets are inserted for four hours at 80°C in driers (specific temperature may change according to different materials, for the purpose of describing the process ABS reinforced with 20% of Carbon Fiber has been taken as reference) to be desiccated from moisture and guarantee the optimal mechanical properties (Ajinjeru et al., 2018). When dried, the material is drawn into the printing head and melted by the extruder. A schematic representation of the system used to melt the pellets is presented below (Fig. 8).

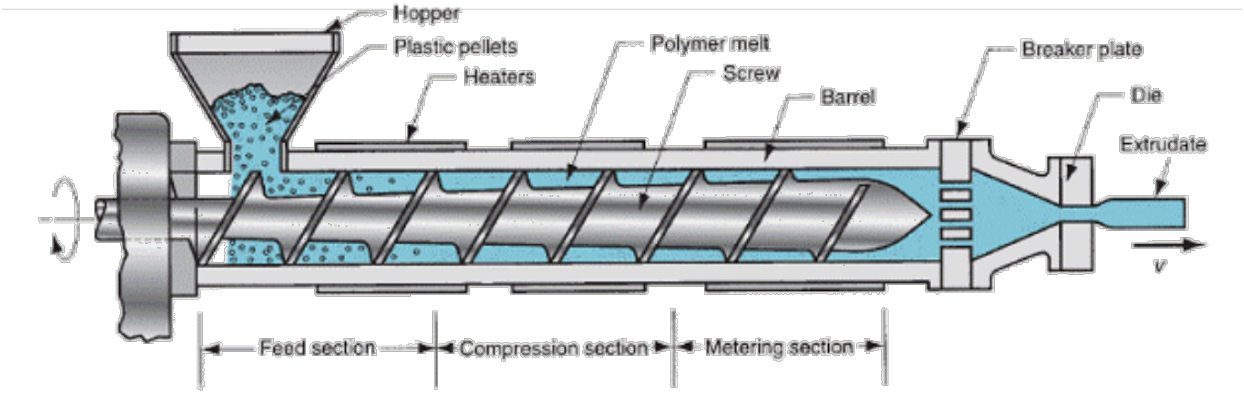

Figure 8 - Representation of a screw extruder for WHAM systems (Courtesy of Ingersoll Machine Tools)

As it can be noticed from the picture, the plastic pellets are sucked into the extruder to be melted at a specific temperature that varies according to the feedstock. The material is melted thanks to the friction and the resistors that are positioned around the screw, indicated in the picture as “heaters”. The rpm of the screw establishes the quantity of material that is extruded by the nozzle. The molten material is then forced out from the die to be selectively deposited where needed. The three zones of

the system, feed section, compression section, and metering section (Fig. 8) plus the zone of the extruder, are set at different increasing temperatures to make the material reach the optimal conditions for the deposition. It is important to assess the correct temperature for each material that needs to be extruded, since incorrect parameters could result in problems for the printed part (Ajinjeru et al., 2018). The extrusion head is then guided in the production process by computerized numeric control (CNC) system that follows a predetermined path established by the controller of the machine. Usually, LFAM machines are capable to move along the three axes (X-Y-Z), when printing, to ensure the correct realization of the product. Since the LFAM systems can vary a lot in dimensions starting from printing volume of 1 m^3, the traditional control systems implemented for FDM technologies, like heated chambers, are not feasible for these kinds of systems. To guarantee the accuracy of the final part and to limit the shrinkage of the product, LFAM leverages on new materials recently developed. In particular, it has been proved by recent studies (Nieto et al., 2019; Tekinalp et al., 2014; Ajinjeru et al., 2018; Post et al., 2017) that carbon fiber reinforced polymers (CFRP) not only have better mechanical properties in terms of stiffness and strength if compared to the neat polymers, but also have lower coefficient of thermal expansion (CTE) by an order of magnitude, making unnecessary to heat the printing chamber to prevent deformation, achieving savings in energy consumption. Moreover, typical material used for FDM, such as filaments, can reach prices around 200 $/kg (Hu et al., 2020), while, since the material used for LFAM are common also for IM, which is widely spread and established as process, the prices are significantly lower, around 18$/kg. Therefore, as previously anticipated, the different materials used by LFAM systems ranged from techno-polymers, such as Polyetherimide (PEI) and Polyether ether ketone (PEEK), Glass Fiber reinforced polymers (GFRP), to CFRP with the percentage of fillers that can vary for the specific application. Going more in depth with this topic, the range of applications for LFAM are various and yet to be studied and exploited. In academic papers (Nieto et al., 2019; Tekinalp et al., 2014; Post et al., 2017) these practical uses are indicated for the technology:

- Rapid prototyping, for the development of products in naval sectors, in particular for models to be used in hydrodynamic tests.
- Molds to be inserted in autoclave, for aerospace, energetic, naval industries and for monitoring and maintenance applications (3D printed molds have

been used for the realization of the robots responsible for the maintenance of the new Ponte San Giorgio in Genova).

- Finished products, for automotive, aerospace, naval, and design sectors.

In the pictures below (Fig. 9-10) it is possible to see some of the before-mentioned applications concerning the LFAM systems. In figure 9a, an additively manufactured blade mold and a produced blade section can be seen. In figure 9b, a partially completed low-pressure blade mold, printed and assembled in different parts can be observed. In figure 10 some printed parts for the naval industry are presented, the first one used as a mold and the second one used to perform hydrodynamic tests for product development.

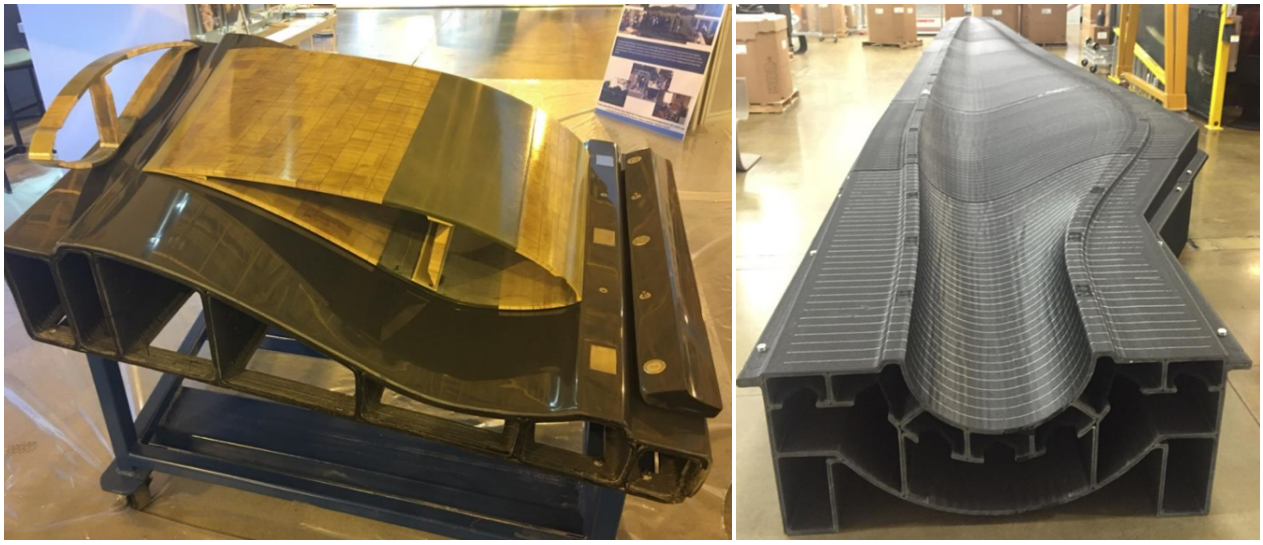

Figure 9a & 9b - On the left, an additively manufactured blade mold and a produced blade section, on the right, a partially completed low pressure blade mold, printed and assembled in different parts (Source: Post et al., 2017)

Figure 10a & 10b – Additively manufactured mold for naval sector (left) and prototype for hydrodynamic tests (right) – courtesy of Camozzi Group

Current research are now focused to enrich the possible sectors of application of Large-format Additive Manufacturing, decreasing costs, developing new materials, and making the process more reliable. In particular, the development of in-situ monitoring for LFAM is core for ensuring the quality of the pieces produced and making the print completely autonomous. Indeed, one of the main difficulties encountered by these systems concerns the replicability of the quality since it depends on numerous factors such as geometry of the piece, extrusion temperature, glass transition temperature (Tg) and degradation onset temperature (DOT) of the printed material, building orientation, and further parameters (Hu et al., 2020; Billah et al., 2020).

1.2 Sustainability of Additive Manufacturing

Additive Manufacturing has established itself as one of the main pillars regarding the new concept of industry denominated as "Industry 4.0". In a world that is always more connected and attentive to environmental issues, Additive Manufacturing is redesigning the concept of sustainable production (Godina et al., 2020; Suarez et al., 2019). The adoption of Additive Manufacturing facilitates and shortens value chains, offering significant benefits in terms of CO_2 reduction. Among the potential benefits that Additive Manufacturing can offer, according to Ford (Ford et al., 2016), three of them emerge:

- Improvement of resource efficiency,
- Extended product life,
- Reconfigured value chains.

Firstly, the enhancement of resource efficiency is mainly characterized by different concepts of manufacturing if compared to the traditional subtractive manufacturing methods. Indeed, the fact that the production is based on building objects from scratch rather than obtaining them from removing material through drilling and milling perfectly represents this shift in mentality. As far as the design is concerned, Additive Manufacturing enables the development of more complex and optimized components thanks to greater freedom in terms of shape and geometry, allowing different structures not obtainable with traditional manufacturing. Optimized geometries lead also to other kinds of savings that are realized along the entire life of the 3D printed object.

The presentation of examples coming from the aerospace sector is particularly effective to understand the potentialities of 3D printing. For instance, aerospace components need high performances and a relatively low scale of production. The manufacturing of these components typically requires a buy-to-fly material ratio of 4:1 (of input material to the weight of the final component) that can reach the ratio of 20:1 in the case of the most complex geometries (Gebler et al., 2014). The use of Additive Manufacturing can lead to significant savings in terms of costs of material, and the redesign of the object by using Design for Additive Manufacturing can achieve lower weights and higher resistance. In the aerospace world where every gram counts when flying, the capability of saving weight can realize reductions in terms of fuel used, limiting the CO_2 emissions during the entire lifecycle of the object (Gebler et al., 2014). At the same time, the capability to develop engineered structures extends the service life of the component.

Similarly to product redesign, Additive Manufacturing can enhance also process redesign. This is the case of molds' development. In fact, AM can realize structures with internal channels carefully designed to improve the cooling of the parts. Molds are very expensive and are realized through complex production processes limited by traditional manufacturing. The possibility of realizing optimized structures aimed at cooling down in a more efficient way can enhance the quality of the production and favor the reaching of higher production volumes.

At the same time, the possibility of producing parts from scratch limits the time to market of a product. Usually, products are produced in advance (using the so-called Make-to-stock policy) resulting in the overuse of raw materials. Moreover, producing pieces not already sold will lead to an increase in inventory costs, reducing profits and increasing the need for space inside the company. Talking about inventories and inventory costs, it is dutiful to consider a wider perspective than the one limited inside the company, expanding the reasoning to the entire supply chain.

Recent studies (Ford et al., 2016; Garcia et al., 2018) have assessed a change in the supply chain for companies that adopt AM. A traditional supply chain is characterized by a wide pool of actors that are responsible for the realization of the product, starting from the production of the raw materials to the final delivery to the customers. A traditional supply chain can be roughly schematized as in the picture below (Fig. 11), where suppliers send raw material to the production plant where the manufacturing activities are performed. Then, the products move from the plant to the warehouses of the company and go through several intermediaries before arriving to the final customers. Another possible path followed by the products involves the presence of intermediate assemblies or reworks that increase even more the total number of layers and movement to reach the final customer.

Along with creating opportunities for new business models, Additive Manufacturing is also changing the distribution of manufacturing activities. Due to the fact that no particular tools are needed to produce an object, it is easily understandable that only raw materials, a 3D printer, and the CAD file of an item are needed to produce it. In such a view, more localized manufacturing could radically change supply and distribution network.

Logistics may be more about delivering digital files and raw materials rather than containers and ships. This shift in perspective considering the deliveries of digital files and basic materials will have substantial positive effects in reducing environmental emissions of transportation. Product and process redesign is going to amplify these effects. For instance, simplifying complex and multi-component products into less or single-component products will simplify the entire value chain (Ford et al., 2016).

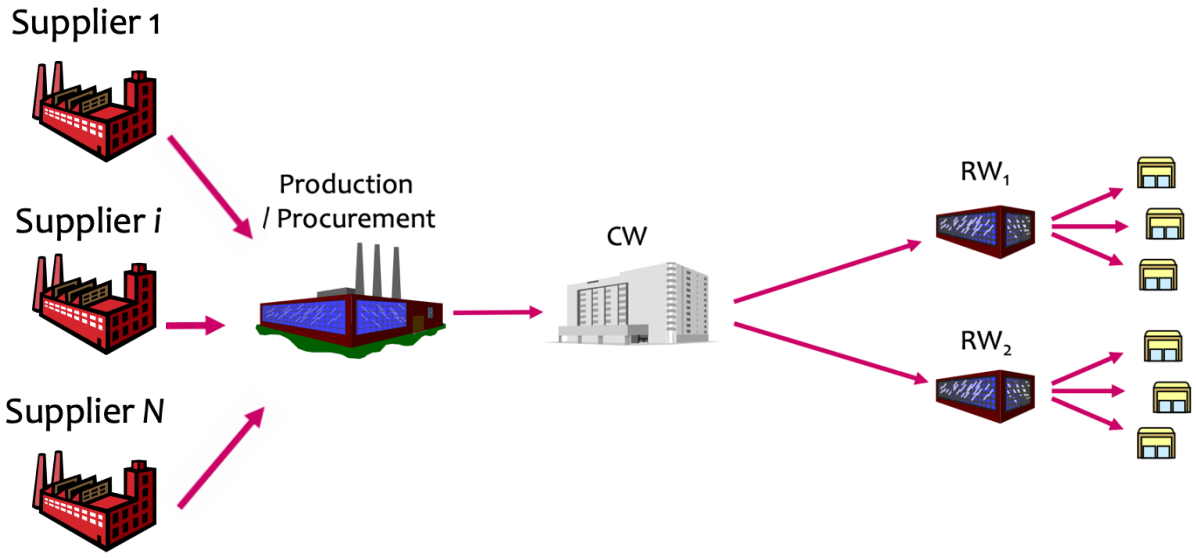

Figure 11 - Schematical representation of a traditional supply chain (Perego et al., 2020)

Moreover, considering the disruptive events caused by the outbreak of the pandemic where shortages of products have been registered all over the world, Additive Manufacturing had the potentiality of improving resilience for the supply chains, limiting the number of trades and encouraging a direct dialogue between the manufacturer and the final users.

The use of AM as a production process can also enhance the flexibility of the supply chain (Alogla et al., 2021) in manufacturing a higher range of products with high customization and low production volume. Thanks to the programmability of the printing and the possibility of producing complex geometries, even if considering the high times required, Additive Manufacturing is competitive in responding to the demand of single-batch pieces and to encounter quick changes on the market.

Indeed, AM is offering new possibilities to produce in a more sustainable way, limiting wastes in terms of production and movement of the goods (Ford et al., 2016).

To conclude the paragraph dedicated to the sustainability, important mentions need to be done regarding the attempts linked with the possibility of "closing the loop", so achieving sustainable production by reusing and recycling the materials. As far as the recycling of the materials is concerned, closing the loop is an important step to achieve a 100% sustainable production, especially today where global warming is in

the spotlight (Ford et al., 2016; Gebler et al., 2014). Due to the high number of materials processable by 3D printing, for the purpose of this thesis, only composites are considered and a brief discussion on recyclability of metal powders is provided. Regarding the latter, the highest recovery of value is achieved locally during the production process when the unused material is reclaimed. To be more precise, it has been estimated (Petrovic et al., 2011) that up to 98% of the material can be recycled. At the same time, the diversity of the material entering the recycling process and the complexity of processes that are required to recover the material leave space for further development. Recycling metals is an activity that has been performed for a long time and they can be recycled, potentially, an infinite amount of time. The situation for composites material is different.

As composites are a mix of a polymer matrix and fibers, the ideas of reusing them in a productive context consist in mainly two options:

- Incineration.
- Recycling.

To be more precise, a third option of landfilling wastes exists and is discussed in the literature (Witik et al., 2013). For the purpose of this work, the option of landfilling wastes waiting for their decomposition is not taken into consideration as cannot be considered a sustainable way to value wastes.

As far as incineration is concerned, this option can be pursued to recover energy by burning the material and using its calorific value to produce electricity. Indeed, incineration is a thermal waste treatment process that converts waste material into ash and heat enabling the release of embodied energy. Modern incinerators burn material into a furnace operating between the temperatures of 800-1000 °C. At the end of the process some ashes remain as waste and need to be landfilled in any case. Processed gases are used to heat a steam boiler and drive a turbine to produce electricity. In some way, this is considered an option to usefully end the life of an object; nonetheless, it cannot be considered as an environmentally friendly way. Considering CO_2 emissions, it is obvious that it is not sustainable for the future, especially with all the objectives set by the institution in terms of reaching the target of “zero emissions”. Moreover, this proceed is not “closing the loop”. Indeed, without reusing and recycling the materials, the objective of a neutrality for carbon emissions will not be achieved. For these reasons, the most promising method to use scrap materials is to recycle them.

Recycling is fundamental in closing the loop and achieving sustainability regarding production. Lots of articles have been written regarding the recycling of polymers and composites, and all of them agree about the fact that three methods of recycling are mostly used:

- Mechanical recycling,
- Thermal recycling,
- Chemical recycling.

These methods differ a lot between themselves but allow to achieve similar results.

1.2.1 Sustainability through material recycling

Mechanical Recycling

The first recycling method that is going to be described is mechanical recycling. Prior to the reprocessing of the materials into new products, the conversion from wastes to new raw materials needs to be achieved (Ragaert et al., 2017). First of all, recycling begins with the collection of the scraps or the wastes that will be reprocessed. Then, the materials need to be baled for transport purposes, because often composites wastes are not processed where collected. A third phase concerns the removal of contaminants, often organics, that could compromise the recycling of the material by altering its composition. Subsequently, the most important phase is called grinding, where the composite material is reduced in dimensions using a shredder similar to the one represented below (Fig. 12). If the pieces introduced in the grinder are too big to be processed, another preliminary phase of size reduction needs to be performed. In particular, for composites reinforced with carbon fiber, this stage is strongly recommended to facilitate the overall process of recycling since the strong mechanical properties of the material could damage the blades and reduce the useful life of the machine.

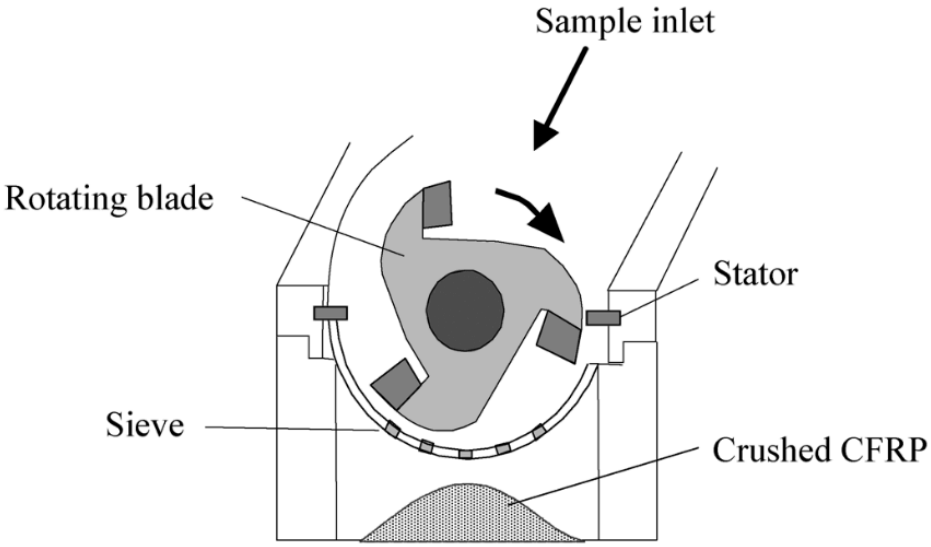

Figure 12 - Scheme of a shredder used to mechanically recycle composites (Source: Ogi et al., 2006)

As it is noticeable from the picture, the materials recovered are introduced in the machine from the top. Subsequently, the shredder reduces the dimensions of the object to the desired ones, regulated by a parameter that can be adjusted directed on the machine. A sieve is placed below the blades to collect the materials with the correct dimensions. This process can be repeated multiple times to have granulates of similar dimensions and to achieve a sort of homogeneity in the minced. The material, treated in this way can be directly reprocessed to produce new objects. However, another optional step of compounding can be performed to reinforce the recycled material with other inserts. The result of the process is a granulate that can be remelted and reused to close the loop in giving a new life to wastes.

This kind of process is well established to recover plastics and composites materials, and it is the most used method to recycle plastics in the world. It is the most energy efficient between the three with an average energy consumption of 2 MJ/kg of recycled material (Howarth et al., 2014), and allows to recover, talking about composites, both the fiber and the matrix in an easy and sustainable way. On the other hand, the efficiency of the process is the lowest among the three methods, despite its 90% ratio between material recycled and material inserted in the machine. Moreover, the mechanical properties of the granulate are expected to be 15/20% less

than the ones of the original material, and the variance of the value of precedent studies suggests a discrete variability of the process (Morsidi et al., 2019).

Thermal recycling

Different from mechanical recycling, thermal methods allow only the recovery of the fibers, while the matrix is distilled to obtain oil and gas to be used as fuel. In this method, the fibers are released from the polymeric matrices through thermal methods. The two main processes used to reclaim the fibers are the pyrolysis and fluidized bed methods (Pakdel et a., 2021).

Among the different methods, pyrolysis has progressed a lot to industrial levels on recent years. Generically, pyrolysis refers to the breaking down of the polymeric matrix in an inert atmosphere at a controlled temperature, usually higher than 400°C and up to 700°C, and at 1 atm of pressure (Pakdel et a., 2021). In this process, the matrix is decomposed into a mix of gas and oils, these are collected using their different molecular weights and used as fuels. The residual products of the process, usually ashes, are collected and landfilled or incinerated. Pyrolysis is a viable method to recover carbon fiber on a large scale and it is estimated that the process consumes an average of 30 MJ/kg of material recycled. At the same time, it has been reported that the new composites made of recycled carbon fiber show a decrease in mechanical properties of -10/15% (Morsidi et al., 2019) with a relatively low variability. Modifying some parameters of the process, such as the percentage of oxygen in the atmosphere and the temperature, can lead to a quicker process but to a more defined loss of mechanical properties (up to 65%).

Different from pyrolysis, fluidized bed is a process in which the polymeric matrix can be separated from the fiber by using a hot stream of air in the presence of a silica sand (Pakdel et a., 2021). Typically, composites wastes are shredded into pieces of variable dimensions (between 6 and 20 mm) before entering the process. The silica sand is used to volatilize the scrap material, decompose the resin and release the fiber. The operating temperature of this process is around 500-550°C. Once the resin is decomposed, the fibers are removed from the gas stream by a cyclone and then collected (Meng et al., 2017). In the picture below is graphically represented the scheme of the fluidized bed process (Fig. 13).

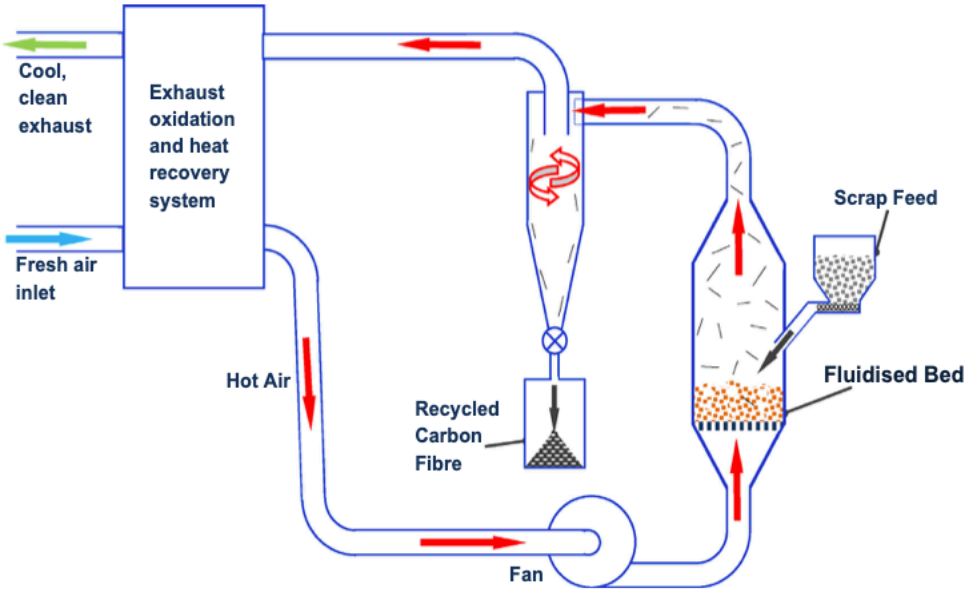

Figure 13 - Fluidized bed process for recovering carbon fibers (Meng et al., 2017)

Because of the high temperature involved in the process, this thermal methods for obtaining recycled carbon fibers are the highest energy-consuming process.
Nevertheless, using fluidized bed processes, the energy required to recover a kilogram of carbon fiber, on average, is equal to 6 MJ, against the 30 MJ required with pyrolysis. At the same time, the mechanical properties register a decrease of 15% on average, as recent studies sustain (Meng et al., 2017).
In terms of efficiency, both the pyrolysis and the fluidized bed technique register a 95-98% on average for carbon fibers recovered, achieving higher percentages if compared to the mechanical recycling.

Chemical recycling

The last category of recycling analyzed for the recovery of the fibers is chemical recycling. As already mentioned, this method is capable only to recover the fiber of the composites, degrading the polymeric matrix. The process of chemically recovering the fiber is called solvolysis. This proceeding breaks down the polymeric matrix into monomers using different types of solvents (Meng et al., 2017): the material is left immersed in the solvents according to the degree of fiber cleaning as well as mechanical properties required. Indeed, the more the material is left in the

critical fluid the more accurate will be the cleaning of the fibers. On the other hand, leaving the material too much time inside the solution will lead to a significant decrease in mechanical properties. On average, solvolysis is able to recover the fiber with a loss in mechanical properties between 5-10% (Meng et al., 2017). Moreover, the efficiency in recovering the fiber is 95% and recent studies assess the energy requirement of the process to 19 MJ per kilogram of carbon fiber since the operating temperature of the process can reach at its peak 400°C and pressures higher than 4 MPa. The main advantages of using this method concerned the obtaining of clean fibers without significant degradation in mechanical properties, the conservation of the length of the fiber, the rapid and selective depolymerization. On the other hand, this recycling process is the most expensive if compared to the one analyzed before, and it is not environmentally sustainable. In fact, the use of solvents makes this process the most dangerous in terms of toxicity, making treatment necessary to disperse waste liquids into the environment.

1.2.2 Sustainability through zero-defects production

A second approach used to enhance sustainability for AM consists in scrap reduction. The idea at the basis of this concept concerns the avoidance of reprocessing and catastrophic failures that could result in the waste of large amount of material. As stated before, the main cause of prevention for the wide adoption of Additive Manufacturing is the fact that 3D printing is not a repetitive and standardized process. The possible ways that have been developed to reduce the quality defects that could arise during the printing of the artifacts include two diametrically opposed strategies:

- Optimization of printing parameters,
- In-situ monitoring.

These two approaches differ in the type of control that is adopted to prevent the onset of defects. In fact, it can be noted that the optimization of printing parameters concerns actions that are perceived a priori in order to optimize the entire printing process. However, once the additive manufacturing process is launched, the main parameters cannot be changed anymore, except for very small values. Due to the non-repeatability of the process, this is an action that need to be performed every time the geometry of the artifacts is changed. This is reflected in tailored time-

consuming pre-production studies that need to be performed before the printing of the object.

On the other hand, the other technique mentioned above concerns in-situ monitoring, which takes place during the printing process. In-situ printing process monitoring is indispensable for detecting quality defects (Fu et al., 2020) and provide early signals if something abnormal is recorded in the machine control parameters. Nowadays, this approach is the costliest in terms of time and preparation but permits a generalization of the quality and provides more consistent results in the long term.

Indeed, the implementation of in-situ monitoring techniques allow the detection of printing problems in real-time and the undertaking of a series of corrective actions to resolve the issues. The final objective is to safeguard the piece in order to reduce waste and continue with the production process. The importance of the direct intervention during the process of Additive Manufacturing can be summarized referring to real cases that occurred during the experience in the company. Indeed, if issues arise early in the process, the restart of the process using new material is not particularly costly. On the other hand, it has happened that some defects have emerged in the final layers of the printing. In this case, the emergence of defects has meant that the entire production of 12 hours for a piece weighing 350 kilograms was cataloged as a waste of production, having to restart from scratch the entire printing process. In particular, since the majority of the products are realized with plastic, the result has been an overproduction of plastic wastes. The possibility of implementing the above-mentioned best practices could have increased the probability of detecting the error as soon as they occurred, saving the process from failure.

To correctly design a monitoring system, firstly, a clear understanding of the possible defects that may arise during the process needs to be pursued. In particular, the entire paragraph 1.3 it is dedicated to fully assess this topic, firstly regarding extrusion-based systems and then focusing on Wide and High Additive Manufacturing systems.

Moreover, to be consistent in the reasoning, in the paragraph 1.4 it is presented an overview of the current in situ-monitoring systems: form the ones that uses the integration of images and machine learning algorithms to sensors and devices used to monitor physical quantities, like the acoustic emissions. To be more precise, the monitoring systems that will be analyzed are presented below:

- 2D vision

- Temperature monitoring
- Vibration monitoring
- 3D vision
- Acoustic emission monitoring
- Force and pressure monitoring
- Electrical quantities monitoring
- Other sensors technology
- Sensors fusion technology.

1.3 Extrusion Based printing part defects

Since the WHAM is part of the extrusion-based printing processes, in order to analyze its problems, it can be useful to provide an overview of the issues that may affect FDM (Fused Deposition Modeling) and FFF (Fused Filament Fabrication) 3D printing processes. In particular, four subcategories of part defects can be identified (Bertoli, 2020):

- Geometrical and Dimensional Defects,
- Cracking and Delamination,
- Porosity,
- Surface Defects.

Geometrical and Dimensional Defects

Geometrical defects refer to divergences in part geometry and shape if compared to the theoretical and nominal ones designed by CAD. On the other hand, dimensional defects influence the dimensional accuracy of the part, accounting for misalignment in the design-required tolerances. These types of defects compromise the operability of the printed part, not meeting the requirements for which the product has been designed and developed. Shrinkage is indicated as an expression of geometrical defects. It is primarily caused by thermal-induced residual stresses and strain inside the parts when it is cooling down. It occurs below the glass transition temperature and ends when the part reaches room temperature (Bertoli 2020; Hu et al., 2020; Yaman 2018). An additional common defect affecting geometrical accuracies and belonging to the family of shrinkage is warping (Fig. 14), also caused by the contraction of the material due to thermal residual stresses (Hu et al., 2020). The combination of shrinkage and warping leads to curling, resulting in curved profiles.

Geometrical and dimensional inaccuracies can be also caused by over-extrusion and under-extrusion of the material, due to incorrect setups or excessive inertia of the material that can cause not desired material leakage (Fig. 15) resulting in material over-deposition over a printed part (Li et al., 2019). These kinds of problems can cause several difficulties for the application of the printed part and, in extreme cases, can lead to a complete reprint of the object, losing time, money, and materials. To provide a comparison of the above-mentioned defects with respect to a normal situation, a typical layer profile with no inaccuracies is also presented (Fig. 16).

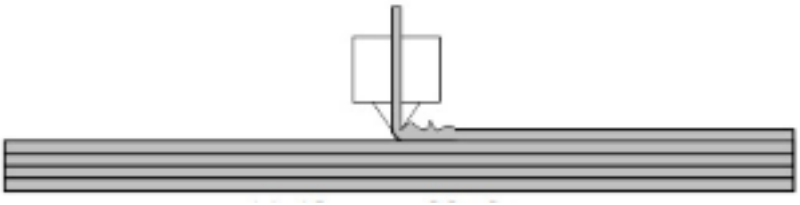

Figure 14 - Incorrect deposition causing inaccuracies (Source: Li et al., 2019)

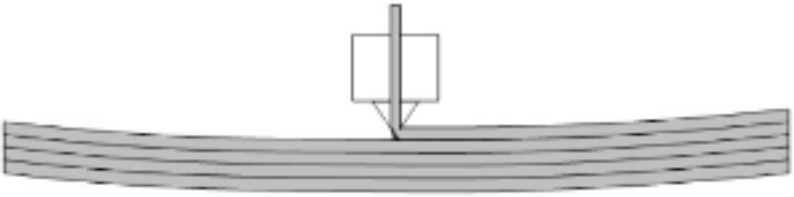

Figure 15 – Example of warping, a curve profile can be noted (Source: Li et al., 2019)

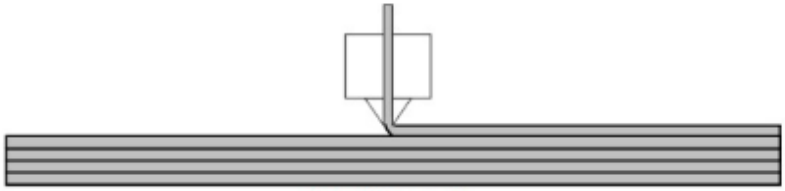

Figure 16 - Layer profile with no inaccuracies (Source: Li et al., 2019)

Cracking and delamination

The second category of part defects is identified by cracking and delamination due to phenomena related to the detachment of the layers. Cracking is the process that forms cracks on the surface of a material due to thermal gradients and fatigue. It brings to progressive and localized structural damage. It also causes deterioration of the thermomechanical properties when it happens on polymers composites and acts

as a catalyst for further issues that may emerge (Bertoli, 2020). Similarly, delamination is seen as a particular and heavy case of cracking when entire layers are detached between each other in a solid part. It is caused when residual stress overcomes the bonding force that keeps the layer together. It also causes massive loss in thermomechanical properties undermining the final application of the object (Roschli et al., 2018; Hu et al., 2020). The only way to cope with severe delamination in 3D printing is to stop the printing and restart the process of manufacturing another object, avoiding the appearance of the phenomena. In figure 17 it is shown an example of a delaminated printed part.

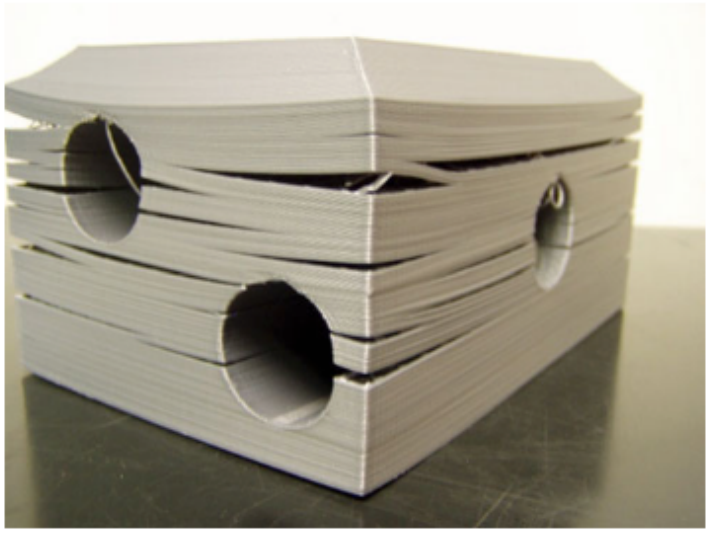

Figure 17 – Examples of cracking and delamination in a printed part (Source: Sbriglia et al., 2016)

Porosity

The third family of part defects concerns porosity problems. Porosity can be defined as the fraction of volume of voids over the total volume of the part. This phenomenon is described as void formation within the material and on external surfaces. In particular, intra-layer porosity refers to empty spaces inside the layer itself, while inter-layer porosity is described as empty spaces between successive layers. The former is mainly present due to non-uniformity in the filament or because of under-extrusion mainly caused by the variable flow of material (Fu Y. et al., 2021),

the latter is caused by the extruder itself. Indeed, even if the nozzle is circular, the pressure applied when the bead is deposited makes the bead to flatten, becoming elliptical, and creates voids triangular-shaped (Fig. 18). Moreover, an increase in void fraction negatively affects the mechanical properties of the final part, resulting in weaker pieces (Tekinalp et al., 2014). Other examples of porosity are caused by air bubbles, arising when the material reaches the nozzle at high temperatures in a liquid state. When the material passes through the nozzle, it produces friction with the sidewalls generating turbulence that facilitates the air aspiration. So that, when the material is finally deposited, air bubbles provoke under-deposition with voids of material in the final part.

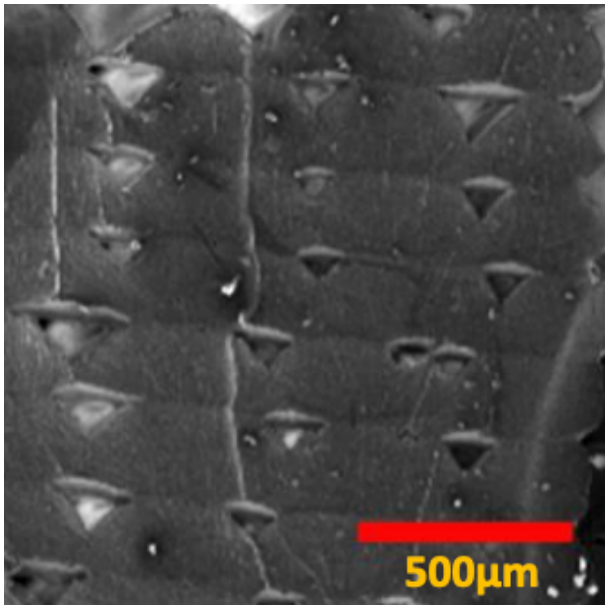

Figure 18 - Triangular shaped porosity (Tekinalp et al., 2014)

Surface defects

The last category of defects concerns surface's defects. These irregularities can alter the quality of the final part mining the conformity for surface roughness requirements. The most well-known defect that is included in the category is the so-called staircase effect (Fig. 19), the trademark of 3D printing due to the peculiarity of the technology. In fact, it is caused by the slicing of the CAD model for the generation of the layer in which the final object will be constituted. Similarly, chordal errors refer to the conversion of curved surfaces in a CAD model into an STL file,

resulting in curved surfaces becoming visible as a series of segments in the final fabricated part. Another example of surface defect can be caused by over-deposition of the material, indeed when more material than required is deposited during 3D printing it can result in deviations concerning the desired geometry as well as surface inaccuracies. Finally, one last example of surface defect regards those surfaces that have been in contact with supports: often, supports are needed to sustain layers that otherwise will fall out but, as they are printed and are physically attached to the part, they need to be removed. The elimination process of those supports can cause irregularities and deviations. Some surface defects, like the staircase effect, are typical of the 3D printing technologies and efforts can be made to reduce the arise of the problems but is nearly impossible to completely avoid them.

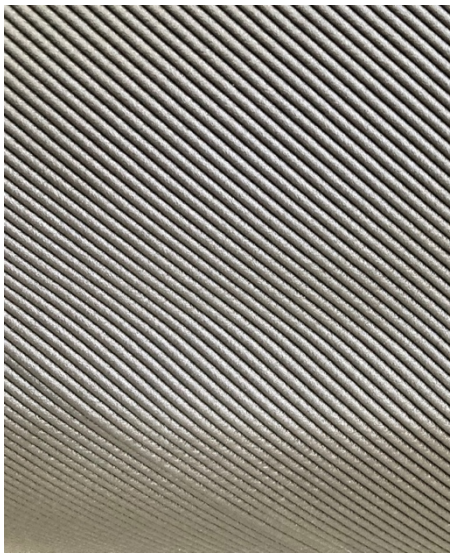

Figure 19 - Picture highlighting the layers and the staircase effect

1.3.1 WHAM defects

Since LFAM and WHAM technologies are relatively new and differ in their key fundamentals from FDM (e.g., in the dimensions of the operating area), different unstudied problems may arise during the printing of the parts. At the same time, they are part of the extrusion-based system, so the defects pointed out in the previous section may arise on a larger scale. To briefly discuss the possible problems of Wide and High Additive Manufacturing an on-field work has been performed. In particular, some weeks of work have been spent at Innse Berardi S.p.A. directly

following the printing of the objects. The materials used by the Ingersoll MasterPrint have been ABS 20% glass fiber reinforced, ABS 20% carbon fiber reinforced, and the techno-polymer "PEI". Next to the problems that occurred during the printing of the artifacts, a confrontation with the operators and the managers that have acquired experience on working with the machine has been useful for the analysis. In particular, the presence of a highly experienced manager of Ingersoll, the company of the group that has designed and manufactured the 3D printer, has helped in collecting and cataloging the printing defects. The two macro-categories identified for a first division of the problems concern the process-related and the part related problems. The difference between these two categories can be identified in the two objects observed: the machine itself and the artifact printed. Indeed, the former category concerns inaccuracies of the proceeding due to failure of the machine, while the latter is more focused on defects that could emerge in the printed object. Regarding the process-related problems, five sub-categories have been identified to better classify the issues:

- Temperature problems
- Deposition problems
- Platform related problems
- Screw related problems and
- Other problems.

Temperature Problems

Temperature problems are issues that can arise due to the incorrect settings of the machine. In particular, there is an extrusion temperature that varies with the material used: for example, PEI's extrusion temperature is above 350°C while for ABS reinforced polymer the extrusion temperature is around 256°C. Theoretically, the material can be extruded just above the glass transition temperature to avoid the insurgence of delamination/deformation problems, but the printing time of a layer causes the object to cool down due to the difference in heat between the object and the environmental temperature, so when the next layer is deposited, if the previous one is not sufficiently warm, can result to adhesion problems. Similarly, a higher extrusion temperature lead to higher costs in terms of energy but ensure the remaining above the Tg (glass transition temperature) for the whole layer printing, enhancing also the flowability of the materials and achieving a higher deposition rate. At the same time, a high extrusion temperature and not correlated layer time

can lead to deformation problems because the lower layers may not be able to sustain the ones deposited later. As easily understandable, the wrong extrusion temperature can lead to geometrical problems for the final object, compromising the printing and leading to errors that cannot be resolved except by restarting the process. In particular, a higher temperature can be managed better if compared to a lower temperature because it can be sufficient slowing down the printing and leave the material to cool down for more time before printing above. Differently, if the temperature falls below the Tg, the piece will be affected by cracking and delamination because, at the moment, there are no devices or instruments that can reheat the printed layers above the Tg to enhance the adhesion.

Deposition Problems

In addition to thermal problems, deposition problems may also arise. This category of problems is influencing the final geometry of the piece and can cause defects and deformations in the final object. The most intuitive problems that can arise regards the incorrect quantity deposition of the material, resulting in over-deposition or under-deposition. These problems are caused by the wrong settings of the machine or by incorrect operations of the feeding systems responsible to bring the pellets inside the screw extruder. Even in this case, there are differences between the final consequences of the issues and the treatment that can be followed to solve them. The over-deposition is not so fatal as the under deposition: the former problems can be caused by simply milling the excess of the material, while the latter, because of the absence of the material where needed, can preclude the piece its structural stability. This can be dangerous considering that some pieces have to work under high pressures and loads. Similarly, other deposition problems are related to the casting of the material and the possible failure to support printing layers. The first issue can arise when the extruder ends the printing of a layer and moves to the starting point of the following. In this case, the extruder should stop the deposition of the material and restart it when correctly posed upon the starting point. Nevertheless, the inertia of the screw and the material already melted inside can lead to continue the extrusion when not requested, depositing material incorrectly. This issue can cause severe geometrical problems compromising the printing of the following layers. On the other hand, the failure in supporting the printing of a layer is related to the incorrect spatial deposition due to the geometry of the piece. In fact, it can happen

that a layer cannot be printed perfectly above the previous one due to a particular feature of the object. If at the same time the development of supports is not possible, the material can pour laterally as it is literally deposited “on air”.

Platform Related Problems

The third category of problems is related to the platform where the pieces are printed. As a matter of fact, to successfully print an object without compromising the first layer, the artifact must be printed above a surface that enhances the adhesion to sustain the first layer but, at the same time, the item must be detached when the printing is over. The surface used by Innse Berardi is an ABS’ panel positioned in the printing area. (Fig. 20).

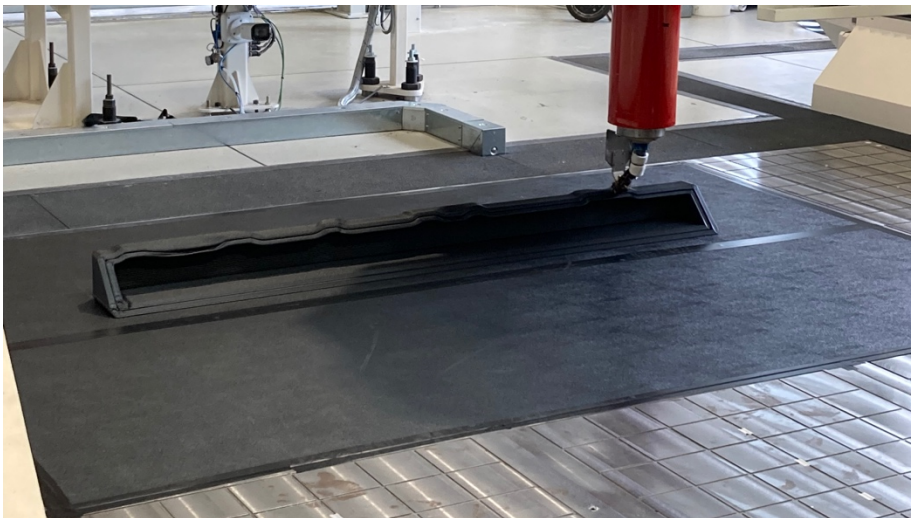

Figure 20 - Printing of a panel over an ABS' platform – courtesy of Camozzi Group

The panel is kept in position by a vacuum system that sucks air between the panel and the floor to maintain it in the correct position. The first issue identified concerns the non-vacuum sealing of the platform. If the panel is not perfectly horizontal and

moves during the printing it can alter the position of the artifact. By altering its position, the object is no more where it is expected to be by the machine, so the deposition and the printing continue in the wrong position. The last problem concerning this category is the detachment of the piece from the platform. If the first layer is not correctly printed and the adhesion between the platform and the object is not insured, the residual stresses of the material caused by cooling can result in forces able to detach the pieces from the platform before the end of the printing, causing unnecessary lifting and printing problems as well as geometrical inaccuracies.

Screw Related Problems

The fourth category of problems identified is related to the screw responsible for the melting of the pellets. To be successfully printed, the pellets are brought from the reservoir where they have been previously dried to the screw extruder responsible for the print of the bead. As a matter of fact, the screw is one of the most important parts of the machine and its integrity and maintenance are really at the core to guarantee an affordable process. The possible issues that could show during the printing of an object are related to the material inside the screw. In particular, when the 3D printer is processing fiber-reinforced polymers, it can happen that the fibers accumulate inside the extruder acting as a plug and slowing down the material flow exiting the extruder. Similarly, when the friction between the deposited fiber and the melted material becomes higher, the plug can be suddenly expelled causing local over-deposition of the material. On the other hand, it may happen that the supply system of the extruder lets enter the air inside the polymerization screw, resulting in a not continuous flow of material. This is the case of the picture below (Fig. 21) where we can notice the phenomena of under-deposition caused by the presence of air inside the material. As we can see, the other layers have been perfectly deposited but when the air has been expelled with the material, it led to unintended results.

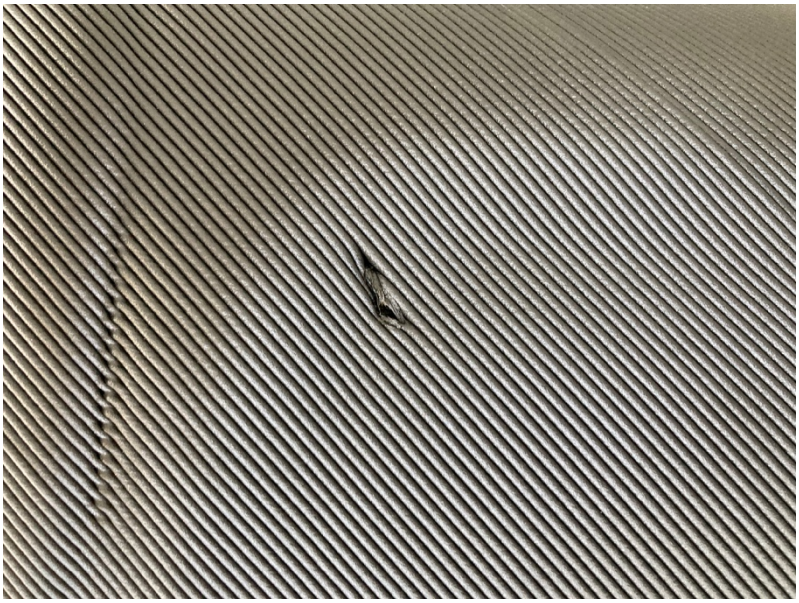

Figure 21 - Effect of under-deposition caused by air bubbles

The last identified problem linked to the screw is related to the material melted left inside the extruder. When the printing process is over the machine stops and the flow of material is interrupted. The material melted will solidify and it is considered as scrap because it will not be reused in the next printing. Indeed, before starting a new process, the machine needs to be dredged and the material inside the screw needs to be removed. When processing composites, leaving the material to solidify is not an issue. On the other hand, letting this happen with techno-polymers like PEI can lead to major issues. In fact, it has been reported that if this kind of material remains inside the machine at the end of the printing, its remelting is not possible. Consequently, the only procedure to restart the process is spending money and time to substitute the screw.

Other Problems

In the last sub-category of problems, those issues that remain excluded from the previous ones have been inserted. In particular, they have been linked to software and hardware problems that can strongly influence the printing but that are not controllable by the operator since depends on other conditions. Similarly, the last identified problem of supports' removal is a peculiarity of the process that can be

limited where possible by the pre-processing of the CAD file. In fact, it cannot be completely avoided but only reduced with smart designs and features.
To be clear, all process-related problems have been summarized in the following tables (Table 1 & 2).

	Category	Possible Problems	Consequences	Frequency	Severity
Process-related problems	Temperature problems	Low temperature of the last layer	Delamination	Low	High
		High temperature of the last layer	Deformation	Low	Medium
	Deposition problems	Material over-deposition	Geometrical inaccuracies	Medium	Low
		Material under-deposition	Inaccuracies and structural problem for the final piece	Low	High
		Material casting	Geometrical inaccuracies	Low	High
		Last layer not supported	Weaker pieces and printing inaccuracies	Medium	Medium

Table 1 - Process related problems (pt.1)

	Category	Possible Problems	Consequences	Frequency	Severity
Process-related problems	Platform related problems	Platform non vacuum sealing	Geometrical inaccuracies	Low	High
		Piece detachment from the platform	Geometrical inaccuracies	High	Low
	Screw related problems	Cooling of the material inside the screw extruder	Printing interruption	Very Low	High
		Air Bubbles	Under-deposition of the material	Low	Medium
		Fiber Accumulation inside the screw extruder	Material over-deposition	Low	Medium
	Other problems	Technical problems (software and hardware)	Printing interruption	Low	High
		Supports removal	Geometrical inaccuracies	Low	Medium

Table 2 - Process related problems (pt.2)

The second macro-category of WHAM defects identified concerns the part's related problems. In particular, these issues arise in the pieces printed by the machine due to, for example, incorrect cooling process, and are also capable to undermine the stability of the printed object compromising its structure and limiting its applications. While following the work of the experts capable of running the Ingersoll MasterPrint and while confronting them about the difficulties of WHAM, the problem identified has been grouped in two different categories:

- Geometrical and shapes problems
- Porosity problems.

Geometrical and shapes problems

Similar to the ones presented before in the paragraph dedicated to FDM defects, geometrical problems refer to divergences between the nominal dimensions of the part to be printed and the final result obtained by the machine. Moreover, these problems are also caused by the incorrect deposition of the material due to unpredicted changes in shapes. In particular for WHAM, the issues related to the over-deposition of the material are not so critical if compared to the under-deposition ones. The main cause of this statement is related to the fact that the artifacts designed for WHAM are realized with material slightly in excess, because of the need of refining the object by milling. The last step is necessary to achieve the desired dimensions and tolerances especially for functional applications like vacuum molds used in autoclaves. On the other hand, the defects based on under-deposition are more critical. Indeed, if excess material is just removed, there is no possibility to re-add raw material where needed if the artifact has cooled down. This fact justifies the fatality of geometrical defects related to the scarcity of the material.

Comparably, shape problems strongly compromise the integrity of the final artifact and are more difficult to be fixed. To be more precise, regarding geometrical and shapes problems, two possible issues have arisen: warping and scarce layers' adhesion. Both issues are caused by an incorrect drop in the temperature of the artifact during the printing process, resulting in an accumulation of internal stresses to the object and causing a detachment between the layers and deformations in the final shape. Moreover, slight displacements of the layers can cause deposition problems also for the subsequent layers, worsening the circumstances. On the other hand, warping is an amplification of these issues that involve even more layers and compromise the structure of the artifact. Even if the presence of fiber reinforcements reduces the coefficient of thermal expansion increasing the thermal stability of the material, these phenomena still arise. As printing technologies continue to scale up in size, warping and delamination caused by thermal stresses remain a major impediment to the widespread adoption of large-scale polymer (Compton et al., 2017). To conclude the paragraph, in the next picture (Fig. 22) are represented both the defects discussed before: at the center of the image, we can notice the detachment of the layers with the manifestation of the delamination, and, similarly, at the bottom

right of the picture it can be noted a slight rising of the piece from the platform, highlighting the beginning of the warping phenomenon.

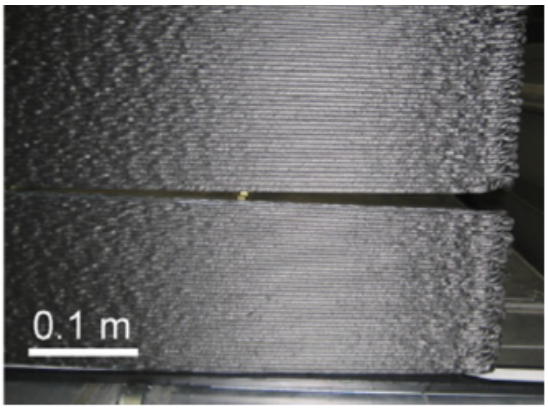

Figure 22 - Picture representing warping and delamination in WHAM (Source: Compton et al., 2017)

Porosity problems

The last category of issues identified as part-related problems concerns porosity. As previously defined for smaller extrusion-based systems, porosity is the fraction of volume of voids over the total volume of the artifact. The porosity in WHAM can be divided into two sub-categories:

- Intra-layer porosity
- Inter-layer porosity.

Intra-layer porosity is referred to the void within the same layer and is caused by the peculiar characteristics of the technology. To exhaust the issue, intra-layer porosity can be primarily caused by the incorrect deposition of the material resulting in voids along the bead. The rise of this problem can cause issues to the stability of the final part, in particular, because of the absence of the material where needed. Typical consequences of this kind of porosity are related to weaker mechanical properties that undermine the functionality of the artifacts and the lack of hermetic sealing, in particular for molds that are designed to be used in autoclave. The criticality of the arising of these issues is highlighted by the fact that, if not solved during the printing, these complications usually show up during the milling phase, requiring last minutes interventions with particular materials that non-negligibly increase its processing time and reduce the quality of the final work.

Comparably, inter-layer porosity refers to the void created between the different beads that form the artifacts. The main consequences are mainly related to the non-hermetic sealing in case of application for molds and the scarce resistance and mechanical properties between the connection of the beads.
The part-related issues are summarized in the table below, also highlighting a qualitative assessment in terms of frequency and severity of the issues. The following and the previous tables have been realized with the assistance of the people responsible for the design and production of pieces with the Ingersoll MasterPrint, and they have been revised by the Ingersoll personnel in the U.S.

	Category	Possible Problems	Consequences	Frequency	Severity
Part-related problems	Geometrical and shapes problems	Warping	Delamination and geometrical inaccuracies	Low	Medium
		Scarce layers' adhesion	Delamination	Low	High
	Porosity problems	Intra-layer porosity	No vacuum sealing (for a mold)	High	Medium
			Weaker mechanical properties		
		Inter-layer porosity	No vacuum sealing (for a mold)	Medium	Medium

Table 3 - Summary of identified part related problems

1.4 In-situ monitoring approaches

To properly assess the topic regarding in situ monitoring, it must be pointed out that the main sources of information for the realization of this section have been the following articles:

- "*Process monitoring for material extrusion additive manufacturing: a state-of-the-art review*" written by Oleff A., Küster B., Stonis M., Overmeyer L., published in 2021,
- "*In situ monitoring for fused filament fabrication process: A review*" written by Fu Y., Downey A., Yuan L., Pratt A., Balogun Y., published in 2020.

Even if the extraordinary potentialities and opportunities offered by Additive Manufacturing are clear, its low process repeatability and standardization are limiting its expansion across the industries. Solving the challenges of qualitative uncertainties in terms of materials and processes, as well as filling process knowledge gaps, it is fundamental to include AM in the industry and limit scraps to enhance sustainability, reducing material usage. To do that, providing tools for quality monitoring is essential. Indeed, measuring process states and parts characteristics during 3D printing is relevant to achieve the objective. In particular, process monitoring enables the assessment of whether the printed parts satisfy the requirements or not. In-situ inspection and analysis increase customer confidence in a product and reduce costs caused by rejection and quality deviations because anomalies are rapidly detected after they occur. Moreover, information from monitoring is necessary for implementing a reliable quality control on parts and processes. Among the different AM technologies, powder-based processes are the ones where in-situ monitoring has been implemented the most. Indeed, the use of expensive materials (titanium alloys, aluminum, copper, etc.), the long processing time, the costly post-processing, and the high-quality standard requested, give an explanation of why there are so many solutions for a low-waste production. At the same time, the growing attention on sustainability and the fact that extrusion processes are the most diffused as 3D printing technologies are making in-situ monitoring critical also for other AM techniques.
To make in-situ monitoring feasible for the implementation, two aspects need to be addressed:

- Machines must be equipped properly with in-situ monitoring devices,
- Process data analytics and statistical monitoring techniques must be developed to target signatures to automatically identify defects and to optimize process' parameters.

Even if, at the beginning, in-situ monitoring has been applied to other technologies, the attention concerning the sensorization of extrusion-based systems has grown. Recent studies conducted by Charalampous et al. (Charalampous et al., 2020) discussed sensor-based quality monitoring before, during and after the Additive Manufacturing process. In particular, they presented nine material-extrusion in-situ process monitoring. Similarly, Lu and Wong presented interesting challenges and developed principles for monitoring through thermal and acoustic sensors. To further focus on in-situ monitoring for material extrusion, a clarification is presented. According to literature and reviews (Oleff et al., 2021; Fu Y. et al., 2021), two main components can be monitored: the material extrusion machine, which has a direct impact on the quality of the printed part, and the part itself.
Clearly, the machine can be monitored as a whole, but to deepen the analysis each component can be kept under surveillance. In particular, these are the main functional components that can be traced:

- Extrusion Head, referred to the mechanism that extrudes and deposits the material.
- Feeding System, intended as the transportation method to feed the extrusion head.
- Build Chamber, in which the peace is printed.
- Build Platform, referred as the surface upon which the piece is printed.
- Axis System, including the motor that moves the extrusion head.

On the other hand, as pointed out previously, the entire part can be monitored. The following are discerned depending on the area monitored:

- Part, intended as the whole piece.
- Layer, equivalent to the building surface.
- Sidewalls of part.

In order to monitor and trace the different components of the machine and to keep under control the printed part, different monitoring systems have been developed

addressing multiple specific aims. The monitoring systems briefly discussed are the following:

- 2D vision
- Temperature monitoring
- Vibration monitoring
- 3D vision
- Acoustic emission monitoring
- Force and pressure monitoring
- Electrical quantities monitoring
- Other sensors technology
- Sensors fusion technology.

To provide a picture of the current status regarding in-situ monitoring for extrusion-based systems, a summary is presented.

2D Vision

The term 2D vision is used to describe the monitoring technologies that acquire two-dimensional images of the object that needs to be observed. As a monitoring technique, it is one of the most used in the industry. 2D vision is mainly used for the inspection of layers, with technical variants used to also monitor the extrusion head. In particular, this technology is used in combination with machine learning algorithms to analyze surfaces images in the area closer to the nozzle, trying to investigate issues related to overfill or underfill (Jin Z. et al., 2020; Makagonov et al., 2017), as exemplified in Fig. 23.

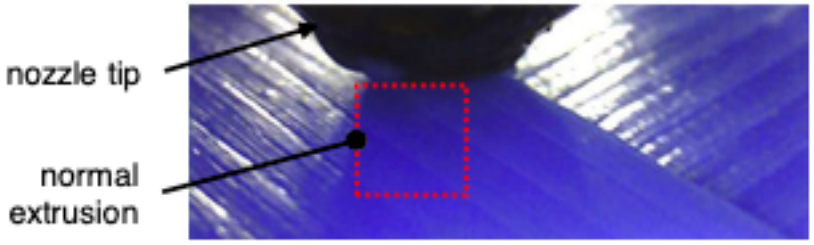

Figure 23 - 2D Vision technology used to identify underfill during extrusion (Source: Oleff et al., 2021)

Moreover, aside from monitoring layers and the extrusion head, 2D sensors can also be used to inspect sidewalls of parts. In this variant, the camera is mounted above the build platform to detect irregularities in printed objects: from detachment to the build platform to lack of material flow (Baumann et al., 2016). This technique has been used also in WHAM because the beads can be easily distinguished from one another with an algorithm. Thanks to that, irregularities can be detected with a monitoring system. Other systems imply the utilization of multiple cameras to monitor the printing and other functional components such as the feeding system of the machine.

Temperature Monitoring

Because the material is melted by applying heat during the extrusion, the data collection of the temperature during the process is a practical method to evaluate the condition of the operations. Temperature sensors are used for controlling the temperature of functional components like the build platform, the extruder, and the build chamber, as well as the heat retention of the material during the extrusion process.

To highlight the importance of the monitoring, for example, Li et al. (Li et al., 2020) have developed a system to control the speed of the extruder in relation to the flow of material: because of the curve path, the extrusion head needs to be slowed down to ensure a correct deposition avoiding over and under-deposition and a correct cooling of the part. Similarly, Müller et al. (Müller et al., 2016) underline the importance of monitoring the process environment, so build chamber and build planform temperature, to minimize variables that can cause undesirable effects. On the other hand, besides sensors that are in contact with the part that needs to be monitored, there are inspection techniques involving temperature determination with thermography. Thermography involves inversion measurement without directly touching the part, using infrared radiation. Thermal cameras are often used for this purpose.

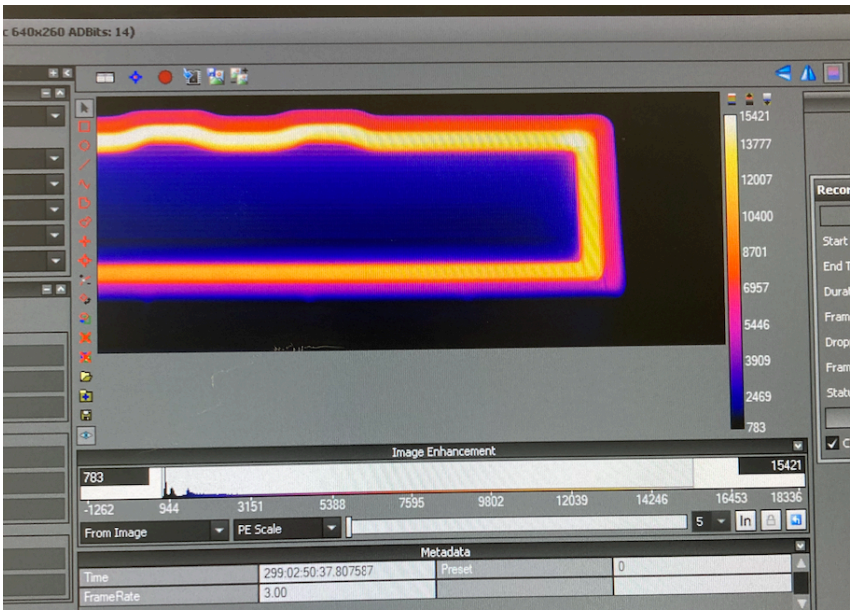

Figure 24 - In-situ temperature monitoring of a printed layer.

Temperature monitoring with thermal cameras has been implemented also in monitoring WHAM, as underlined in literature (Borish et al., 2019; Compton et al., 2017), to provide in-situ feedback to improve process parameters, detect errors and inaccuracies at early stage, providing explanations for the arise of defects during the printing of an object. In the picture above (Fig. 24) it is presented an image related to the collection of data related to the temperature of a printed layer, used to analyze the cooling process of a 3D printed part in WHAM.

Vibrations Monitoring

Vibrations can be measured at many of the mechanical and functional components of a 3D printer. Usually, this way of monitoring is used to inspect the extruder, attaching an accelerometer to determine nozzle clogging conditions. It has been observed that the vibrations increase non-linearly with the decreasing of effective nozzle diameter, providing signals of congestion in the extrusion of the material. To detect these signals, real-time statistical analysis is needed to prevent the evolution of the system from a normal to a critical situation (Liu C., 2019). Another research work has seen the installation of accelerometers to build platform and extrusion head in order to identify, respectively, parts deformation and incorrect extrusion conditions.

As far as the mechanical components are concerned, Yen and Chuang (Yen et al., 2019) investigated axle failure using neural network and backpropagation algorithm using data collected by accelerometers, to determine the status of the 3D printing and avoid faults.

3D Vision

Compared to 2D vision, 3D vision allows the collection of data related to the height of the piece. These sensors are used to expand the vision of the monitored part and to capture information linked with error detection. A reference point, to be used to compare 3D capture images with the nominal dimension of the piece to find geometrical or dimensional inaccuracies, could be the G-code developed to guide the machine during printing. On the other hand, laser triangulation is used to record a single height profile. The combination of multiple triangulations can generate a 3D point cloud to obtain a complete view of the printed part. Once generated, the image is reported to the original CAD file to highlight differences between the designed and the realized parts. More easily, 3D images that give information about all the dimensions of a printed part can be used to monitor in real-time the piece while printing. Indeed, the operators are not always capable of observing the printed object at 360°. It can also happen that dangerous materials that require a protective environment or devices for individual protection are used, so the process needs to be monitored mandatory respecting a safety distance. The adoption of 3D cameras solves the problems related to a visual need in the inspection of the machine or the 3D printed object.

Acoustic Emissions Monitoring

The main working principles of acoustic emission monitoring are linked with the fact that various actuators and mechanical components of a 3D printer generate sound. Indeed, if anomalies occur, they will cause changes in acoustic emissions. In literature, acoustic monitoring is often referred to the control of the extrusion head, leveraging on the non-intrusiveness of the process. As a matter of fact, acoustic sensors are attached in strategic positions closer to the nozzle to record information and collect data both in time and frequency. An important step to be performed in order to correctly process these kinds of data consists in the filtering phase. The objective of this step is to eliminate noise's sources that could damage the reliability

of the data. If data are properly collected, acoustic emissions analysis can be implemented, analyzing variations in the sound of the components. Yang and Lin (Yang et al., 2018) used this method to provide real-time information about filament breakage while printing. Other studies present sensors mounted directly on the build platform next to the printed part. This arrangement could detect detachment of the part from the build platform and cracking or deformation. In fact, the defective part can come into contact with the extrusion head causing abnormal acoustic emissions. Similarly, Becker et al. (Becker et al., 2020) used microphones mounted in the build chamber to detect anomalies concerning the build chamber. They recorded specific sounds that, once analyzed using machine learning algorithm, can provide information about the state of the printer and the printing. In the picture below (Fig. 25) it is presented a typical setup for the measurement of acoustic emissions related to the extrusion head of a 3D FDM printer.

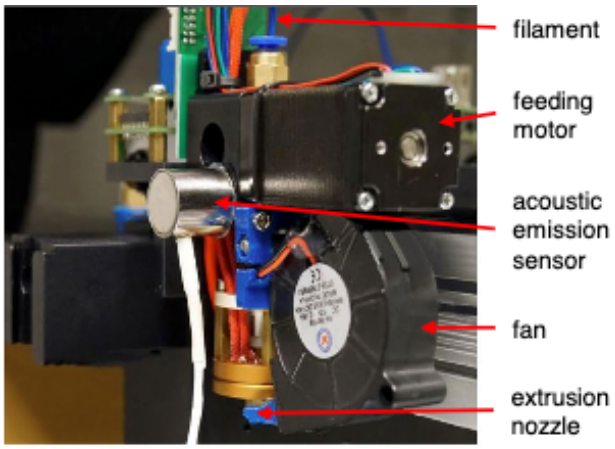

Figure 25 – Experimental setup for measuring acoustic emissions of extrusion head (Source: Oleff et al., 2021)

Force and Pressure Monitoring

As far as force and pressure monitoring is concerned, they are mainly referred to the investigations of extrusion head elements. It has been shown that extrusion force in a piston-based extrusion is directly related to the flow characteristics of the material, being an indicator for the correct extrusion of the material. The main sensors used for monitoring force and pressure are load cells. Furthermore, in the extrusion of continuous fibers, the ones that are not fed at a sufficient rate result in a noticeable change in terms of measured forces. At the same time, extremely high forces caused

by unnecessary contact between the extruder and the part can cause operating failure. Kemperle et al. (Kemperle et al., 2016) developed a patent involving load cells to detect this kind of problem, even without providing a way to manage the data collected.

Electrical Quantities Monitoring

This category of sensors is used to monitor the currents of the motors of the 3D printer, in particular, those that push the filament through the extrusion head or that move the axis. As a matter of fact, nozzle blockages and incorrect axis movement or fatal blocks cause changes in the motor current and can be detected and evaluated. Specific studies (Kim et al., 2015) have found correlations between the motor current and the level of extrusion pressure. Indeed, the extrusion pressure depends on the size of the nozzle outlet and on the distance between the nozzle and the printed part. If the part is not aligned with the correct disposition, it can cause a diminishing in the distance between the outlet and the substrate, causing changes in the motor current that can be detected by the sensors. On the other hand, other studies (Gatlin et al., 2019) proposed an approach to continuously monitor the current supplied to each individual actuator during the manufacturing process and detecting anomalies to X-Y-Z axis motors. These monitoring systems have the characteristic of not being invasive, without affecting the printing time while monitoring in normal conditions.

Other Sensor Technology

The monitoring systems not included in the previous paragraphs have been included in this category. In particular, other sensors attached to monitor the printing refer, for example, to ultrasonic control to analyze part structures, encoders to determine the positions of the axis in order to implement a closed-loop control, fiber Gragg grating sensors for measuring strains. In this kind of system optical fibers are placed on unfinished parts and subsequently overprinted with additional material, measuring if deformation occurs during the printing proves. It is clear that these sensors technologies are not diffused as the above-mentioned; nevertheless, the studies regarding new approaches for in-situ monitoring are increasing and further results are expected to come in the next years.

Sensor Fusion Technology

In order to monitor a larger number of features at time, a powerful method adopted concerns the combination of the just presented sensors. On the other hand, systems such as 2D vision and 3D vision are rarely combined with other sensor technology due to the large amount of information provided by optical inspection systems. Moreover, these technologies are used to inspect the quality characteristic of a part. Differently, to inspect the condition of the 3D printer and the printing process more aspects need to be considered. A priori, an effective way to design in-situ monitoring does not exist, due to the high number of possibilities offered by the sensor technologies and the high number of features that can be monitored during the printing. Because of that, every case should be evaluated on the specific requirements or research purpose for which the monitoring system is needed, considering the integration of the different systems presented above to better exploit the possibility of improving the processes and the quality of the printed parts as well as limiting the arise of problems and issues that could show up during the printing.

To sum up the possible in-situ monitoring technique presented and the related controlled part, it has been decided to present two tables (Table 4 and Table 5) that summarize the publications that have been considered for the realization of this paragraph. The "Xs" presented in some cells represent fields that have been nominated in the paragraph but for which no articles are cited. For a deep understanding of the topics, please refer to the articles cited at the beginning of the paragraph that have been fundamental for the draft of this chapter.

	System Monitoring				
	Extrusion head	**Feeding system**	**Build platform**	**Axis system**	**Build chamber**
2D Vision	Jin Z. et al., 2020	X		X	
Temperature monitoring	Li N. et al., 2020		Müller. et al., 2016		
Vibration monitoring	X		Liu C., 2019	Yen C.T. et al., 2019	Yen C.T. et al., 2019
Acoustic emission monitoring	Yang Z. et al., 2018		X	X	Becker P. et al., 2020
Force and pressure monitoring	Kemperle A. et al., 2016	X			
Electrical quantities monitoring	Kim C. et al., 2015			Gatlin J. et al., 2019	
Other sensor technology	X	X	X	X	X
Sensor fusion technology	X	X	X	X	X

Table 4 – Summary of system monitoring articles

	Part Monitoring		
	Entire part	**Layers**	**Sidewalls part**
2D Vision	Makagonov N.G, et al., 2017	X	Baumann et al., 2016
Temperature monitoring		Compton et al., 2017	X
Vibration monitoring			
3D Vision	X	X	X
Electrical quantities monitoring	X		
Other sensor technology	X	X	
Sensor fusion technology	X	X	X

Table 5 - Summary of part monitoring articles

2. Recycling and reuse of ABS CF 20%

One approach that has been followed in pursuing the objective of reducing wastes for WHAM has been the exploration of using recycled material for printing new pieces. In particular, because of its high cost in terms of supply, the efforts have been concentrated on the techno-polymer ABS filled at 20% with short carbon fibers. Strategically, the choice has fallen on this material because of its cost, which is around 18€ per kilogram. Moreover, lots of studies have been performed on the quality of recycled composites, but no studies that concern the reuse of 3D-printed material coming from Wide and High Additive Manufacturing have been identified. The objectives of the experimentation concern the evaluation of the feasibility for the reuse of recycled material and the assessment of the application, in terms of mechanical properties, for pieces printed with recycled material. In the literature, regarding the mechanical recycling of composites, savings equal to 60% of the total costs are indicated (Pimenta et al., 2011). Moreover, processes to produce carbon fibers consume up to 286 MJ/kg, while the most energy demanding recycling process for carbon fiber consume, at maximum, 30 MJ/kg (Meng et al., 2017). The first paragraph of this chapter will discuss the choice of the recycling method selected to recycle ABS filled with 20% carbon fibers, comparing the various methods previously presented from the point of view of emissions, costs and expected results in terms of mechanical properties. The discussion will continue with a presentation of the selected recycling method and the amount of material produced. Once this point has been completed, we will move on in evaluating the economic and environmental sustainability of the selected recycling process, examining also the mechanical properties of the recycled material for assessing its practical applications.

2.1 Preliminary evaluation of recycling systems

As mentioned above, three recycling methods have been identified to make the material classified as production waste reusable:

- Mechanical recycling,
- Thermal recycling,
- Chemical recycling.

The first factor considered in selecting the recycling method to be adopted to reuse carbon-fiber-filled ABS was the expected output. For expected output is intended the material that will come out as the result of the recycling processes. As mentioned before, mechanical recycling is the only method, among those selected, able to recover both the matrix and the fibers of the material providing a consistent output with respect to the objective of reusing all the material. In parallel, the remaining recycling methods mentioned above are only able to recover the carbon fibers immersed in the polymer matrix, being processes based on the thermal or chemical degradation of the polymer.

From the point of view of the expected output, mechanical recycling can be considered as the process that allows to recover the greatest amount of material with the lowest processing time.

Turning to the economic and environmental sustainability of recycling processes, previous studies have been identified in the literature to quantify the cost of obtaining a kilogram of recycled material in terms of energy consumed. At the same time, it must be considered that in the case of mechanical recycling it is obtained a recycled kilogram of ABS filled with carbon fiber, while, in the case of thermal and chemical recycling processes, it is obtained a kilogram of recycled carbon fibers.

After the preliminary observations, the aforementioned recycling methods have been assessed by considering costs, environmental impact, and loss in mechanical properties after one cycle of material recycling. To compare the expected costs of recycling between the various methods, it has been decided to consider the amount of energy required by the various recycling methods to produce one kilogram of recycled material. Based on studies performed between 2014 and 2017, assessments have been made regarding the energy consumption required to recycle one kilogram of ABS filled with carbon fibers. In particular, studies (Howarth et al., 2014) quantify the energy needed to recover a kilogram of CFRP with mechanical recycling at 2.03

MJ/kg, considering only the shredding. On the other hand, thermal and chemical recycling processes require a much higher amount of energy, as well as particular process parameters such as the use of high temperatures or solvents capable of degrading the polymer matrix. Respectively, these processes require 30 MJ/kg and 19.2 MJ/kg on average to obtain the recycled material (Meng et al., 2017). Consequently, with respect to energy consumption, the environmental impact of recycling processes is proportional to the energy used. With this in mind, the most environmentally friendly process is the mechanical recycling.

The last variable to be examined consists in the expected mechanical properties. Considering the strong applicative character of this work, it has been decided to focus the bibliographic research of this part on the ultimate tensile strength (UTS) of recyclates, considered by the MasterPrint managers as the key parameter to define the functional boundaries of the material. Based on the articles by Morsidi et al., 2019, and Raharjo et al., 2021, the ultimate tensile strengths of materials obtained from different recycling processes were compared. In particular, there was a decrease in UTS for mechanically recycled material of 15-20% compared to virgin material. Similar values were found for fibers recycled by thermal processes, while a less pronounced decrease in mechanical properties, around 5-10%, was recorded for the chemical recycling process. To clearly summarize what has been presented so far, the following table (Table 6) has been presented.

	Material recovered	**Energy required**	**Costs**	**Environmental impact**	**Mechanical properties**
Mechanical recycling	Matrix and fibers	2.03 [MJ/kg]	€	Low	-15/20%
Thermal recycling	Fibers	30 [MJ/kg]	€€€	High	-15%
Chemical recycling	Fibers	19.2 [MJ/kg]	€€	High	-5/10%

Table 6 - Comparison table for recycling processes

Considering the analysis presented above, mechanical recycling has been identified as the most suitable method to recycle ABS filled with carbon fiber. In the next

paragraph more detail about the chosen recycling method will be given, describing the phases and preparing the definition of the case study.

2.2 Evaluation of carbon emissions and recycling costs

It has been decided, together with Camozzi Group and Innse Berardi S.p.A., the formal owner of the printing, to pursue the objective of recycling the scrap material coming from errors in production or end-of-life products. Among the different types of recycling methods that have been presented before, the mechanical recycling has been the most promising one in enhancing sustainability and being valuable in terms of costs reduction. Indeed, due to its characteristics, this process allows the recovery of both the matrix and the fibers. Moreover, the mechanical recycling method is the one that emits less pollution in terms of equivalent CO_2 produced per kilogram of material recycled, as stated in previous paragraphs. Once the recycling mode has been decided, the research efforts were addressed towards the identification of the steps required for material recycling, as well as the estimation of CO_2 emissions and costs. These issues have been solved thanks to the help of another company of Camozzi Group operating in the field of injection molding, "Camozzi Technopolymers".

Figure 26 - Production scraps of the Ingersoll MasterPrint

The company had the expertise and the machines capable of reprocessing production scraps, like the ones represented in the previous image (Fig. 26), and end-of-life products. The following paragraphs will discuss the workflow for material recycling through grinding, the environmental impact and the cost sustained for material reuse.
In each paragraph, general considerations on the methodology for material recycling will be made, and they will be followed by some reflections on a case study application. More in details, the identified workflow, as well as the evaluation of costs and CO_2 emissions, will be applied to the recycling of 100 kg of ABS filled with 20% of carbon fibers production scraps.

2.2.1 Recycling workflow

Generally speaking, when thermoplastic scraps are recycled via material grinding, five main steps are usually performed. The first step to be performed in mechanically recycling composites is the collection phase, that can be generalized in the physical recuperation of the wasted materials. Usually, the subsequent process to the collecting phase is related to the cleaning and sorting of the material. In fact, different types of plastics and composites can be recycled, but every category need to be treated on their own to avoid undesirable mix. Moreover, debris of other undesired materials could be present, they need to be separated from the rest to avoid problems in the recycling process. The following phase is the cutting phase. Indeed, it is possible that some pieces have dimensions that are too big to be processed, so their extent need to be reduced to make them suitable for the proceeding. The final step is the grinding phase, performed with a shredder. When the waste is ground to the desired dimensions, it is ready to be reprocessed and reused.
In collaboration with Camozzi Technopolymers, we verified that this workflow is almost entirely suitable for the company needs and compliant with MasterPrint's production scraps. Thus, a workflow composed by five steps has been formalized, as depicted in the next figure (Fig. 27), and it is described hereafter, following the path of the production scraps we have been able to recover.
As stated before, the first step has been the collection phase. Assuming that production wastes were collected on board the production line, no logistics is considered. Consequently, this phase can be generalized as the collection of these production waste. The following phase concerned the sorting of the material. In this

particular phase, since the material sent to the company was homogeneous ABS carbon-fiber-reinforced, the sorting phase was not necessary. Indeed, next to the machine, the company has containers to differentiate the materials used, as presented in figure 28.

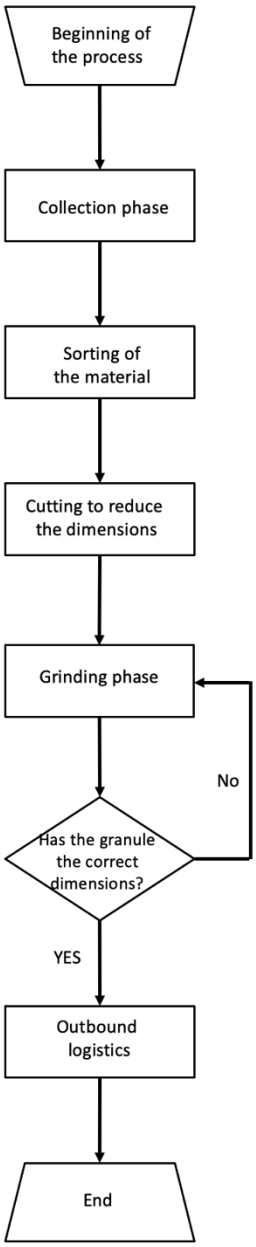

Figure 27 - Scheme of the mechanical recycling process

Figure 28 - Sorting of the material inside the factory

The next phase has been the cutting. Since the production scraps coming from a WHAM system usually have important dimensions, they need to be manually reduced in smaller pieces, using a saw, to be finally processed by the grinding machines. The dimensions of these pieces vary according to the capacity of the machine capable to process them. In particular, the production scraps used to obtain the recycled material have been reduced approximately to pieces that measured 120x120x120 millimeters to be processed by shredders (Fig. 29).

Figure 29 - Shredder similar to the model used to process MasterPrint's scraps

According to the managers in charge of the process, the cutting phase has been the most time-consuming activity due to the tenacity of the material as well as the final dimensions required compared to the initial ones. The subsequent phase has been the grinding phase with the use of the shredder. Since the company is specialized in injection molded plastics, they have small grinding machines capable of processing wastes up to the dimensions previously indicated. In order to achieve the correct dimensions for the recycled material, a pitch of 4 millimeters has been set for the augers of the shredder. At the end of this phase, a qualitative control concerning the final dimensions of the granulate needed to be performed to evaluate the compliance to the requested ones. If the proportions were not satisfied, a new transit through the grinding machine would have been necessary. When the dimensions have been compliant to the sought required by the specifications, the process has been considered as complete. The just-presented path has been followed by 100 kilograms of ABS carbon fiber reinforced recovered from the MasterPrint's production scraps. In the end, the recycled material has been shipped back to the production plant in Milan to be used as raw material for the experimentations. To conclude the paragraph, it must be reported that the process efficiency stands at 90%, because some materials reduced to powders during the grinding phase could not be reused. The entire recycling process had a duration of 70 hours, excluding the logistics. The activity that took the longest time has been the cutting, this phase took about 60 man-hours. On the other hand, the grinding process took a total of 10 hours to be completed.
In the next paragraph, an analysis concerning the evaluation for footprint reduction and economic feasibility for the mechanical recycling have been performed, considering the comparison in terms of CO_2 emissions and costs for producing the virgin material.

2.2.2 Analysis on footprint reduction

In this paragraph we presented a model to compute CO_2 emissions reduction for material recycling in WHAM, and the results of the discussed case study. Considering the different operations required for material recycling (see Figure 27) the components of total CO_2 emissions are:

$$Total\ CO_{2,Recycling} = CO_{2,Logistics} + CO_{2,Cutting} + CO_{2,Grinding} + CO_{2,Mixing}$$

Considering that we are assuming that the recycling process is performed in-house near to the production line and cutting operations can be performed manually with a saw, we assume that the contribution of these two variables, in terms of CO_2 emissions, is null. Moreover, the mixing phase between virgin and recycled material is performed manually, and it is beyond the boundaries of the recycling process, so its contribution in terms of emissions, is considered as null. For our specific case study, we considered two different scenarios according to the size of the grinder:

- Recycling by using a small shredder for pieces produced by injection molding.
- Recycling by using an industrial shredder.

Considering the recycling process discussed in the paragraph 2.2.1, and the hypothesis above-mentioned, the only emissions related to the mechanical recycling, in both cases, have been the ones associated to the shredder. The model has been elaborated as follow:

$$Total\ CO_{2,Recycling} = CO_{2,Grinding} = \frac{P_s}{\eta_{gas\_t}} \times m \times\ t_{s,1kg}$$

where:
P_s: electrical power absorbed by the shredder (small or industrial),
η_{gas_t}: gas turbine efficiency (since in Italy almost 50% of electrical power is generated by turbogas turbine),
m: kg of CO_2 produced for obtaining a gross kWh from burning gas,
$t_{s,1kg}$: time used by the shredder for processing a kilogram of material.

For this case study, we have considered the following data coming from reliable sources, and reasonable hypothesis. According to Terna, an Italian company for energy distribution, the 50% of the energy produced in Italy comes from gas plants, so it is reasonable considering the electricity as produced by a gas turbine. In particular, the efficiency for a gas turbine is supposed equal to 0.32 and the kg of CO_2 produced to obtain a gross kWh are assumed to be 0.365 kg.
The other factors, P_s and $t_{s,1kg}$ depend on the machine used. In particular, for the small shredder, it has been possible to recover reliable data thanks to Camozzi Technopolymers. Indeed, the shredder used had a power of 7 kWh and the time used

to process a kilogram of material has been equal to 0.1 hours. Similar calculations have been made for the industrial shredder, this time making hypothesis with the managers of Camozzi. With their expertise, a power of 15 kWh and a processing time of 0.125 hours have been considered for the calculations. Based on data just presented, the CO_2 emissions related for the scenario involving the small shredder have been calculated and are equal to 0.8 kg. On the other hand, by using the industrial shredder, this number increase to 2.1 kg.
In order to understand the environmental advantages of recycling material through grinding, we also computed the emissions related to the virgin material procurement and we compared them with those related to material recycling. The supplier for the ABS filled with 20% of carbon fibers is the company Airtech Europe, which has its production plant in Luxembourg. This information is important to evaluate the emissions for the transportation of the material. Made these premises, the model concerning the emissions of this scenario can be written.
The following variables have been considered:

- The CO_2 emissions to produce one kilogram of the polymer ABS.
- The CO_2 emissions for the production of one kilogram of carbon fiber.
- The CO_2 emissions produced to mix the two components together and create the composite.
- The CO_2 emissions related for the transportation by truck of the raw materials from Luxembourg to the plant in Milan.

The model can be summarized as follow:

$$Total\ CO_2 = CO_{2,ABS} + CO_{2,CF} + CO_{2,Mixing} + CO_{2,Logistics}$$

Since the emissions related for mixing the two components have not been found in the literature, this variable has been considered equal to zero. Therefore, the estimate of the CO_2 emissions for this model can be interpreted as a lower bound.
The model has been elaborated as follow:

$$Total\ CO_2 = 0.8 \times CO_{2,ABS} + 0.2 \times CO_{2,CF} + CO_{2,Logistics}$$

where:
$CO_{2,ABS}$: are the kilograms of CO_2 produced to obtain a kilogram of ABS
$CO_{2,CF}$: are the kilograms of CO_2 produced to obtain a kilogram of CF

$CO_{2,Logistics}$: are the kilograms of CO_2 produced by the transportation of the material from the supplier to the production plant.

In particular, since the material is 80% ABS and 20% CF in terms of weight, the CO_2 emissions have been weighted on the percentages of the compound. The voices of the model have been calculated as follow: the emissions to produce a kilogram of ABS are equal to 3.5 $\frac{kg\ CO2}{kg}$ (source: City of Winnipeg website), the emissions related for the production of a kilogram of CF are equal to 29.5 $\frac{kg\ CO2}{kg}$ (source: renewable-carbon.eu website), the carbon emissions related to the logistics are equal to 0.11 $\frac{kg\ CO2}{t \times km}$ (source: EU parliament, 2010) multiplied for the distance between the supplier and the production plant, equal to 860 km. By using these data and the model above-mentioned, it has been possible to calculate the CO_2 emissions associated to the production of one kilogram of virgin material, equal to 8.8 kg.
The graph in the figure below (Fig. 30) summarizes the result just presented, including the recycling process and grouping the emissions in their related categories.

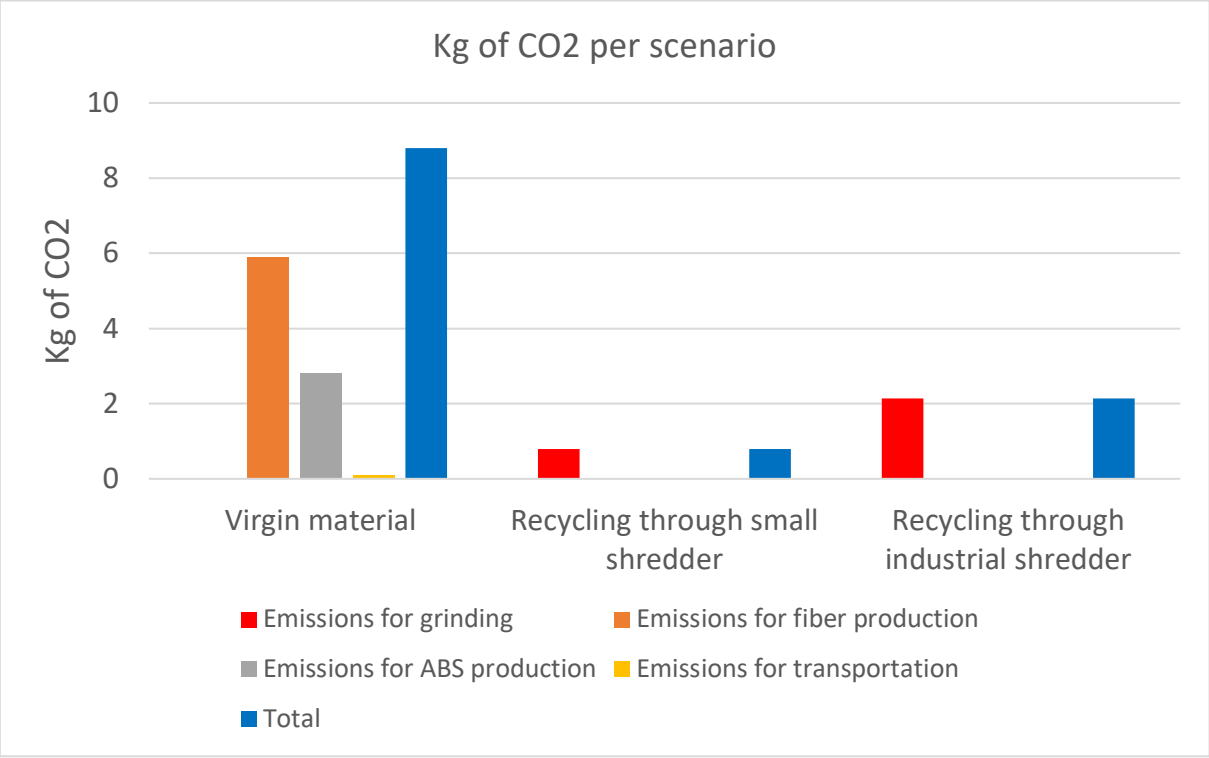

Figure 30 - Scenario analysis for ABS 20% CF emissions

To conclude the paragraph, it must be considered that the new material processed by the machine, for the purpose of this work, is not fully recycled, but is a blended material obtained by mixing 80% of virgin material and 20% of recycled material. In the next graph (Fig. 31) the variation of CO_2 emissions for a kilogram of blended material by varying the percentage of the recycled material in the compound is presented. The benchmark is given by the yellow line, which represents the emissions related to the virgin material. As we can see from the picture, adding recycled material to the compound is always worthy for reducing the environmental impact, due to the high energy requirements for producing carbon fibers, as presented before.

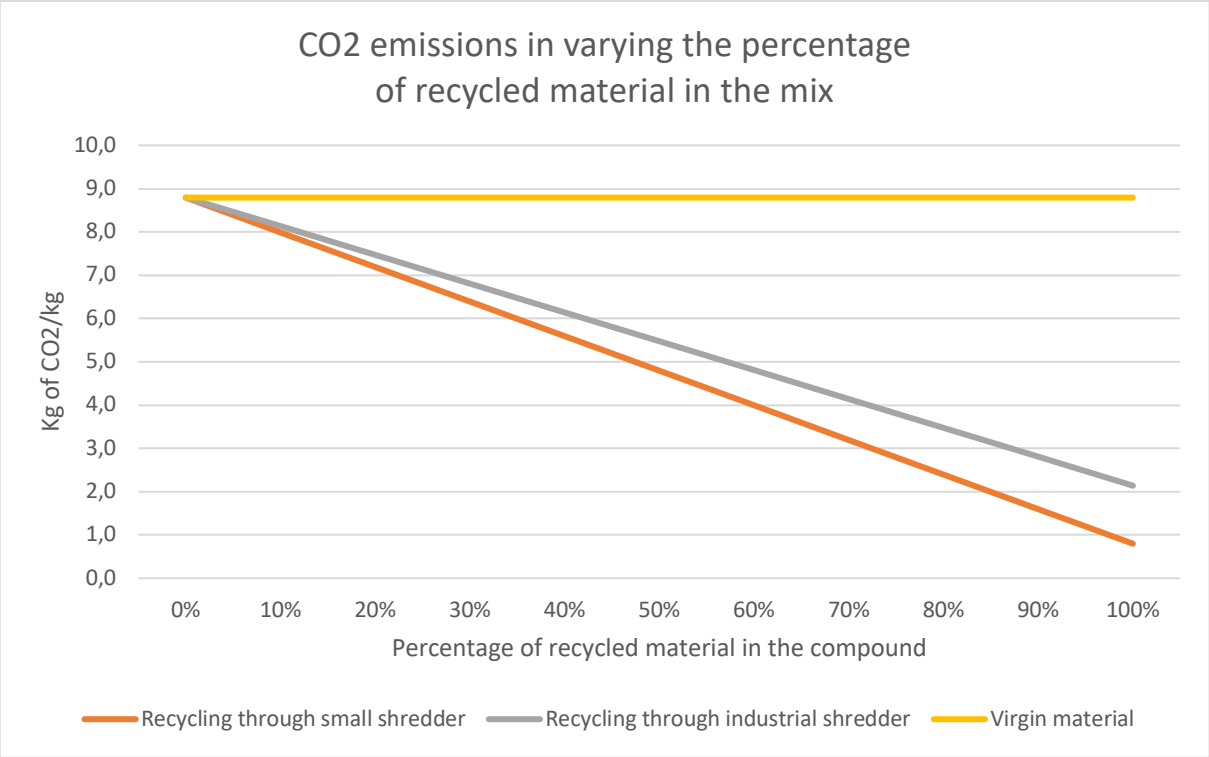

Figure 31 - Emissions related to the possible blended material when varying the percentage of the recyclate

To conclude the assessment, a cost analysis will be presented in the next paragraph, discussing the effective cost for recycling the material, as estimated by Camozzi Technopolymers, and comparing it to the purchasing cost of the virgin one.

2.2.3 Costs model and economical evaluation

Similarly for the scenarios presented for assessing the environmental impact for the production of the virgin material and its recycling, the cost evaluation has been performed following the paths above presented. Three scenarios have been considered:

- Mechanically recycling the material through a small shredder.
- Mechanically recycling the material through an industrial shredder.
- Purchasing the virgin material from the supplier.

The reasoning and the cost model for the recycling are based on the recycling process illustrated in paragraph 2.2.
The cost model can be depicted as follow:

$$C_{recycling} = C_{Logistics} + C_{cutting} + C_{grinding} + C_{mixing} + C_{depreciation}$$

At the same time, hypothesis have been made to simplify the model:

- Logistics costs are not considered since the recycling is intended to be performed in-house.
- The costs related to the mixing of virgin and recycled material are taken as negligible since they require a small amount of time compared to the other activities.
- It won't be employed a full-time operator for the recycling, but spare time of the operators is used.
- The investment is intended in buying one shredder, small or industrial.

Even in this case the two models for the two scenarios are equal, only the parameters typical of the shredders and the processing times are changing. Considering these premises, the cost model related to the recycling of the material has been established as follow:

$$C_{recycling} = C_{cutting} + C_{grinding} + C_{depreciation}$$

Each cost item can be broken down to go into the singular voices to assess the actual cost of recycling considering the quantity recycled in a year.

The first variable considered is the cost of cutting, which is made manually and change between the different type of shredder, depending on the dimensions that the machines is capable to process. The voices for the cost of cutting are the following:

$$C_{cutting} = t_{cut} \times c_{op} \times q_{kg/y}$$

where:
t_{cut}: it is the time used for obtaining a kilogram of material to be processed by the shredder,
c_{op}: it is the hourly cost for an operator, equal to 25.4 €/h
$q_{kg/y}$: it is the quantity of material recycled in a year.

Similarly for the cutting's costs, the grinding's costs are related to the operator's cost for the first part, then they are linked to the electrical consumption of the machine. The costs of grinding are divided as follow:

$$C_{grinding} = (t_{op} \times c_{op} + t_g \times P_g \times c_{el}) \times q_{kg/y}$$

where:
t_{op}: it is the time spent by the operator for the movement of the material for grinding,
c_{op}: it is the hourly cost for an operator, equal to 25.4 €/h,
t_g: it is the time to grind a kilogram of material,
P_g: it is the power requested by the shredder,
c_{el}: it is the cost of the electricity for industrial applications, equal to 0.234 €/kWh (average for the Italian market, source: Sorgenia.com),
$q_{kg/y}$: it is the quantity of material recycled in a year.

The last category of costs is related to the depreciation of the machinery used for the recycling process. For the yearly costs, it is a function of the year of investments.
The depreciation costs have been declined as follow:

$$C_{depreciation} = \frac{Total\ investment\ for\ the\ shredder}{Years\ of\ investments}$$

This is the fixed part of the yearly costs. In order to calculate the costs of recycling one kilogram of ABS 20% filled with carbon fibers, the total costs must be divided by

the yearly quantity of material recycled. It is a direct consequence that the fixed part of the costs will be smaller as the yearly kilograms of material recycled will grow. Before performing a sensitivity analysis regarding the variations for the material quantity, data regarding the calculation of the previous model, for the small shredder and the industrial one, must be provided. In particular, the data for the small shredder are known since they have been collected from the recycling process performed at Camozzi Technopolymers. In particular:

- $t_{cut} = 0.6\ hours,$
- $t_{op} = 0.02\ hours,$
- $t_g = 0.1\ hours,$
- $P_g = 7\ kWh,$
- $Total\ investment\ for\ the\ shredder = 7000€,$
- $Years\ of\ investments = 6.$

At the same time, as regards the evaluation of costs using the industrial shredder, the variables t_{cut}, t_{op}, t_g and P_g were assumed as follows, following a discussion with the managers of Technopolymers regarding the size of the new machine:

- $t_{cut} = 0.15\ hours,$
- $t_{op} = 0.02\ hours,$
- $t_g = 0.125\ hours,$
- $P_g = 15\ kWh.$

On the other hands, the years of investments have remained equal and the economical spending for an industrial shredder has been quantified in around 50000€.

Regarding the assessment of the costs for the virgin material, only the purchasing from the supplier, equal to 18 €/kg, is considered. A particular agreement with Airtech Europe, moreover, let the costs decrease to 17 €/ kg if the quantity purchased in a year overcome 2000 kilograms. The model considered has been the following:

$$C_{virgin\ material} = C_{purchasing}$$

Having used those inputs in assessing the yearly costs, a sensitivity analysis considering the yearly quantity of recycled material to be processed has been performed. The results are summarized in the graph below (Fig. 32).

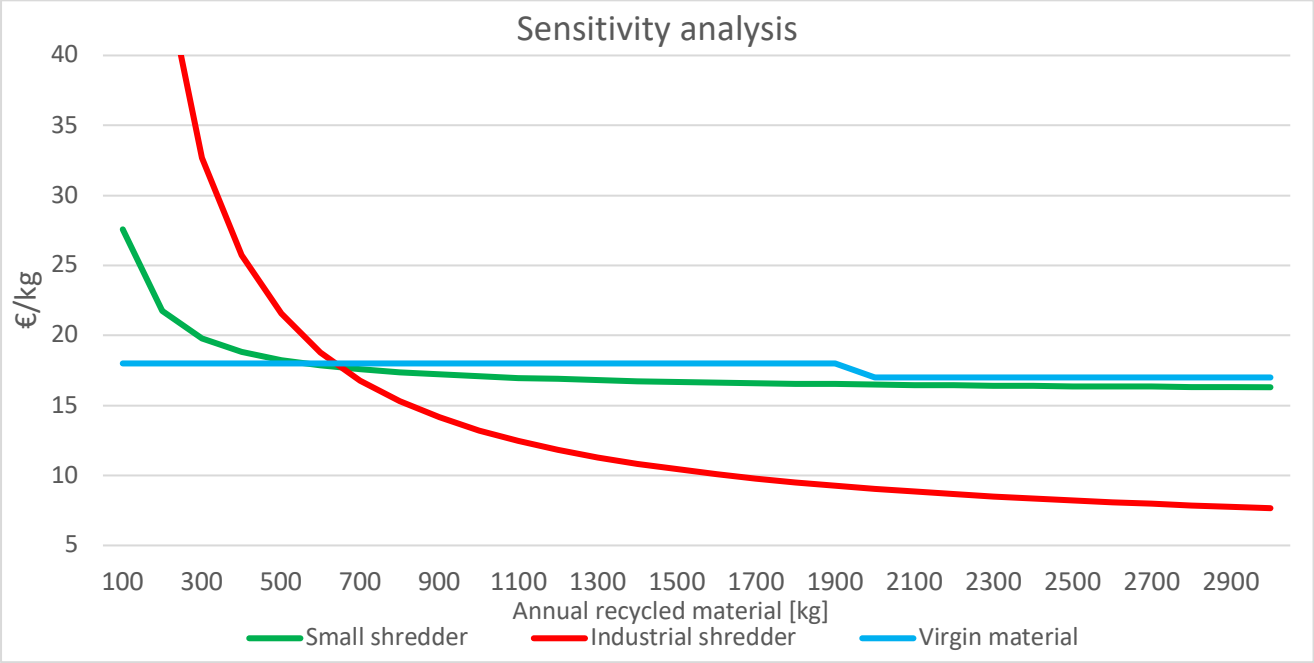

Figure 32 - Sensitivity analysis for annual material recycled

As stated by the graph above, where the models are summarized, three regions can be identified: the first region from 0 to 500 kg of recycled material in which it is economically convenient purchasing only virgin material, the second region from 500 to 700 kg where it is convenient to adopt a strategy based on recycling the material through the small shredder, and a third region above 700 kilograms where the €/kg for the recycled material through the industrial shredder become more competitive than the others. Based on this premises, it can be concluded that above an annual quantity of 500 kilograms, the recycling of this material is a viable opportunity.
To conclude this chapter, the investigation of mechanical properties for evaluating the changes after the recycling process is discussed in the next paragraph.

2.3 Investigation on mechanical properties changes after recycling

As mentioned in the introductory paragraph, in order to reduce waste that concern Wide and High Additive Manufacturing, it has been developed a project for assessing the feasibility of recycling ABS filled at 20% with short carbon fibers. Based on data provided by Ingersoll, the company of Camozzi Group which has designed the Ingersoll MasterPrint, the afore-mentioned material is the most consumed by the machine to fabricate final products with functional application. Due to the peculiarity of the process and considering that an average piece manufactured by the 3D printing weights around 400 kilograms, finding a way to enhance sustainability and, at the same time, saving costs ensuring functional applications can help the development of the technology and its adoption worldwide as a valid alternative to traditional manufacturing, especially when it comes to single-batch products like molds or prototypes.
100 kilograms of material have been recycled, and once assessed its environmental impact and costs, the next step concerned the evaluation of its mechanical properties. To do that, an experimental campaign has been arranged. The design of experiment and its results will be presented in the following paragraphs.

2.3.1 Experimental Campaign

In order to evaluate the feasibility of using recycled material as a raw material to produce functional parts, it has been decided to plan an experimental campaign with the aim of evaluating the statistical influence of the type of material used in affecting the mechanical properties. Forty specimens were produced with virgin and recycled material to realize tensile strength tests. The raw material consists in virgin ABS filled with 20% of carbon fibers produced by Airtech Europe and 100 kilograms of the same, mechanical recycled, material. The granulometry of recycled feedstock material was around 4 mm and the shape was irregular. For further details on production of recycled material see the paragraph before (Par. 2.2). The recycled feedstock was mixed with the virgin one in a ratio equal to 80:20.

Figure 33 - Bucket of recycled and virgin ABS 20% CF-reinforced

As we can see in the picture above (Fig. 33), the two materials appear very similar when mixed, only a slight color difference can be noticed: indeed, the recycled material emerges as grey against the black of virgin material. On the other hand, if analyzed closer, the grain of recycled material come into view with an irregular shape if compared to the perfect cylindrical shape of the pellets of the virgin material. Then, a printing functional to extract testing samples has been designed. The optimal shape chosen to obtain these kinds of parts has been octagon. Indeed, every side of the printed shape can be used to draw out a variable number of samples according to the requests. In order to successfully compare the mechanical properties of the virgin and recycled material, two octagons of different material needed to be printed:

- 100% virgin ABS 20% CF-reinforced
- 80% virgin ABS 20% CF-reinforced + 20% mechanical recycled ABS 20% CF-reinforced.

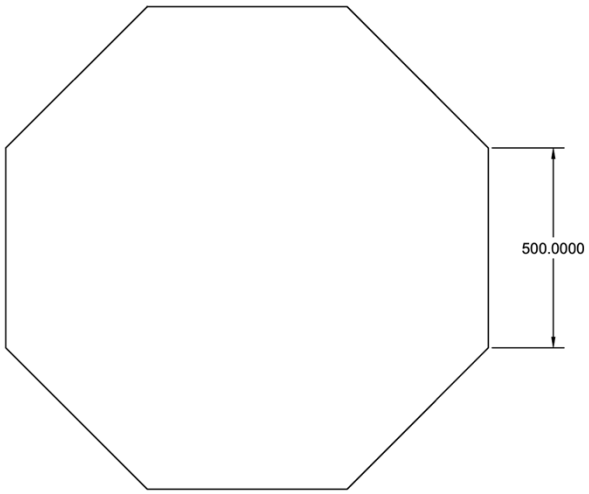

Figure 34 - Technical drawing of the printed octagon, dimension in mm

The final dimensions of the polygon have been the result of previous experience of the operators and managers running the machines. To be more precise, a side of the shape measure 500 mm for a height of 390 mm. The width of the bead was equal to 19 mm. Above it is presented a technical drawing (Fig. 34) used to represent the dimensions of the printed shape. Subsequently to the programming phase of the printing, the realization phase has occurred. In fact, the two shapes have been realized one after the other, in two consecutive days. The printings have been surveilled by the operators and no problems have occurred. Whether there was certainty about the successful printing of the virgin material, for the blended material there was no known data. As planned, the first printing went successfully and, to be sure of avoiding possible problems, the second printing was surveilled visually by the operators. No problems occurred during the second printing and the question mark related to the printability of the material was solved. To be more precise but without giving details, the printing was a success and the parameters used have been similar to the ones settled for the 100% virgin material. So, the first objective of verifying the printability of the blended material was achieved. To clarify the result of the printing and to show the result, hereafter (Fig. 35) is presented an image of the recycled octagon.

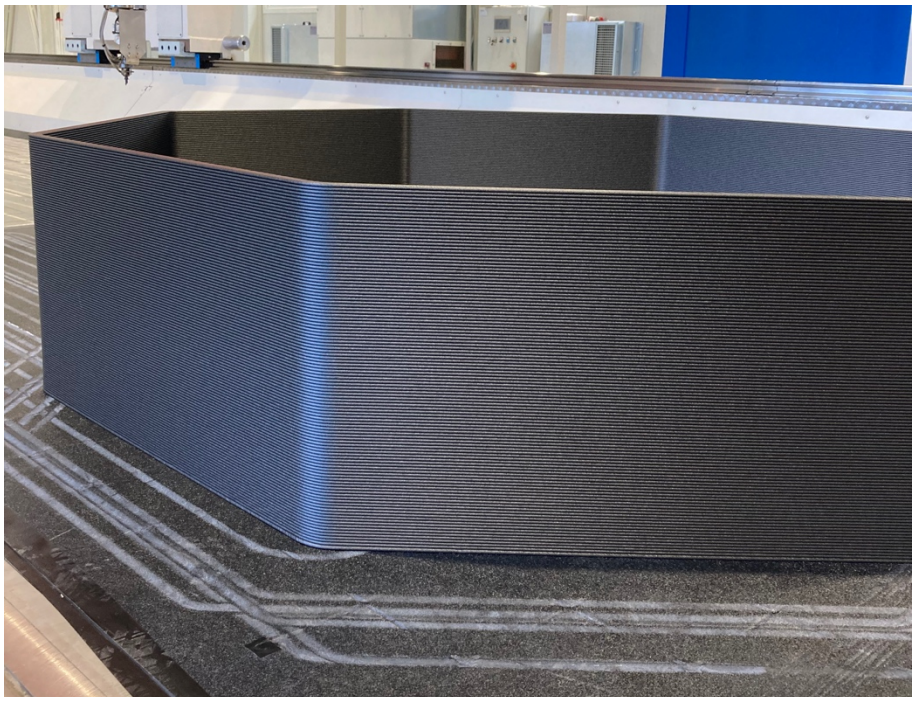

Figure 35 - Octagon printed in recycled material

Due to the impossibility of extracting and testing samples from the rough octagon, the sides have been cut to obtain eight single panels. Since the width of a bead, as indicated previously, was equal to 19 mm, the surface needed also to be milled to achieve the standard required for the mechanical characterization of reinforced composites. The reference standard for the mechanical testing of fiber-reinforced composites used has been the ISO 527-4:1997. With a required width up to 10 mm, the panels have been milled to achieve a 9 mm thickness. Since each panel had to be clamped to a block to keep it in place while milling, the useful surface to extract the panel has been reduced from 500x390x9 mm to 420x390x9 mm.

Considering previous experiences with mechanical tests performed on WHAM printed materials, the machine managers also pointed out a substantial difference in properties depending on the direction of specimen extraction, along the bead or between the beads. This is due to the characteristics of the process, in fact, if a

specimen is tested along the deposition direction, axis x in the picture below (Fig. 36) the mechanical properties will be given by the material. In contrast, if the specimen is tested along the direction perpendicular to the printing direction, z axis in the image, the mechanical properties are given by the adhesion of between the layers.

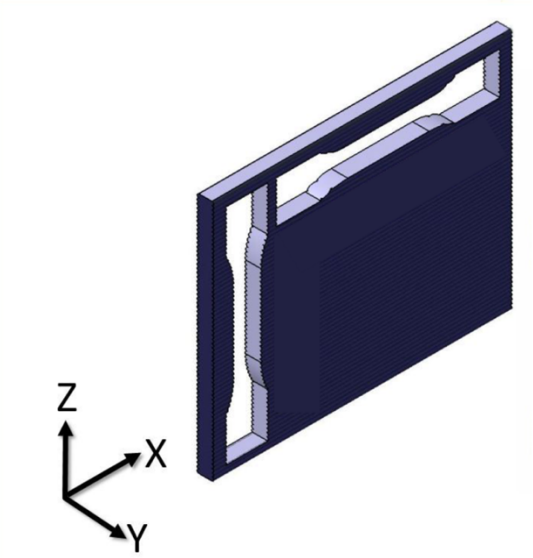

Figure 36 - Representation of the panel used to extract the specimens with the related orientation

According to the standard previously introduced, specimens "dog-bone-shaped", as represented in the following figure (Fig. 37), has been designed, respecting the parameters that are indicated in Table 7, compliant to the ISO 527-4:1997 standards.

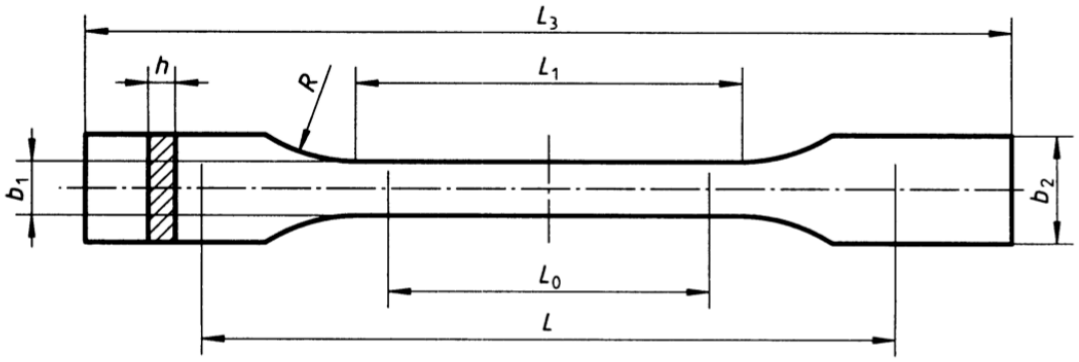

Figure 37 - Specimens' shape

Parameter	Name	Value
b_1	Width of narrow portion	10 mm
b_2	Width at ends	20 mm
L	Initial distance between grips	115 mm
L_0	Gauge length	50 mm
L_1	Length of narrow parallel-sided portion	60 mm
L_3	Overall length	200 mm
h	Thickness	9 mm
R	Radius	60 mm

Table 7 - Summary of the specimen parameters

As previously anticipated, the output variables to be analyzed are the mechanical properties of the materials. In particular, the results requested by the managers have been:

- Tensile modulus
- Young's Modulus.

The variables that have been decided to be tested linked to the expected responses are the following:

- Type of material (Virgin – Blended)
- Orientation of extraction (Along the bead – Between the beads)

According to the experience of the managers supervising the project, it has been decided to test 10 specimens for each combination of the variables. The total number of specimens extracted and tested has been 40. The following step to be achieved has been the design for the correct extraction plan of the specimens from the panels.
Hereafter (Fig. 38 and Fig. 39) are represented the finished panels from which the samples have been produced. The letter on the top-left side of the image represents the material of the panel: "R" indicates the blend material while "V" indicates the virgin one.

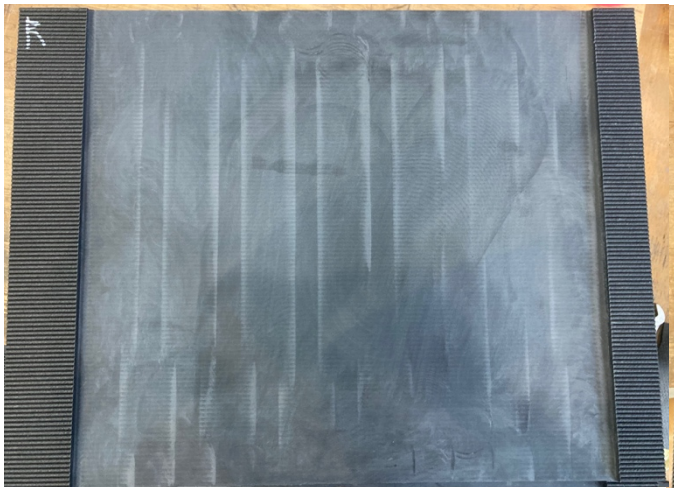

Figure 38 - Recycled panel

Figure 39 - Virgin panel

As anticipated before, the useful area to extract the specimens has been reduced to 420x390x9 mm, due to the unfinished surfaces visible in the pictures above. To enhance the variability and contain costs and complexity related to the extraction of the samples, it has been decided to use the lowest numbers of panels utilizing at least two panels per material. To do that, a maximum of 10 specimens could be extracted from the same panel. With this constraint, the work of designing a suitable extraction plan has begun. Due to the sample's dimensions previously reported, it has not been possible to include 10 shapes in every console. The alignment has been rearranged and a maximum of 8 specimens, 4 for every extraction dimension, have been settled. Moreover, all samples have been marked to be recognized and to potentially reconstruct their position within the panel. In the next image it is presented a picture of the extraction plan (Fig. 40) and the relative position of each specimen in the panel.

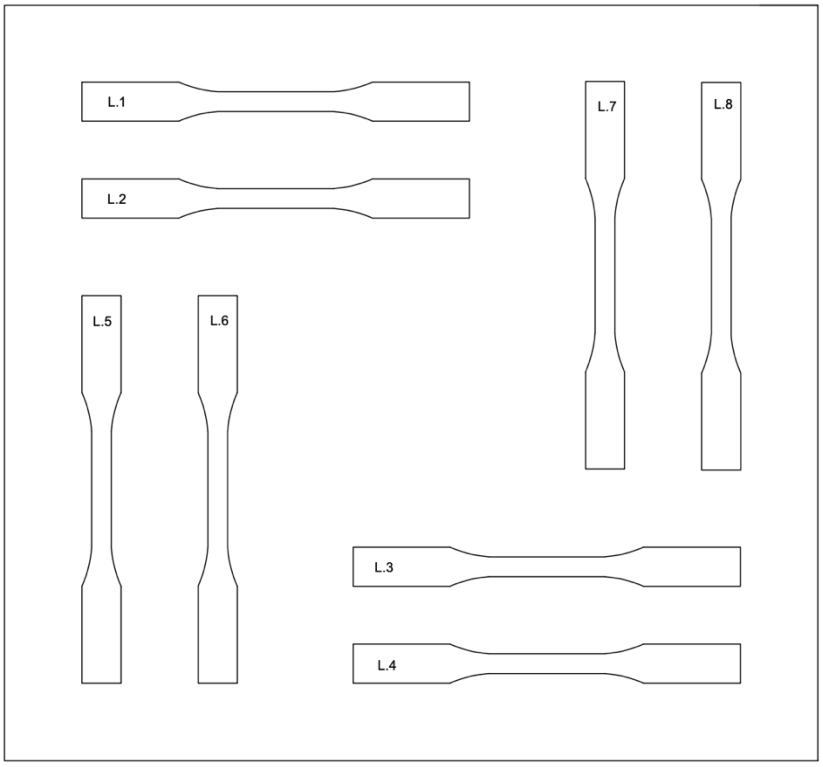

Figure 40 - Specimens' position inside the panel and related notation

To be more precise and provide reference points, the capital letter "L" represents the number of the panel (ranging 2 to 7) from which the specimens have been extracted, while the following numbers have helped to take note of the position of the specimens inside the panel. As it is noticeable, from 1 to 4 are numbered the samples that have been extracted along the x direction, or along the deposition direction of the beads, while the numbers from 5 to 8 indicates those specimens extracted along the z direction. To provide a complete picture of the position of the specimens it is worth noting that the upper part of the panel shown in the figure above represents the top of the panel.

To remove the specimens from the panels it has been used a waterjet cutting machine with a water pressure of 380 MPa mixed with abrasive sand, since the water itself at that pressure would not have been able to drill the material. To compensate the waterjet process, the width of the specimens has been increased by 0.2 mm. On a working day, a total of forty-eight specimens have been extracted, forty for the actual experimentation and to be mechanically tested, and the remaining eight as backup in

case something would not have gone according to the planning phase. The above-presented notification to recognize the specimens have also been used as reference order to extract the specimens from the panels, as exemplified in the picture below (Fig. 41).

Figure 41 - Cutting of specimens 1-2-3-4 from panel V3

In particular, in the picture above the cutting of the specimens numbered as 3.1-3.2-3.3-3.4 can be seen, as well as the striations due to the milling process can be noted. Moreover, the side bands of the layers give another indication of the extraction direction of the samples. Once extracted, the specimens have been tagged in order to be recognized and prepared for the mechanical testing.
In the next paragraph the results of the mechanical tests will be presented and discussed.

2.3.2 Results of mechanical tests

As previously mentioned, mechanical tests have been performed on the specimens previously described and following the standard reference for composite materials ISO 527:4:1997. The two factors considered for the analysis have been the material used to print the specimens and the orientation of extraction. The output data related to those factors have been the ultimate tensile strength and the tensile modulus or

Young's modulus. To analyze the relationships between the input variables and the outputs, the statistics technique of ANOVA has been used. As mentioned before, the DOE has been designed using two factors selected as relevant with two values, for a total of four combinations for the factors. Every run for each combination has been repeated ten times, for a grand total of eighty output values. The DOE just described is summarized in the following table (Table 8).

	Factors		Ultimate Tensile Strength			Young's Modulus		
Scenario	**Material**	**Orientation**	1	…	10	1	…	10
1	Virgin	X						
2	Virgin	Z						
3	Blend	X						
4	Blend	Z						

Table 8 - Summary of the DOE

The results have then been processed by the software Minitab to perform the ANOVA analysis and to obtain meaningful results aimed at representing the influence of the studied factors on the outputs of mechanical properties.
In the picture below (Fig. 42) the individual value plot for the values of ultimate tensile strength is presented.

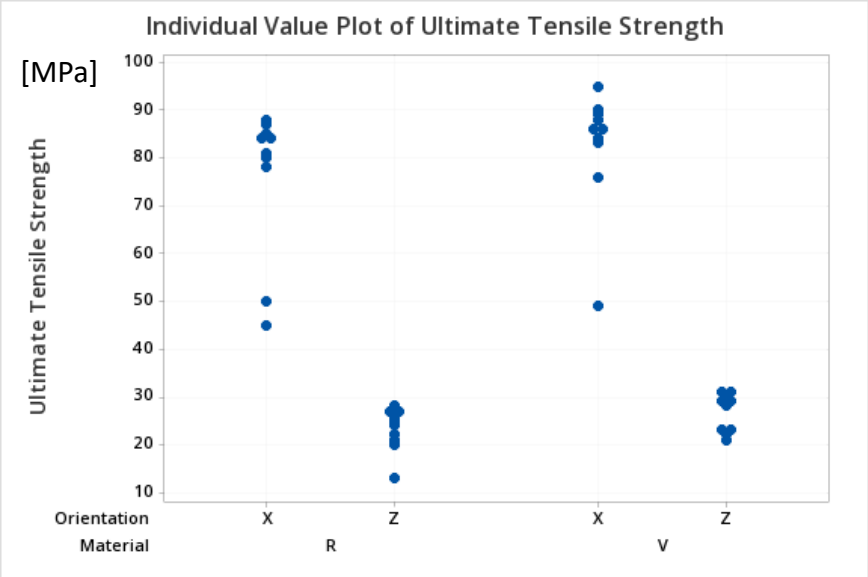

Figure 42 - Individual value plot for tensile strength

As can be noticed form the previous picture, data are grouped for the two variables analyzed, the material, indicated as "R" for blended and "V" for virgin, and the orientation of the specimens. As also predicted by the material data sheets, there is a clear difference in mechanical properties, taking the same material as a reference, between the x and z orientation. Excluding the three outliers related to the extraction direction x and considering, this time, the material, it cannot be highlighted a marked difference in properties between the virgin and the blended material. Moreover, the variability of the results is visible in the results for both the orientations. At the same time, percentage variability is higher for the orientation on the z axis.
In order to deepen the analysis and to draw results based on quantitative analysis, it has been decided to report the interaction plot concerning the ultimate tensile strength (Fig. 43).

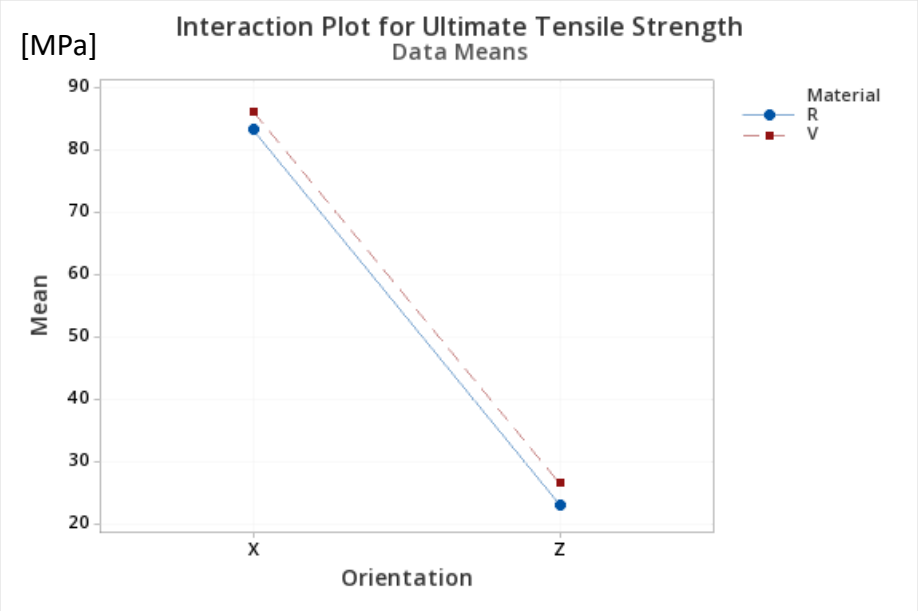

Figure 43 - Interaction plot for Ultimate Tensile Strength

From the image just presented, the orientation of extraction of the specimens is predominant in the evaluation of the mechanical properties of the material, with the average tensile strength that change from 26 MPa to 86 MPa depending on the orientation considered. On the other hand, it can also be seen that the material also plays an important role in the value of the mechanical properties. In fact, the blue line representing the blended material is slightly below the line representing the properties of the virgin material, underlining a decrease in the values considered due to the recycling process of the material.

In order to complete the quantitative assessment and draw conclusions regarding the impact of the material and the orientation on ultimate tensile strength, it has been decided to perform an ANOVA analysis and analyze the results, excluding the values previously identified as outliers. The next image (Fig. 45) shows the analysis as processed using Minitab software. To properly perform the ANOVA analysis, a data transformation indicated as optimal directly by the software and represented in the first point of the image was applied. As can be seen in the "Analysis of Variance" section, particular attention should be paid to the p-value which indicates the statistical incidence of the parameter considered in influencing the output, in this case the ultimate tensile strength. As a threshold value for the p-value, it is usually taken 0.05, so if the value is lower it means that the parameter considered has a statistical impact on the output.

WORKSHEET 1

General Linear Model: Ultimate Tensile Strength versus Material; Orientation

Method

Factor coding	(-1; 0; +1)

Box-Cox transformation	
Rounded λ	1
Estimated λ	1,01337
95% CI for λ	(0,670874; 1,35987)

Factor Information

Factor	Type	Levels	Values
Material	Fixed	2	R; V
Orientation	Fixed	2	X; Z

Analysis of Variance

Source	DF	Adj SS	Adj MS	F-Value	P-Value
Material	1	92,7	92,7	4,84	0,035
Orientation	1	32858,8	32858,8	1715,52	0,000
Material*Orientation	1	0,4	0,4	0,02	0,879
Error	33	632,1	19,2		
Total	36	33743,2			

Model Summary

S	R-sq	R-sq(adj)	R-sq(pred)
4,37650	98,13%	97,96%	97,65%

Figure 44 - ANOVA results for Ultimate Tensile Strength

Made this premise and considering the results of the analysis, it can be noted that both variables have a statistical influence on the output, with the orientation being predominant having a higher F-value. On the other hand, the interaction between the variable does not have any influence on the output. Moreover, the R-sq (adj) of the model, used to evaluate its accuracy, is particularly effective in predicting the outcomes. To certify the accuracy of the results, it should also be added that both tests to verify the normality of the residuals and the equal variances have been carried out successfully.
Considering the analysis presented above, it can be concluded that both variables, material and orientation, are statistically significant in influencing the ultimate tensile strength of the specimens, causing a reduction equal to 3 MPa for both the directions.

Hereafter the same analysis regarding the Young's Modulus is presented.
As well as the analysis performed for the ultimate tensile strength, the same steps have been followed in analyzing the impact of the material and orientation variables with respect to Young's modulus. The first step involved the graphical representation of the values obtained experimentally for the Young's Modulus of all the specimens. In the next picture (Fig. 45) the individual value plot of the values is presented.

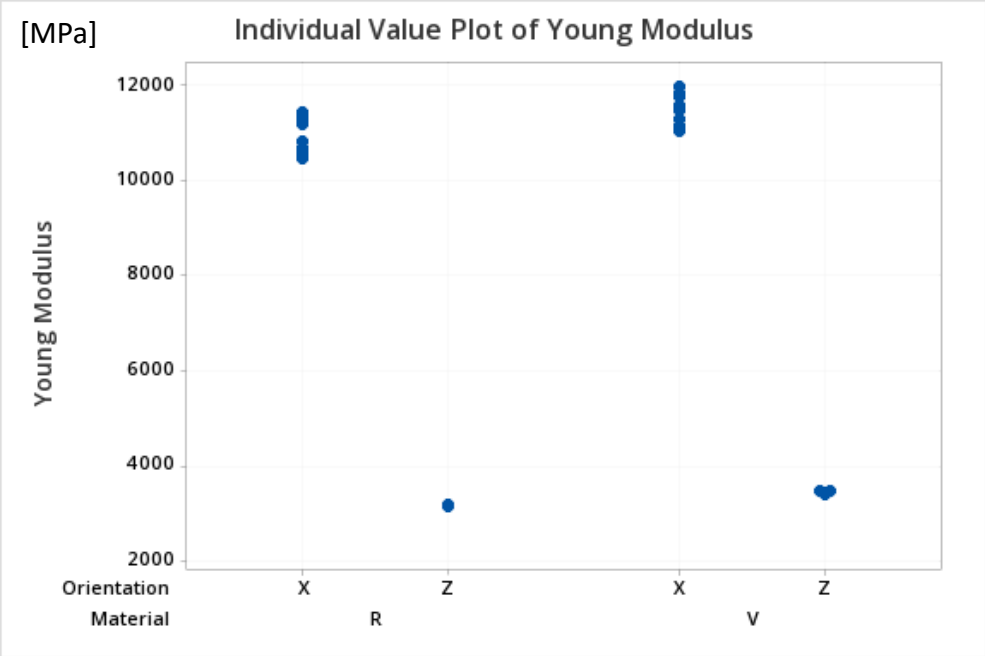

Figure 45 - Individual value plot for the Young's modulus

As can be seen from the image, in this case and unlike the ultimate tensile strength values, all values are consistent with each other and there are no outliers to eliminate before proceeding with the analysis. As in the previous case, the next step involved the elaboration of the interaction plot (Fig. 46) in order to provide a first assessment of the impact of the variables on the outcome considered. Similarly to the previous analysis, it can be seen that the Young's Modulus is significantly different when considering the orientation extraction of the specimens, while it differs to a much lesser extent when looking at the type of material. Indeed, the virgin material turns out to have higher values for both orientations. However, even in this case, the z orientation has significantly lower values in terms of mechanical properties than the x orientation. Moreover, the recycled material turns out to have, in general, worse mechanical properties than the virgin material.

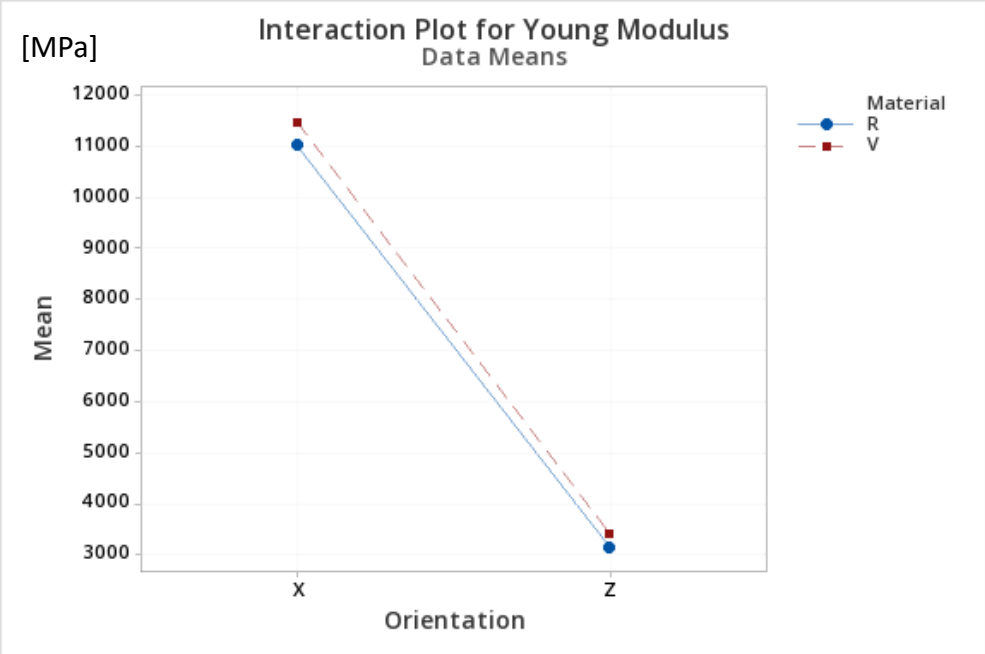

Figure 46 - Interaction plot for Young's Modulus

To complete the quantitative assessment and draw conclusions regarding the impact of the material and the orientation on Young's Modulus, an ANOVA analysis has been performed. Even in this case, to properly perform the ANOVA, a data transformation indicated as optimal was applied, as indicated in the first part of figure 47. As pointed out in the section concerning the "Analysis of Variance", in this case the variables and its interaction are statistically relevant in influencing the

outcome. Even in this case the orientation is the dominant factor when looking at the F-value. The reference parameter for evaluating the model, the R-sq (adj), is very high and close to 100%, showing the accuracy of the statistical model developed by the software Minitab. To be more precise, even in this case, the normality of the residuals and the test for equal variances have been performed and verified. Considering the above-stated results, thanks to the ANOVA analysis just presented, it can be concluded that the factors material, orientation and also their interaction affect the Young Modulus causing a decrease quantified in 500 MPa.

WORKSHEET 1

General Linear Model: Young Modulus versus Material; Orientation

Method

Factor coding	(-1; 0; +1)

Box-Cox transformation	
Rounded λ	-1
Estimated λ	-1,10159
95% CI for λ	(*; *)

Factor Information

Factor	Type	Levels	Values
Material	Fixed	2	R; V
Orientation	Fixed	2	X; Z

Analysis of Variance for Transformed Response

Source	DF	Adj SS	Adj MS	F-Value	P-Value
Material	1	0,000000	0,000000	301,03	0,000
Orientation	1	0,000000	0,000000	71965,97	0,000
Material*Orientation	1	0,000000	0,000000	161,11	0,000
Error	36	0,000000	0,000000		
Total	39	0,000000			

Model Summary for Transformed Response

S	R-sq	R-sq(adj)	R-sq(pred)
0,0000025	99,95%	99,95%	99,94%

Figure 47 - ANOVA results for Young Modulus

However, it should be noted that, since the variability of Young Modulus of z-orientation is almost null (even after Box-Cox transformation), the result of ANOVA must be interpreted carefully. Nevertheless, figure 44 highlight similar results of ultimate tensile strength, i.e., modest reduction of performances along x-orientation.

In the next paragraph the results of this chapter are summarized, discussing the environmental sustainability of the process of mechanically recycling the material, its economic feasibility and the evaluation of the mechanical properties just presented.

2.3.3 Final remarks

This section is intended to briefly summarize everything discussed in this chapter. Firstly, it has been demonstrated that it is convenient from an environmentally point of view pursuing a strategy for mechanical recycling the 3D printed polymer ABS filled with 20% of carbon fiber. In fact, for producing 1 kg of the virgin material, 8,8 kg of CO_2 are emitted into the atmosphere, against the 0,8 kg and 2,1 kg for its recycling, depending on the type of machinery considered for the grinding process. Similarly, the economic feasibility of the process has been evaluated considering two different scenarios for the purchase of two different shredders, a small shredder traditionally used for injection molded parts and an industrial one. In this case, it has been demonstrated that recycling quantity bigger than 500 kg a year it is economically convenient. For further details see paragraph 2.2.2. Finally, the mechanical properties of the blended material composed by 80% of virgin material and 20% of recycled material has been tested through the ISO 527-4:1997 standards. The results of the mechanical tests, in particular for the Ultimate Tensile Strength and the Young's Modulus, have highlighted a statistical dependence of the output variables with respect to the studied variables, the material and the extraction's orientations. In particular, the blended material has obtained lower results in terms of mechanical properties than the virgin material.
The next chapter will discuss the second part of this work, concerning the thermal analysis of data collected during printing in order to better understand the characteristics of the process.

3. Thermal monitoring for WHAM

As anticipated previously, in this section the work performed on the Ingersoll MasterPrint in analyzing the cooling process of the layers from a single-layer perspective is presented. The objective of thermal monitoring of the WHAM printing process is to better understand the peculiarity of the proceeding and to clarify the mechanisms that play a significant role in material cooling. As pointed out before, material cooling is a critical process concerning the quality of the printed part. In fact, an incorrect colling of the part could result in defects like delamination and warping, preventing the application of the printed part and resulting in material waste. This is a preliminary evaluation for thermal monitoring a WHAM 3D printed part. Firstly, the experiment setup will be described, discussing the instrumentation used for data collection. Then, before the analysis of the result and the conclusions, a section is dedicated for the discussion of the extraction and the pre-processing of the thermal data.
Further developments of this work may consist of economical and practical evaluation for installing in-situ monitoring devices to actively control the process.

3.1 Experimental campaign

To achieve the aforementioned objectives, we have monitored the realization of an artifact produced by the Ingersoll Masterprint. In particular, it has been monitored the printing at 45° of a decorative panel realized in ABS reinforced with 20% of short glass fibers. The possibility to print with the nozzle inclined at 45 degrees respect to the printing plane, as represented in the next figure (Fig. 48), has made possible the realization of the piece with an internal cavity without using supports, allowing to save material and to decrease the final weight of the object. The nominal dimensions of the panel are 2 meters x 1 meter x 0.15 meters.

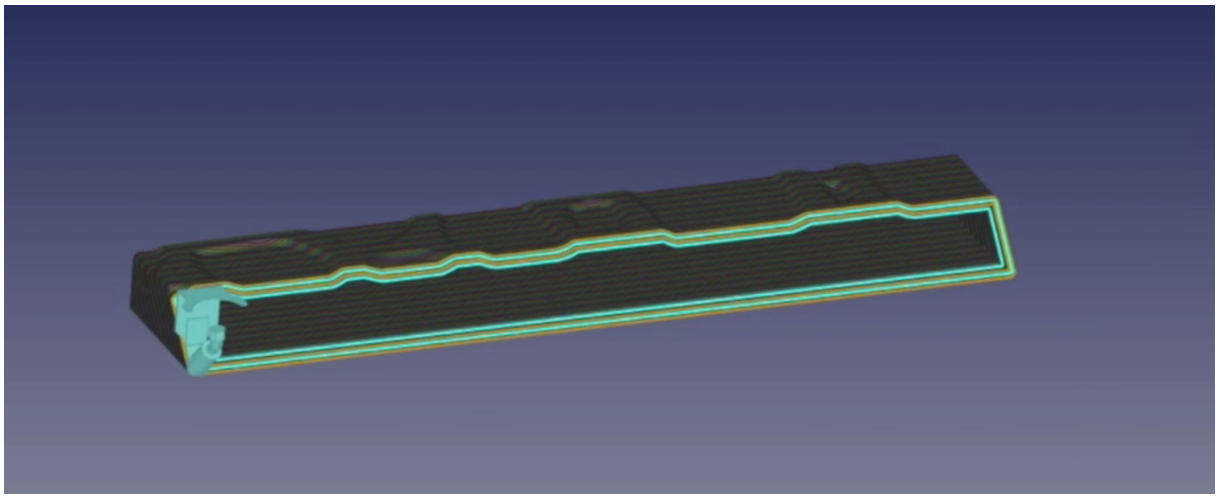

Figure 48 - Simulation of 45° printing of the panel

Following the productive process, the material has been dried for a total of 5 hours at 93°C in order to remove moisture from the pellets and prevent printing problems. The layer time has been set to 160 seconds, giving the material the time to cool down before the deposition of the subsequent layer. Consequently, the extrusion speed has been about 60 mm/second for a deposition rate of almost 18 kilograms/hour. The extrusion temperature indicated by the supplier for this material is 256°C, so the machine has been set to deposit the material at the temperature already indicated. The air temperature at the time was around 18°C. Moreover, the artifact has been printed on a sheet of ABS positioned on the printing plane to enhance the final detachment of the piece. The main characteristic of the printed part concerns the number of beads in one layer: indeed, two beads per layer have been printed. Hereafter (Fig. 49) an image of the piece during the printing is presented, showing the double-bead structure.

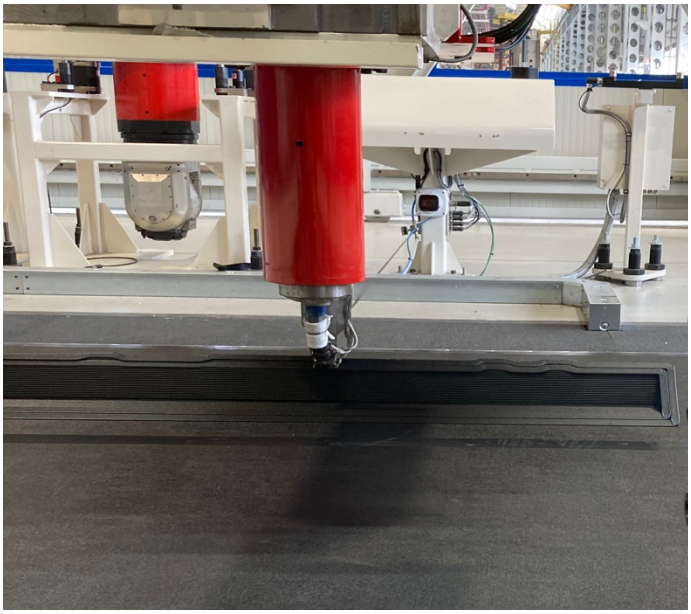

Figure 49 - Printing of the decorative panel, it is noticeable the double-bead structure

Process parameters are reported in the following table (Table 9) summarizing information regarding the environmental condition of the printing.

Parameter	Value
Air temperature	18°C
Material used	ABS 20% glass fiber reinforced
Extrusion temperature (process parameters)	256°C
Heated chamber	No
Heated platform	No
Extrusion speed	60 mm/sec
Density of the material	1.24 g/cm^3

Table 9 – Environmental conditions

To monitor the process from a thermal point of view, some devices have been brought directly to the printing chamber to assemble a monitoring system to collect

precious data. To be more precise, the instrumentation used for the experiment was composed by:

- Scientific thermo-camera FLIR X6900 SC, sensitivity of 20 mK
- 25mm focal lens to collect data from the different parts of the layer
- Tripod
- Computer capable of processing .ats files (for the collection of data coming from the images detected by the camera)
- Monitor used to visualize the parameters of the camera.

The thermal imaging camera, installed on the tripod, was positioned at 3.5 meters from the printed part in order to frame the entire section of the part during printing, using the 25 mm lens. After some iteration to determine the acquisition parameters to capture the material temperature, the video recording began. In particular, the parameters set on the thermo-camera concerned the emissivity of the material, the temperature range for collecting data, the frequency for image acquisition and the recorded time per video. All the parameters set have been reported in the following table (Table 10).

Parameter	Value
Distance nozzle-camera	3.5 meters
Emissivity of the material	0.92
Frequency of image collection	0.5 Hz
Frames recorded	170
Effective time recorded	340 seconds
Temperature range recorded	146-350°C
Interval between two consecutive videos	10 seconds

Table 10 - Parameters set on the thermo-camera

It can be noticed that, even if the layer time was equal to 160 seconds, the duration of the acquisition for one video has been 340 seconds. This number has been chosen considering the acquisition of two entire layers with a 20-second safety-interval to

ensure the correct acquisition. Moreover, a time window of 10 seconds has been left to ensure the correct saving of the video on the computer.
To give a complete perspective of the experiment, in the following figure (Fig. 50) is presented a picture and a scheme to clarify the physical setup and to explain the phase of preparation. As we can notice, on the right side of the image there is the FLIR's camera used for the data collection while, on the left side of the picture, there is the ongoing printing of the panel in ABS reinforced with 20% of short glass fibers. Below them, it is presented a lateral view of the setup. As previously anticipated, the focal length of the camera was equal to 25 mm, able to embrace the entire layer's figure inside the video. On the other hand, the scheme represents the setup seen from above and laterally, showing the position of the camera respect to the printed piece. In particular, the thermal imaging camera has been positioned to get a central perspective of the printed part.

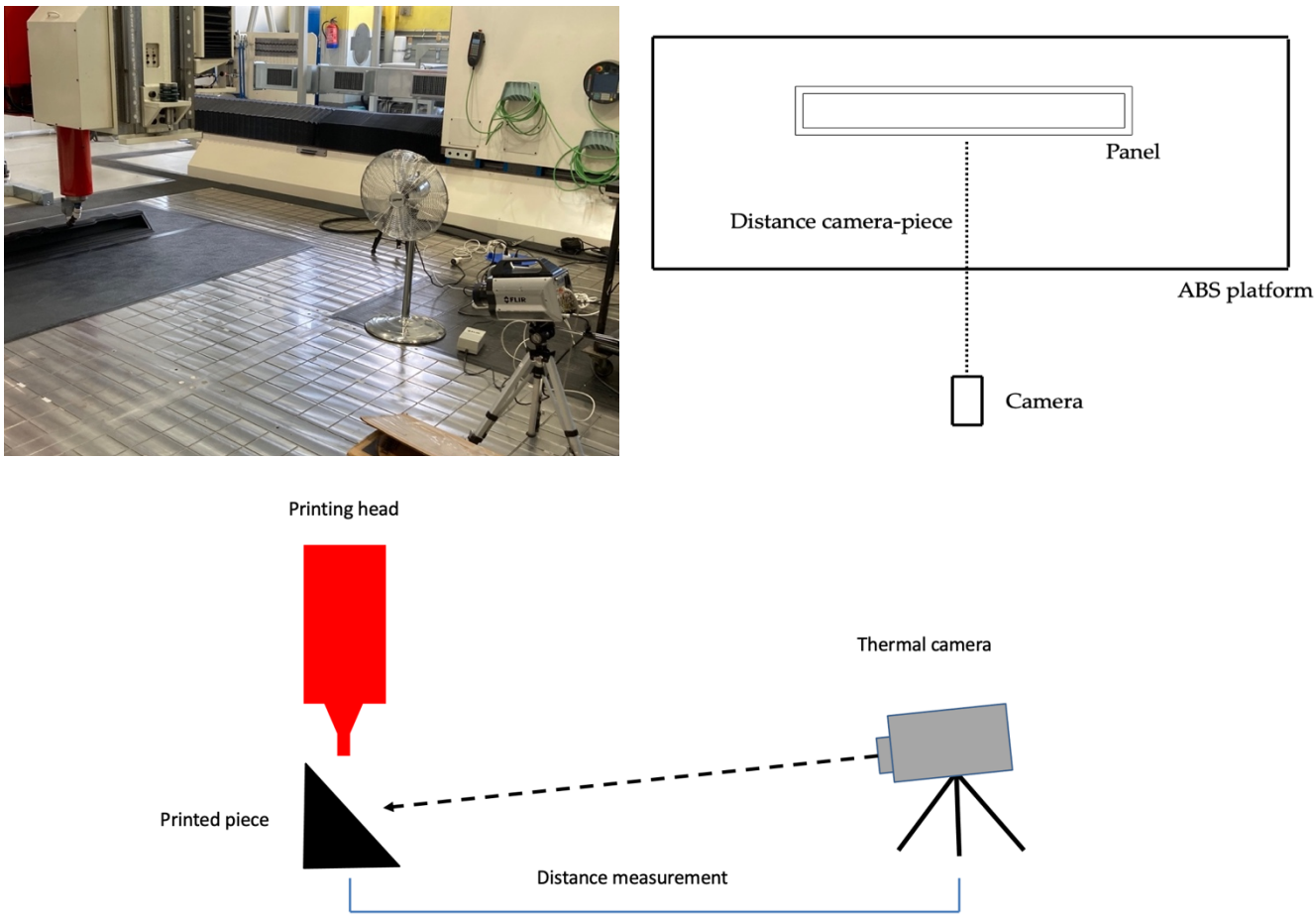

Figure 50 - Setup for data collection and schemes

With this arrangement of the instrumentation and with the parameters set as described above, four videos have been recorded around layer number twenty, filming the deposition of eight consecutive layers. They have been called Video L0, Video L2, Video L4 and Video L6, assigning the numbers to the first layer captured for each video. In the next paragraphs the methodologies for data collection and data preprocessing will be presented. Finally, an entire section will be dedicated to the qualitative analysis of the temperature profile, reaching important conclusions based on data collected.

3.2 Data extraction

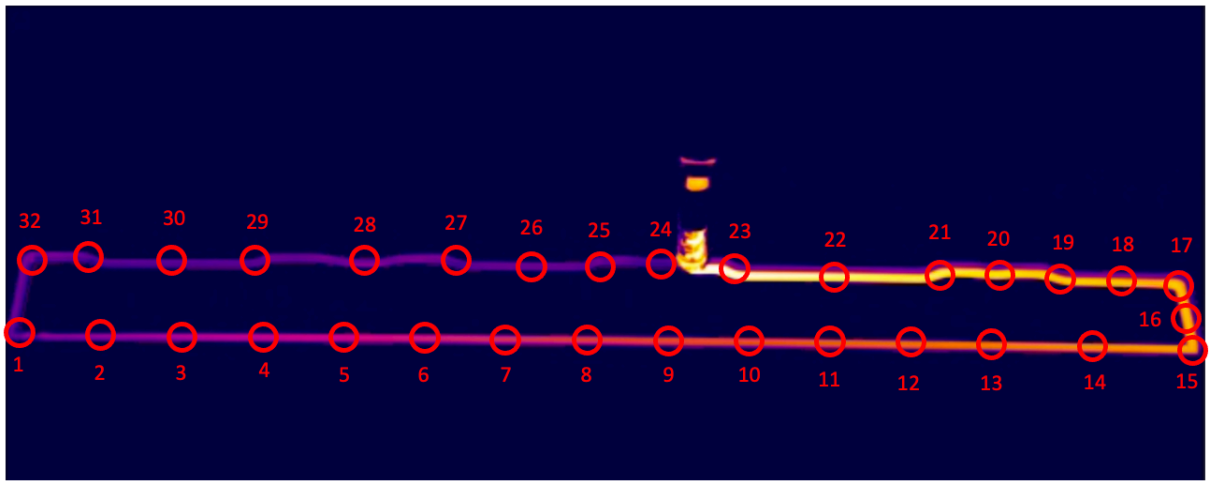

Figure 51 - Representation of the selected ROI with related numbers

To collect meaningful and consistent data, some regions of interest (ROIs) have been defined on the printed part. In particular, the complete area caught by the camera is a window of 640x512 pixels in which the cooling of the layers has been recorded. Since the printed artifact is composed of a double-bead layer, it has been decided to consider the ROIs on both the external and internal bead. Considering the part's nominal length, it was possible to estimate the pixel dimension to 3,2 mm. A single ROI consists in a region of 9 pixels, using a 3x3 area. The average temperature of the area is reported as a single data. This process has been possible because the width of one bead was equal to 6 pixels (19.2 mm). In total 32 ROIs have been identified along the layer profile for the internal and external beads. The ROIs have been named in

ascending order following the extruder path, starting from the low-left angle. In figure 47 only the ROIs for the internal bead are presented, to avoid the overlapping of the markers. For completeness, it must be reported that the ROIs identified on the external bead have been taken exactly in correspondence of those for the internal bead in order to evaluate the behavior of both the beads. Moreover, apart from the 4 angles indicated as regions 1-15-17-32, the regions between 2 and 14 have been chosen as equidistant from one another, and the ones between 18 and 31 have been chosen in correspondence of rectilinear and curve paths of the extruder.
In particular, it was noted that for ROI number 32 the data were not in line with those collected due to a prolonged overlap with the extruder, so they have been eliminated from the dataset. To exemplify the concept hereafter is presented a graph for ROI 32 (Fig. 52).

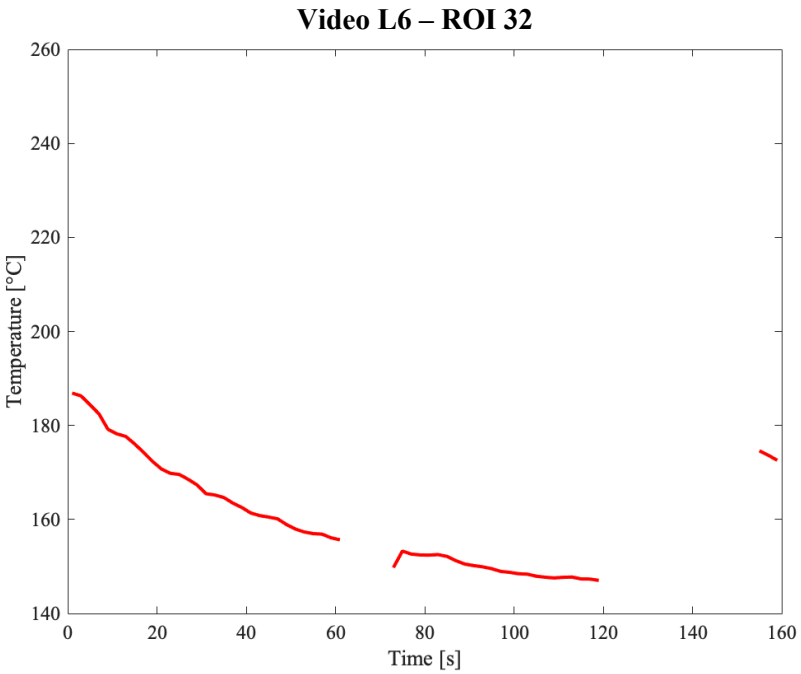

Figure 52 - Graph for ROI 32, Video L6

Once defined the ROIs, the following step has been the collection of thermal data from the selected region starting from the video recorded. To do that, a MATLAB script capable of analyzing fixed coordinates of the .ats files registered by the camera have been used. At the beginning of the data collection phase, it has been noted that, due to the low definition of the images, the ROIs tended to move and alter its coordinates along the video. To overcome this problem and ensure the ROIs to

remain stable during data acquisition, a dynamic method of selecting coordinates and making graphs have been developed. Based on variables of the original code, which is not reported due to its length, a way of visualizing the correct data acquisition point has been developed. The code has been developed in MATLAB. In particular, the following instructions has been used:

Algorithm 1 Area visualization	
1:	Create the figure
2:	Create a mask to be overlapped to the image used for data collection
3:	Select the coordinates for the mask on the map of the video
4:	Return the image of the mask overlapped the video
5:	Select the required frame to be shown for the video

To clarify the usefulness of this step, the following images have been presented (Fig. 53 and Fig. 54).

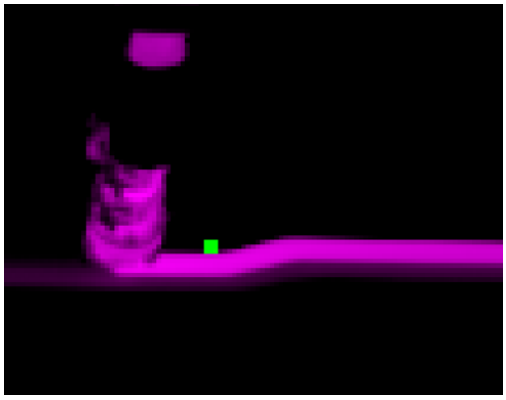

Figure 53 - Wrong area for data collection

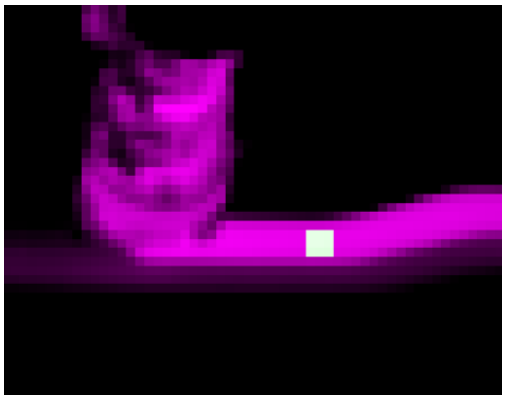

Figure 54 - Correct area for data collection

As it is noticeable from the figure above, the selection of the correct area in order to collect the thermal data it is fundamental. In fact, since the data returned is the mean of data coming from the nine-pixels-area, the wrong zone selection can lead to incorrect acquisition. The code above-mentioned has helped in the definition of the correct zone and in guaranteeing the consistency of the data collected.

Once the area has been successfully identified, the following step consisted in acquiring data from every ROI identified for every video recorded. Since every video included, on average, the printing of two consecutive layers, it has been decided to

focus on the thermal data of one complete layer, since the acquisition of other data has been compromised by the 10-seconds lag between two consecutive videos.
In the next paragraph the method for data preparation will be discussed.

3.3 Data preprocessing

Hereafter (Fig. 55) is presented a first graphical output returned for ROI number 25, video L0, exemplifying all the others collected. The line represents the changing in temperature during time for the area considered, and the spikes and the valleys are present due to the transit of the extrusion nozzle in front of the region of interest. In fact, the passing of the nozzle is unavoidable and its overlapping with the ROI alter the data collected. In particular, when data are acquired from the areas of the nozzle that are insulated the spike is addressed to 146°C. On the other hand, when it comes to parts where the heat of the material gets through the components, we have upward spikes.

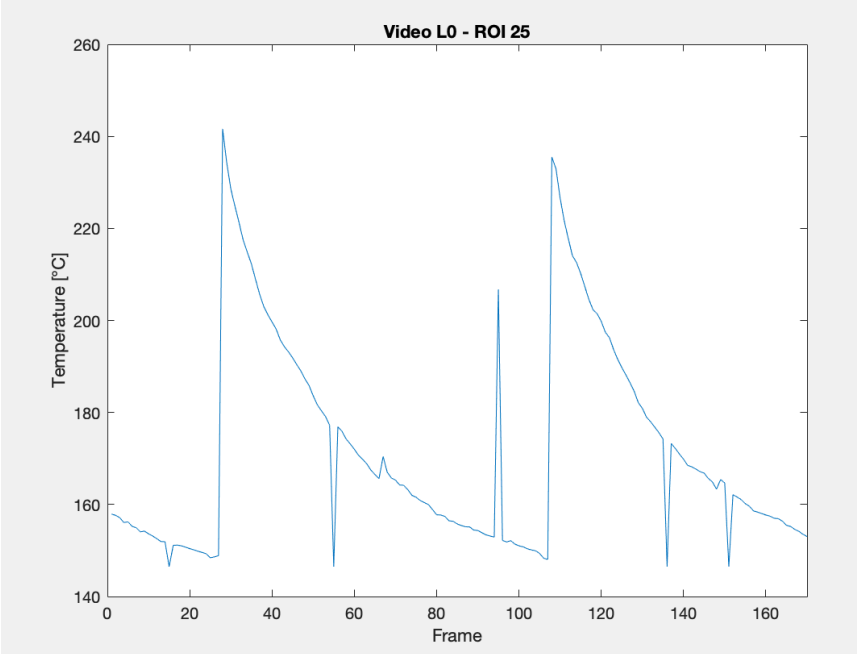

Figure 55 - Graphical representation of ROI 25 for video L0

As can be seen from the figure above, given the sampling interval longer than the time to deposit two layers, there are two partial cooling profiles and only one is

completed. Given this characteristic of the data collected, it has been decided to consider and analyze the layer's profile without missing data. The dataset dimension has been cut to 20000 data due to this shrewdness. The next step necessary to analyze the collected data involved a qualitative analysis to assess the consistency of the data. As mentioned before, data concerning ROI number 32 have been eliminated due to the prolonged overlap of the extruder. This is due to a prolonged extruder overlap in the data collection area due to the adjacent positioning of the start and stop point for the beginning of the new layer.

Another operation that was carried out on the data to eliminate the values vitiated by the passage of the extruder in front of the collection area, was the cancellation of the peaks and valleys created by this overlap. In fact, as we can see from the next figure (Fig. 56), there are two peaks and a valley that cannot be explained by the cooling of the material but are proven by the passage of the extruder in the point of interest. In particular, it can be seen that the ROI considered, number 17 for Video L0, is located in the upper right corner: this explains the inconsistent data exactly in the middle of the graph, due to the passage of the extruder in the adjacent bead. The last peak, instead, is due to the deposition of the next layer in the data collection point.

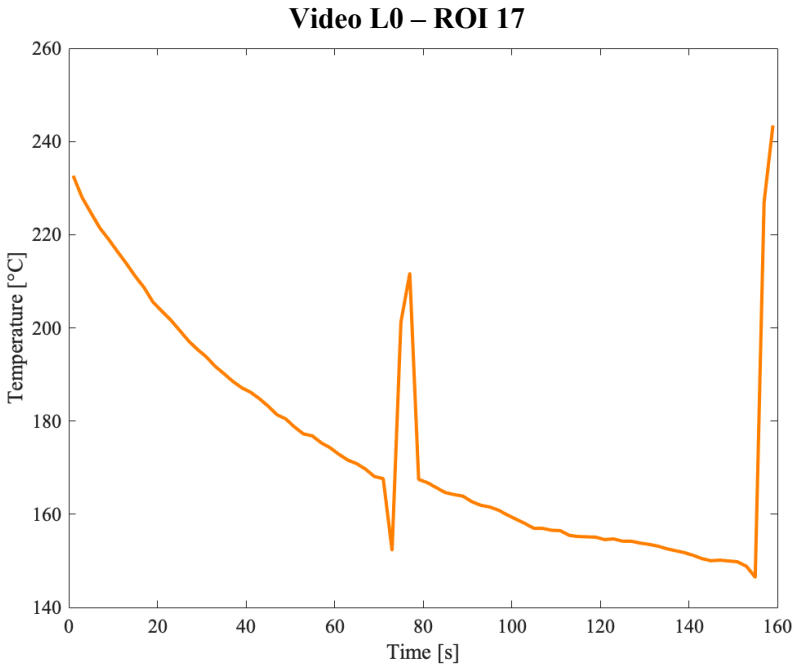

Figure 56 - Thermal profile for ROI 17 before data pre-processing

In order to eliminate these inconsistent data, simple operations were performed on data whose gradients overcome the ± 3-sigma confidence interval from data average. A critical issue that was present for ROIs between #1 and #15 in the external bead involved the loss of collected data. Since the set temperature range ranged from 146 to 350°C, all values below the lower bound result in a plateau. This is exemplified by the following figure (Fig. 57).

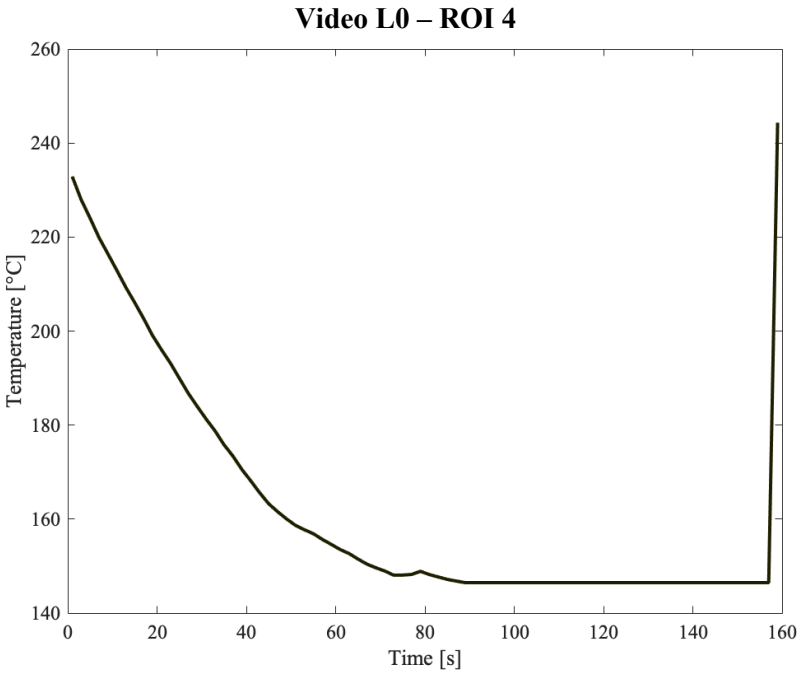

Figure 57 - Image for ROI 4, from 90 s to 150 s the plateau can be seen

In order to clean the dataset from those inconsistent value, some lines of code have been written to directly solve the last issues identified, changing those values with NaN values.

The result of these operations has led to a more consistent dataset, returning graphs without peaks, valleys or plateaus due to factors unrelated to the cooling of the material. An example of a "clean" profile can be seen in the following figure (Fig. 58), where the previously reported code has been applied for ROI number 17, represented in figure 52.

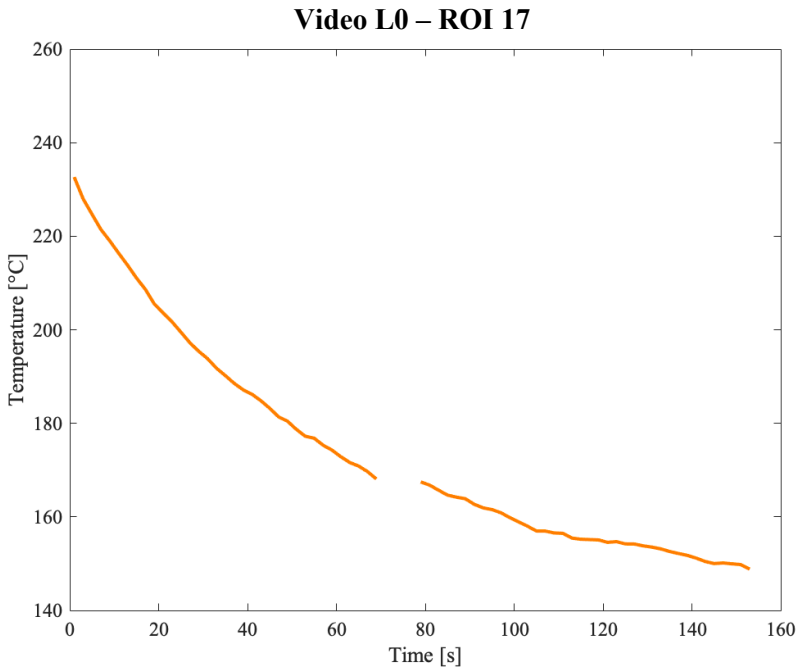

Figure 58 - Profile for ROI 17, with data preprocessing applied

Having concluded the premise regarding the way in which the data have been processed to draw optimal conclusions, in the next paragraphs will be discussed the qualitative analysis carried out on the dataset modified as indicated above. In particular, the objective of this experimentation is a preliminary evaluation of the cooling process for WHAM. Mainly qualitative evaluation will be presented, even if based on data gathered by the thermal camera during the experimentation.

3.4 Temperature profile analysis

In this paragraph we will describe the procedures adopted to draw initial qualitative conclusions on the thermal analysis of the cooling process for Wide and High Additive Manufacturing. Firstly, there have been charted the cooling profiles of all

ROIs, sorted by color, identified for each video, separating, for overlapping issues, the ROIs collected on the external bead from those on the internal bead. The profiles are presented in the figure hereafter (Fig. 59).

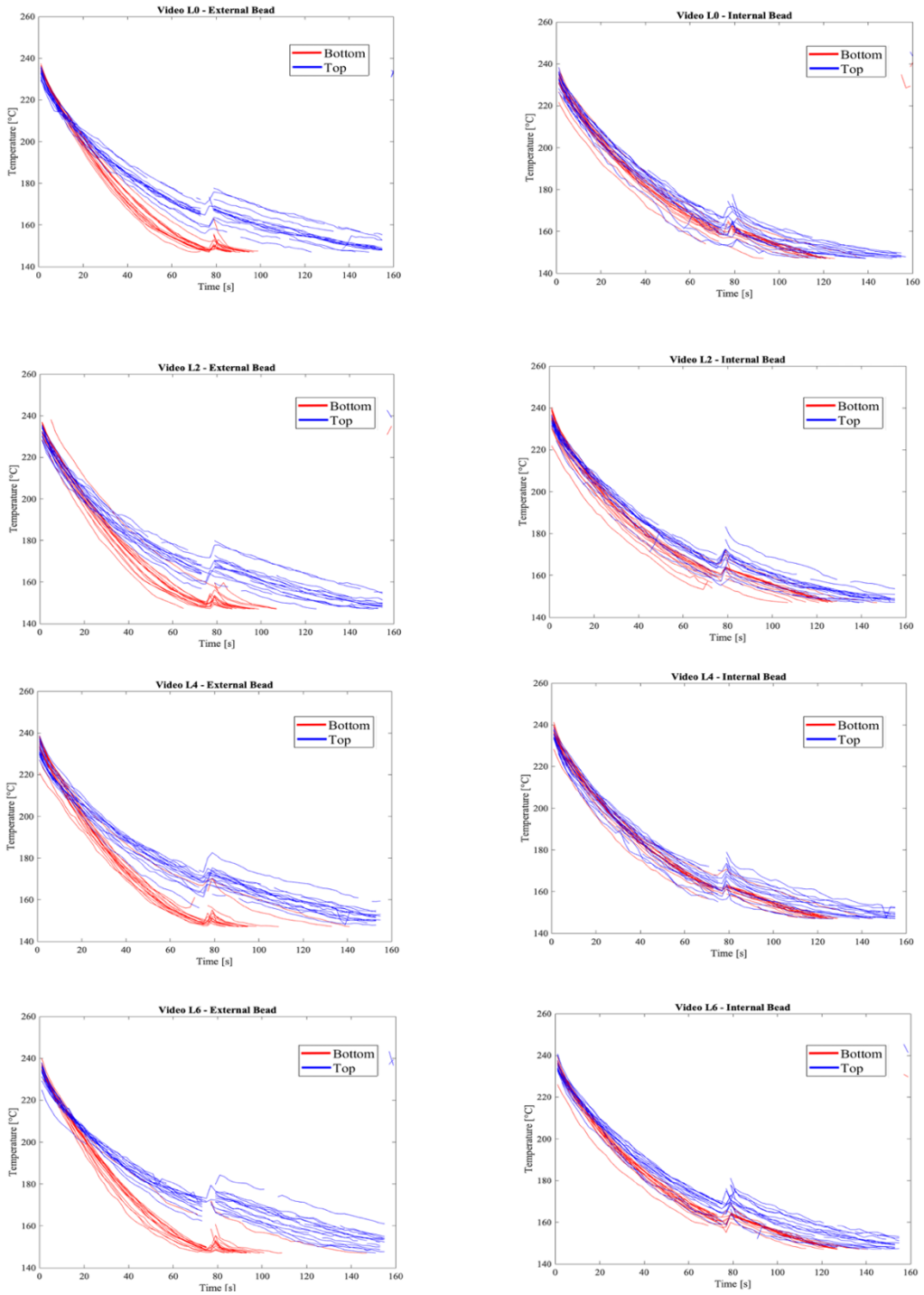

Figure 59 - Thermal profiles for the video analyzed

The ROIs identified in the bottom part of the structure (1-15) are indicated in red, while the ones located in the top part (16-32) are highlighted in blue. As can be seen from the figures presented above, there is a significant difference between the inner and outer bead cooling for the identified ROIs. In fact, in the profiles related to the external bead, a different cooling behavior can be noticed for the ROIs identified in the upper and lower part of the printed object. In particular, referring to the colors indicated before, it can be seen that the ROIs located at the bottom, in contact with the ABS platform resting on the floor, cool faster than the ROIs located at the top of the structure. This fact does not seem to occur for ROIs located in the inner bead, besides their position. Although the red profiles related to ROIs from 1 to 15 lie lower than the others, there is no marked difference as for the outer bead. The next figure (Fig. 60) it is used to stress even more this point. In particular, the individual plot of the average cooling rates of the ROIs, grouped by the different videos, are presented. As we can see, the external bead positioned at the bottom of the structure present lower values in terms of cooling rate if compared to the others, juxtapose to the top of the external bead. A slight difference, as anticipated before, can be noted in the internal bead also, but it is less evident, highlighting a similar cooling behavior between the top and the bottom part.

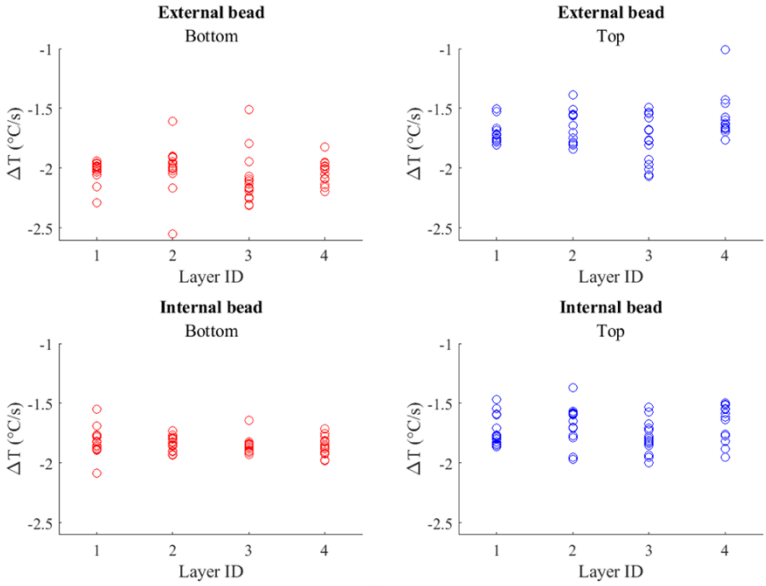

Figure 60 - Individual plot of the cooling rates

The explanation regards the part's cooling mechanisms. The external bead, staying on the ABS platform in contact with the steel surface upon which the printing occurs,

dissipates heat principally by conduction, thus much faster than the other parts of the structure. Unlike the external bead, in the internal bead the ROIs located in the lower part of the structure benefit from a sort of "insulation" provided by the external layer resting on the floor, resulting in a slower cooling process not comparable to the one just described, as can be noted in the figures above (Fig. 59-60). In order to further stress what has just been stated, two graphs, depicting the average thermal profiles and the 95% confidence intervals in order to underline the differences among beads are presented (Fig. 61 and Fig. 62).

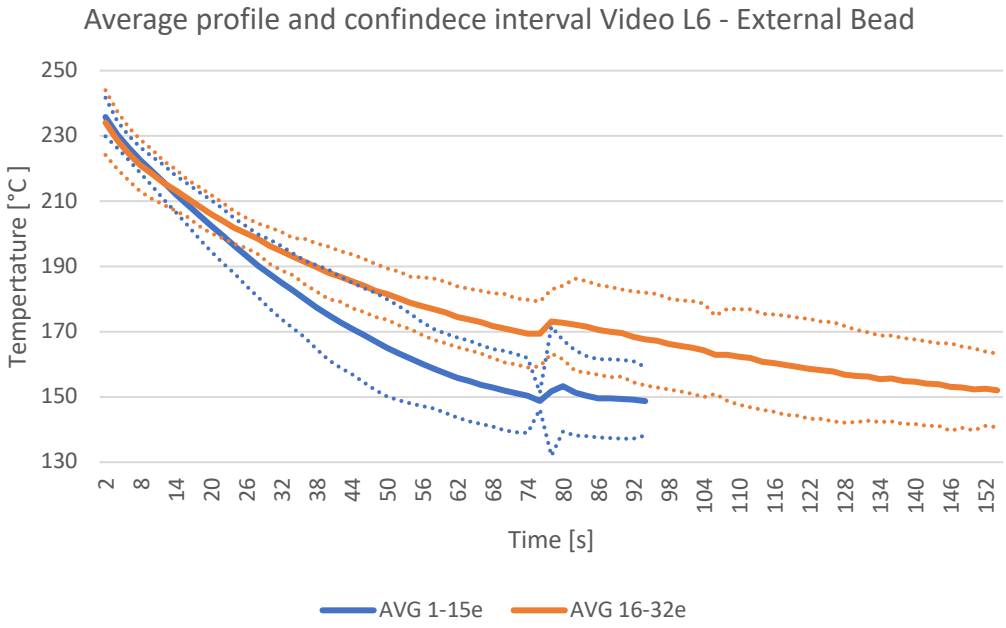

Figure 61 - Video D, external bead, average profiles and confidence interval

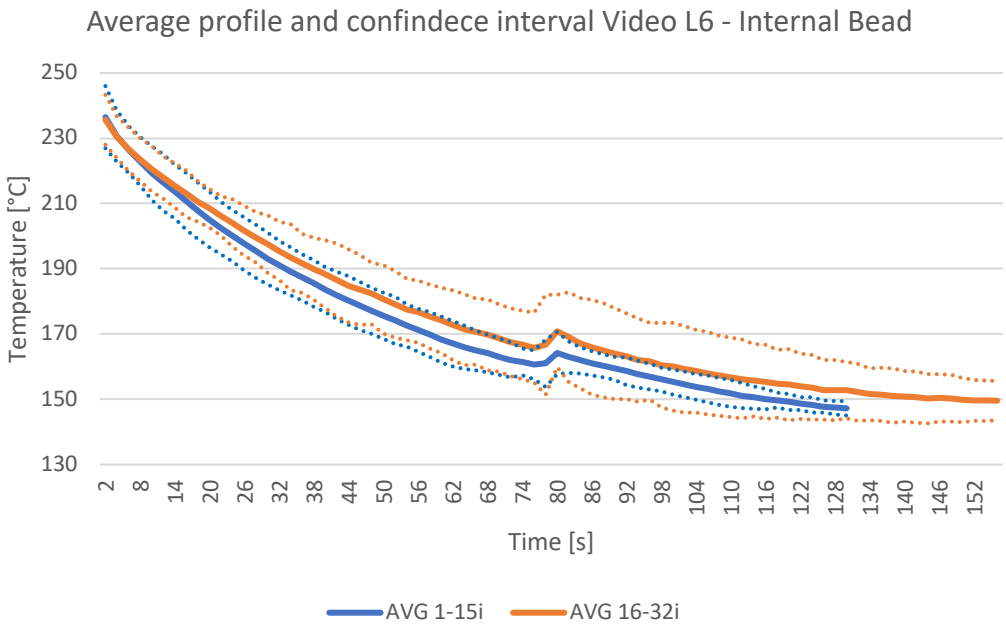

Figure 62 - Video D, internal bead, average profiles and confidence interval

As can be seen from these graphs, the different behaviors for the cooling of the inner and outer beads are clear. Once again, in both cases, the ROIs identified between 1 and 15 lie lower than ROIs 16 through 32, highlighting faster cooling. This difference, however, turns out to be more pronounced for the outer bead, for the reasons identified earlier in the paragraph.

Another qualitative observation that can be made by looking at the previous graphs (Fig. 61 and Fig. 62) concerns what happens exactly in the midpoint of the time scale, around the second 80. At this point a rise in temperature of about 6°C can be seen. This does not only occur for video L6, but is present in all videos, regardless of whether we consider the external or internal bead. Contrary to what it might be thought considering what has been said in the data preprocessing, this increase is not due to overlapping ROIs with the extruder, otherwise it would have been much larger than the one observed. This fact is directly explained by the passage of the extruder on the adjacent bead since they lean against each other. Indeed, if we consider the outer bead, it can be explained by the passage on the inner bead and vice versa. This slight increase in temperature, although very small, can be considered a desirable effect in a dilated layer time perspective, as it slows down the

cooling of the material and causes the temperature to remain above the glass transition temperature, even if for a short time.

As an additional qualitative assessment, we evaluated the possible difference between the ROIs located in the top bead. More in details, we investigated the difference between ROIs on straight bead's segment and ROIs located in turning points. As shown in the previous figures, there are no differences in terms of cooling between these two sections. For this geometry, short curvilinear sections do not influence the cooling process of the part by significantly changing the thermal gradient.

Finally, the last aspect that must be discussed concerns the evolution of the thermal gradient along time. In particular, in the next figure (Fig. 63) it is reported the behavior of the cooling rate for ROI number 17, video L0, as representative of all the ROIs considered. As can be noticed in the figure, despite some irregularities in the profile, the tendency of the gradient is to approach zero as the piece cool down. This is due to the fact that the more time passes, the more the temperature difference between the artifact and the surrounding environment decreases, slowing the heat exchange between the actors involved. This is perfectly in line with the expected results.

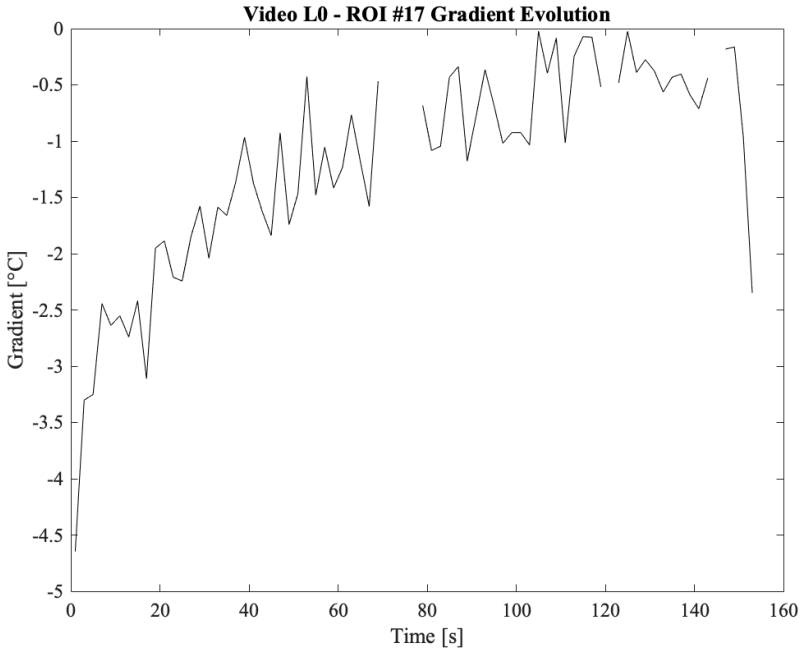

Figure 63 - Gradient evolution along time for ROI #17 - Video L0

Even in this case, the absence of values in the graph is explained by some inconsistent data present because of the reasons identified in the previous sections of this chapter. Moreover, data coming from the reheating of the extruder have been eliminated to focus the attention on values concerning the cooling of the artifacts.

The next chapter will be dedicated to the conclusions that this thesis work has brought, with a final in-depth study dedicated to the possible developments of the paths pursued.

4. Conclusion and future developments

In these days, environmental sustainability is a central theme for the correct development of the economies. The overuse of materials and plastics leads to an increase in pollution and CO_2 emissions, implying a rise in costs for companies, particularly for the manufacturing sector.

In this thesis we investigated the possibility of reducing CO_2 emissions in WHAM, a new technology for the production of large-scale functional 3D printed parts. Two paths have been followed to enhance sustainability. Firstly, an exploratory study on the feasibility for recycling ABS filled with 20% of carbon fiber have been conducted. More in details, this study identified the steps needed for mechanical recycling and it presents an evaluation of its footprint impact and economical assessment. The results have shown a significant difference in CO_2 emissions between producing the virgin material and mechanically recycling it. In particular, while 8.8 kg of CO_2 are produced for virgin material, the recycling lead to a generation of carbon emissions between 0.8 and 2.1 kg. From an economic point of view, the results show a convenience in recycling the material for quantities that exceed 500 kg a year. Finally, the mechanical tests conducted on the blended material composed for 80% of virgin material and 20% by recyclates have shown a slight decrease in mechanical properties, in particular ultimate tensile strength and Young's Modulus. This decrease has been proven to relate with the presence of the recycled material inside the mix. Moreover, a change in mechanical properties have been noted when varying the extraction's direction from x to z.

On the other hand, in order to reduce the quantity of material used for the production, scraps reduction has been pursued by inline identifying the arising parts flaws through in-situ monitoring. Here, we have presented a preliminary investigation on thermal signature and potential acquisition, data processing and automatic detection issues. No defects have shown during the experimentation, but the data collected has given useful information to better understand the cooling

process of the pieces produced using WHAM. In particular, it has been demonstrated that the lower parts of the structures tend to cool faster if compared to the higher parts, due to the contact with the platform. Moreover, in the case of a multiple bead structure, for the internal beads this behavior is not observed, so the cooling rates are similar for the lower and the higher parts of the structure. Another fact pointed out by the data analysis has been the effect of reheating caused by the extruder in the adjacent bead. Considering a multi-bead structure, when the extruder passes on one bead, on the adjacent one a slight increase in temperature (5-6°C) is registered. Another conclusion concerns the cooling of the straight bead's segment and the turning ones. There are no differences between the cooling rates for these portions. Finally, it must be said that the cooling rate of the ROIs considered tend to decrease with the decrease of the material's temperature, due to the gradual approach to the environmental temperature.

As regards future developments, variation of the percentage of recycled material within the compound used as raw material should be evaluated. In fact, if the conclusions previously reported in terms of mechanical tests and costs concerned a mix made up of 80% virgin material and 20% recycled material, further functional evaluations can be made by increasing the percentage of recovered material. Because it is economically convenient, above certain quantities, to recycle ABS filled with 20% of carbon fibers, increasing the percentage of recycled material in the mix will bring further advantages in terms of costs. The DOE used for this work, and the fact that the mechanical properties of the virgin material have already been tested, should further simplify this work by serving as a benchmark for future testing, leaving the opportunity to focus on studying the variation of mechanical properties as a function of the amount of recycled material in the compound. On the other hand, considering the environmental benefits in terms of reduction of CO_2 emissions, the increase in the percentage of recycled material can only benefit the cause and further decrease pollution caused by the production. Further developments regarding recycling could also be undertaken by considering other materials used by Ingersoll MasterPrint, which are also composites materials theoretically suitable for recycling.

Concerning achieving production as close to zero-defects as possible, in-situ thermal monitoring of the 3D printing is certainly a valuable solution in understanding early signals of defect occurrence. New acquisition setups can be tested, as well as different methodologies for the automatic identification of the defects. Feedback and

feedforward control could be implemented to mitigate or to eliminate the defects while printing. The goal would be to intervene promptly and avoid material wasting by saving the part from being classified as scrap. To do this, taking advantage of the work and knowledge acquired during this experiment regarding thermal monitoring, the company will evaluate the implementation of a system for the real-time thermal control of the 3D printed parts by the Ingersoll MasterPrint.

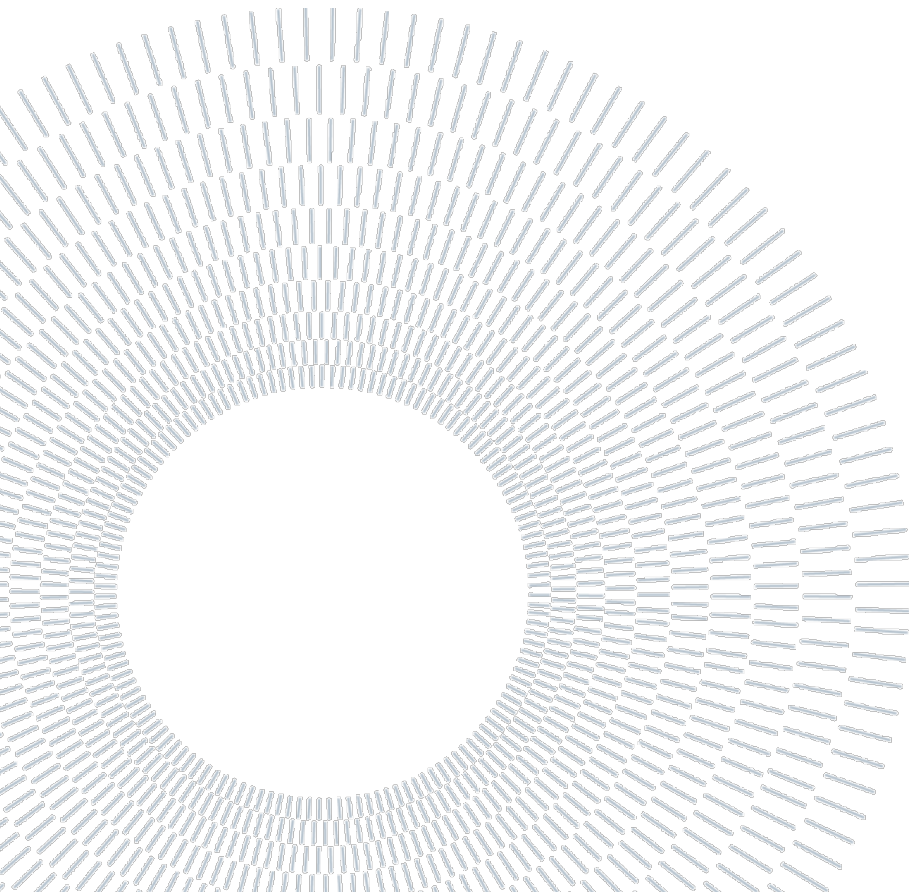

Bibliography

Witten E., Mathes V., Sauer M., Kühnel M., Composites market report 2018, Market developments, trends, outlooks and challenges, Federation of reinforced plastics

EOS, https://www.eos.info/en/industrial-3d-printing/additive-manufacturing-how-it-works (last access: 13/09/2021)

Ugur D., Bahar G., Ulas Y., Melik D., The role of additive manufacturing in the era of Industry 4.0, 27th International Conference on Flexible Automation and Intelligent Manufacturing, FAIM2017, 27-30 June 2017, Modena, Italy

Gibson I., Rosen D., Stucker B., Additive Manufacturing Technologies: 3D Printing, Rapid Prototyping, and Direct Digital Manufacturing, 2nd ed., Springer Link, 2015

Wholers Associates, http://www.wohlersassociates.com/history2014.pdf (last access: 13/09/2021)

Siemens, https://www.plm.automation.siemens.com/global/en/our-story/glossary/vat-photopolymerization/53338 (last access: 13/09/2021)

ISO/ASTM standards, https://www.iso.org/obp/ui/#iso:std:iso:3252:ed-4:v1:en (last access: 13/09/2021)

EOS, https://www.eos.info/en/3d-printing-examples-applications (last access: 13/09/2021)

Andrzejewski J., Mohanty A. K., Misra M., Development of hybrid composites reinforced with biocarbon/carbon fiber system. The comparative study for PC, ABS and PC/ABS based materials, Composites Part B, 2020

Billah K. M., Lorenzana F. A. R., Martinez N. L., Wicker R. B., Espalin D., Thermomechanical characterization of short carbon fiber and short glass fiber-reinforced ABS used in large format additive manufacturing, Additive Manufacturing 35, 2020

Colosimo B. M., Slides of Additive Manufacturing course, 2020

ISO/ASTM standards, https://www.iso.org/obp/ui/#iso:std:iso-astm:52900:dis:ed-2:v1:en (last access: 13/09/2021)

Taisch M., Slides of Operations Management course, Politecnico di Milano, Management Engineering course, 2020

Spieske A., Birkel H, Improving supply chain resilience through industry 4.0: A systematic literature review under the impressions of the COVID-19 pandemic, Computers & Industrial Engineering 158, 2021

Brian N. Turner, Robert Strong and Scott A. Gold, A review of melt extrusion additive manufacturing processes: I. Process design and modeling, Rapid Prototyping Journal, Volume 20 · Number 3 · 2014 · 192–204

Wohlers, T.T. (2011), Wohlers Report 2011: Additive Manufacturing and 3D Printing State of the Industry Annual Worldwide Progress Report, Wohlers Associates, Inc., Fort Collins, CO

R.Singh ,S.Singh, M.S.J.Hashmi, Implant Materials and Their Processing Technologies, Reference Module in Materials Science and Materials Engineering, 2016

Alex Roschli, Katherine T. Gaul, Alex M. Boulger, Brian K. Post, Phillip C. Chesser, Lonnie J. Love, Fletcher Blue, Michael Borish, Designing for BAAM, Additive Manufacturing Journal, 2018

3D Shop, https://top3dshop.com/blog/fff-vs-fdm-difference-and-best-printers#anchor2 (last access: 14/09/2021)

Verlag C.H., Droplets to beat of millisecond, Kunstsoffe International, 2018

Valkenaers H., Vogeler F., Ferraris E, Voet A., Kruth J-P, A novel approach to additive manufacturing: screw extrusion 3D printing, Conference: 10th International Conference on Multi-Material Micro Manufacture, 2013

Chad E et al, Structure and mechanical behavior of Big Area Additive Manufacturing (BAAM) materials, Rapid Prototyping Journal, Volume 23 · Number 1 · 2017 · 181–189

3D Natives, https://www.3dnatives.com/en/four-types-fdm-3d-printers140620174/

3D Printing, Hype or game changer? A global EY report, 2019

Deepak P., Swapnil V, Shaliendra K., Fused deposition modelling: a review, Rapid Prototyping Journal, Volume 26 · Number 1 · 2019 · 176–201

Chartier T., Badev A., Handbook of advanced ceramics (Second Edition), 2013

Post B., Richardson B., Lind R., Love L., Lloyd P., Kunc V.,Rhyne B., Roschli A., Big Area Additive Manufacturing Application in Wind Turbine Molds, 2017

Post B., Lind R., Love L., Lloyd P., Kunc V., Linhal J.M., The economics of big area additive manufacturing, Solid Freeform Fabrication 2016: Proceedings of the 276th Annual International Solid Freeform Fabrication Symposium – An Additive Manufacturing Conference, 2016

Nieto M., Molina S., Large-format fused deposition additive manufacturing: a review, Rapid Prototyping Journal Volume 26 · Number 5 · 2019 · 793–799, 2019

Brian K. Post, Bradley Richardson, Randall Lind, Lonnie J. Love, Peter Lloyd, Vlastimil Kunc, Breanna J. Rhyne, Alex Roschli, Big Area Additive

Manufacturing Application in wind turbine molds, Solid Freeform Fabrication 2017: Proceedings of the 28th Annual International Solid Freeform Fabrication Symposium – An Additive Manufacturing Conference, 2017

Office of Technology Transition, U.S. Department of Energy, Development of BAAM System Spurs Birth of an Industry, 2019

Holshouser C., Newell C., Palas S., Out of Bounds Additive Manufacturing, Advanced Material and Processes, 2013

Ajinjeru C., Kishore V., Liu P., Lindahl J., Hassen A.A., Kunc V., Post B., Love L., Duty C., Determination of melt processing conditions for high performance amorphous thermoplastics for large format additive manufacturing, Additive Manufacturing 21, 125-132, 2018

Hu C., Qin Q., Advances in fused deposition modeling of discontinuous fiber/ polymer composites, Current Opinion in Solid State & Material Science, 2020

Yaman, U., Shrinkage compensation of holes via shrinkage of interior structure in FDM process. International Journal of Advanced Manufacturing Technology, 94(5–8), 2187–2197, 2018

Li Y., Zhao, W., Li, Q., Wang, T., & Wang, G., In-situ monitoring and diagnosing for fused filament fabrication process based on vibration sensors. Sensors (Switzerland), 19(11), 2019

Fu Y., Downey A., Yuan L., Pratt A., Balogun Y., In-situ monitoring for fused filament fabrication process: A review, Additive Manufacturing Volume 38, 2021

Tekinalpa H.L., Kuncb V., Velez-Garcia G., Dutyb C.E., Love L., Naskara A.K., Blueb C.A., Ozcana S., Highly Oriented Carbon Fiber in Polymer Composite Structures via Additive Manufacturing

Charalampous P, Kostavelis I, Tzovaras D., Non-destructive quality control methods in additive manufacturing: a survey. Rapid Prototyp J 26:777–790, 2020 https://doi.org/10.1108/ RPJ-08-2019-0224

Lu Q.Y., Wong C.H., Additive manufacturing process monitoring and control by non-destructive testing techniques: challenges and in-process monitoring. Virtual Phys Prototyp. 13:39–48, 2018 https://doi.org/10.1080/17452759.2017.1351201

Oleff A., Küster B., Stonis M., Overmeyer L., Process monitoring for material extrusion additive manufacturing: a state-of-the-art review, Progress in Additive Manufacturing, Springer, 2021

Borish M., Post B.K., Roschli A., Chesser P.C., Love L. J., Gaul K. T., Sallas M., Tsiamis N., In-Situ Thermal Imaging for Single Layer Build Time Alteration in Large-Scale Polymer Additive Manufacturing, Procedia Manufacturing 34:482–488, 2019

Kim C, Espalin D, Cuaron A., A study to detect a material deposition status in fused deposition modeling tech- nology. IEEE Int Conf Adv Intell Mechatron (AIM):779–783, 2015

Jin Z., Zang Z., Gu G.X., Automated real time detection and prediction of Interlayer imperfection in additive manufacturing processes using artificial intelligence, Advanced Intelligent Systems, 2020

Baumann F, Roller D., Vision based error detection for 3D printing processes, MATEC Web Conf., 2016

Makagonov N.G., Blinova E. M., Bezukladinkov I. I., Development of Visual Inspection Systems, 017 IEEE Conf Russ Young Res Electr Electron Eng (EICon-Rus):1463–1465, 2017

Müller M., Wings E., An Architecture for Hybrid Manufacturing Combining 3D Printing and CNC Machining, International Journal of Manufacturing Engineering Volume 2016, 2016

Liu C., Smart additive manufacturing using advanced data analytics and closed loop control, Dissertation, Virginia Polytechnic Institute and State University, 2019

Yen C-T., Chuang P-C., Application of a neural network integrated with the internet of things sensing technology for 3D printer fault diagnosis, Microsystem Technologies, Springer, 2019

Yang Z., Jin L., Yan Y., Mei Y., Filament Breakage Monitoring in Fused Deposition Modeling Using Acoustic Emission Technique, 2018

Becker P., Roth C., Roennau A., Dillmann R., Acoustic Anomaly Detection in Additive Manufacturing with Long Short-Term Memory Neural Networks, Conference Paper, 2020

Kemperle A, Gelman F, Schmehl PJ, Three-dimensional printer with force detection. US Patent 10556381B2, 2016

Kim C, Espalin D, Cuaron A et al (2015) A study to detect a material deposition status in fused deposition modeling technology. IEEE Int Conf Adv Intell Mechatron (AIM):779–783.

Gatlin J, Belikovetsky S, Moore SB, Detecting sabotage attacks in additive manufacturing using actuator power signatures. IEEE Access 7:133421–133432, 2019

Chesser P, Post B, Roschli A, Carnal C, Lind R, Borish M, Love L, Extrusion control for high quality printing on Big Area Additive T Manufacturing (BAAM) systems, Additive Manufacturing 28 ppg. 445-455, 2019

Howarth J, Mareddy S.S.R, Mativenga P.T, Energy intensity and environmental analysis of mechanical recycling of carbon fibre composite, Journal of Cleaner Production 81, 2014

Ragaert K, Delva L, Van Geem K, Mechanical and chemical recycling of solid plastic waste, Waste Management 69, ppg 24-58, 2017

Pakdel E, Kashi S, Varley R, Wang X, Recent progress in recycling carbon fibre reinforced composites and dry carbon fibre wastes, Resources, Conservation & Recycling 166, 2021

Meng F, McKechnie J, Turner T.A, Pickering S,J, Energy and environmental assessment and reuse of fluidised bed recycled carbon fibres, Composites: Part A 100, ppg. 216-214, 2017

Morsidi M, Mativenga P.T, Fahad M, Fused Deposition Modelling Filament with Recyclate Fibre Reinforcement, Procedia CIRP 85, ppg. 353-358, 2019

Oliveux G, Dandy L.O, Leeke G.A, Current status of recycling of fibre reinforced polymers: Review of technologies, reuse and resulting properties, Progress in Materials Science 72 ppg. 61-99, 2015

Garcia F.L, da Silva Moris A, Nunes A.O, Aparecido Lopes Silva D, Environmental performance of additive manufacturing process – an overview, Rapid Prototyping Journal ppg. 1166-1177, 2018

Witik R.A, Teuscher R, Michaud V, Ludwig C, Månson J.-A. E, Carbon fibre reinforced composite waste: An environmental assessment of recycling, energy recovery and landfilling, Composites: Part A 49 ppg. 89-99, 2013

Pimenta S., Pinho S.T., Recycling carbon fibre reinforced polymers for structural applications: technology review and market outlook, Waste Management 31, 378–392, 2011

https://www.winnipeg.ca/finance/findata/matmgt/documents/2012/682-2012/682-2012_Appendix_H-WSTP_South_End_Plant_Process_Selection_Report/Appendix%207.pdf

https://renewable-carbon.eu/news/natural-fibres-show-outstandingly-low-co2-footprint-compared-to-glass-and-mineral-fibres/

EU parliament, La logistica quale strumento per contrastare il cambiamento climatico, studio, 2010

Bonalumi D., Vercesi P., Slides from the course of Fisica Tecnica and Sistemi Energetici, Politecninco di Milano, 2019

https://www.sorgenia.it/guida-energia/costo-kwh-industriale

www.all3dp.com

Raharjo W.W., Panji A., Ariawan D., Sukanto H., Kusharjanta B., The influence of chemical recycling process on the carbon fiber properties, wettability, and interface bonding of carbon fiber and unsaturated polyester, Journal of Applied Science and Engineering, Vol. 24, No 6, Page 875-882 , 2021

Compton B. G., Post B. K., Duty C. E., Love L., Kunc V., Thermal analysis of additive manufacturing of large-scale thermoplastic polymer composites, Additive Manufacturing 17 (2017) 77–86 , 2021

Ogi K., Nishikawa T., Okano Y., Taketa I., Mechanical properties of ABS resin reinforced with recycled CFRP, Adv. Composite Mater., Vol. 16, No. 2, pp. 181–194, 2006

Alogla A. A., Baumers M., Tuck C., Elmadih W., The Impact of Additive Manufacturing on the Flexibility of a Manufacturing Supply Chain, Applied Science, 2021

Gebler M., Uiterkamp A., Vesser C., A global sustainability perspective on 3D printing technologies, Energy Policy 74 158–167, 2014

Ford S., Despeisse M., Additive manufacturing and sustainability: an exploratory study of the advantages and challenges, Journal of Cleaner Production 137 1573-1587, 2016

Suarez L., Dominguez M., Sustainability and environmental impact of fused deposition modelling (FDM) technologies, The International Journal of Advanced Manufacturing Technology 106:1267–1279, 2020

Godina R., Ribeiro I., Matos F., Ferreira B., Carvalho H., Peças P., Impact Assessment of Additive Manufacturing on Sustainable Business Models in Industry 4.0 Context, Sustainability Journal, 2020

Bertoli L., In-Situ Monitoring of Extrusion-based Additive Manufacturing Processes via Image Analysis and Supervised Machine Learning, Politecnico di Milano, 2020

Wakimoto T., Takamori R., Growable Robot with Additive Manufacturing, 2018

Sbriglia L. R., Baker A. M., Thompson J. M., Morgan V.R., Wachtor A. J., Bernardin J. D., Embedding Sensors in FDM Plastic Parts During Additive Manufacturing, Topics in Modal Analysis & Testing, Volume 10, 2016

Petrovic, V., Vicente Haro Gonzalez, J., Jorda Ferrando, O., Delgado Gordillo, J., Ramon Blasco Puchades, J. and Portoles Grinan, L., "Additive layered manufacturing: sectors of industrial application shown through case studies", International Journal of Production Research, Vol. 49 No. 4, pp. 1061-1079, 2011

Li N., Link G., Jelonnek J., 3D microwave printing temperature control of continuous carbon fiber reinforced composites, Composites Science and Technology 187, 2020

List of Figures

List of Tables

5. Acknowledgements

I would like to thank, first of all, my supervisor, Professor Bianca Maria Colosimo, for giving me the opportunity to carry out a thesis focused on innovation and on the practical application of the concepts developed along the path.
I would also like to thank the Camozzi Group and Innse Berardi for having welcomed me. A special thanks goes to Mirco Chiodi and Fabio Caltanissetta for having followed, supported and endured me in the development of the thesis. I would like to thank those who participated in the endless meetings and had the patience to answer my countless questions. I thank my family and all my friends, the historical ones and the new ones that I had the pleasure to meet here in Milan, without your help I don't know if I would have lived this beautiful experience at Politecnico di Milano in this way.